uOttawa

L'Université canadienne
Canada's university

Photonic Integrated Circuits for Microwave Photonics

Jianping Yao

Microwave Photonics Research Laboratory
School of Electrical Engineering and Computer Science
University of Ottawa

Université d'Ottawa | University of Ottawa

www.uOttawa.ca

Outline

- Introduction to Microwave Photonics (MWP)
- SiP-based MWP systems
  - Photonic generation of microwave waveforms
  - Photonic processing of microwave signals
  - A fully SiP integrated MWP filter
- InP-based signal processing
  - A fully reconfigurable photonic signal processor
  - A fully InP integrated MWP filter
- SiN-based MWP systems
  - True time delay beamforming
  - Reconfigurable signal processor
- Conclusion

Materials systems

Three materials systems:

1) Indium Phosphide (InP)
2) Silicon Nitride (Si_3N_4)
3) Silicon Photonics (SiP)

1)InP:

- Able to monolithically integrate both active and passive photonic components
- High loss, and large size
- Difficulty to integrate with electronics

Materials systems

2) Si_3N_4:

•Very low loss, <0.2 dB/cm

•no active components such as light sources, modulators, amplifiers and photodetectors can be supported, thus full monolithic integration is hard to achieve

3) SiP:

•A technology that allows optical devices to be made economically using the standard and well-developed CMOS fabrication process

•Most of the optical components, both passive and active, can be fabricate

•The key advantages include much **smaller footprint**, **low loss**, and **simple fabrication process**

•No optical amplification and light generation

Introduction to Microwave Photonics

Microwave Photonics (RF Photonics) is an field that studies the **generation**, **processing**, **control,** and **transmission** of microwave signals by means of photonics for applications such as wireless communications, radar, sensing, imaging, and instrumentation.

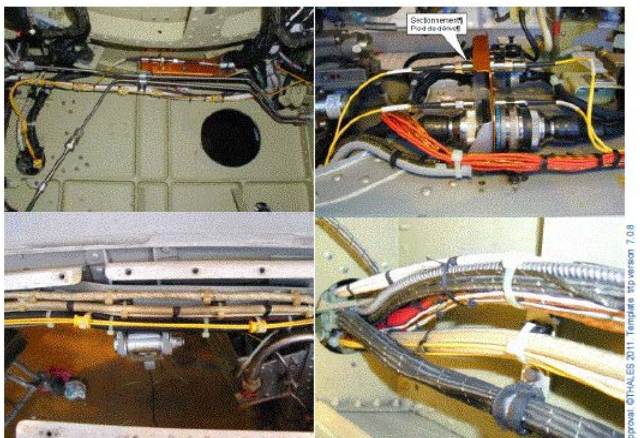

DASSAULT AVIATION

What is Microwave Photonics (MWP)?

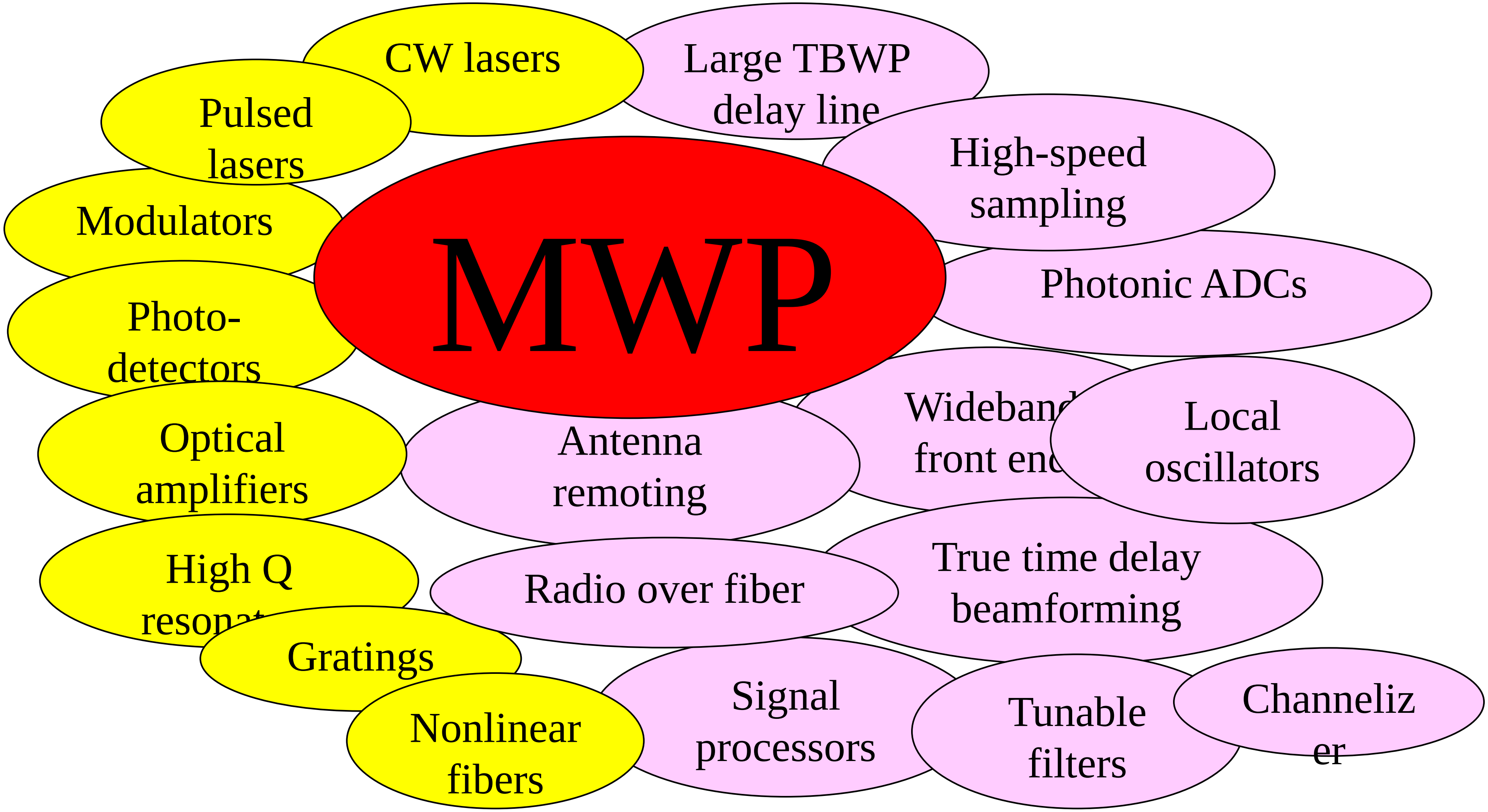

Applications of Microwave Photonics

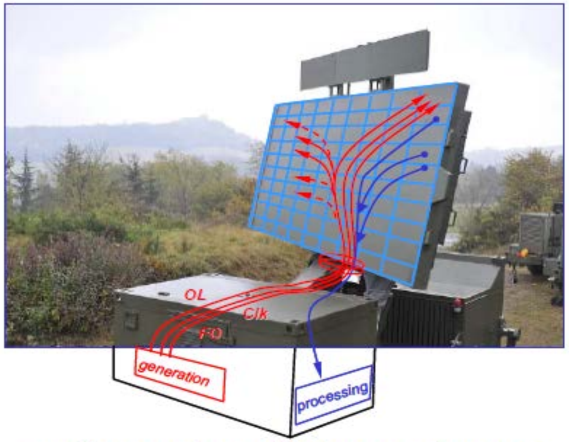

surface radars with large antennas

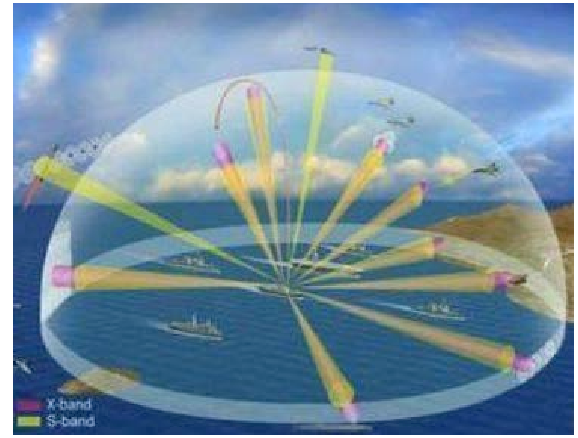

The Atacama Large Millimeter Antenna (ALMA) Array

Outline

- Introduction to Microwave Photonics (MWP)
- SiP-based MWP systems
  - **Photonic generation of microwave waveforms**
  - Photonic processing of microwave waveforms
  - A fully SiP integrated MWP filter
- In-P signal processing
  - A fully reconfigurable photonic signal processor
  - A fully InP integrated MWP filter
- SiN-based MWP systems
  - True time delay beamforming
  - Reconfigurable signal processor
- Conclusion

Chirped microwave waveform generation

Chirp-free pulse

Chirped pulse

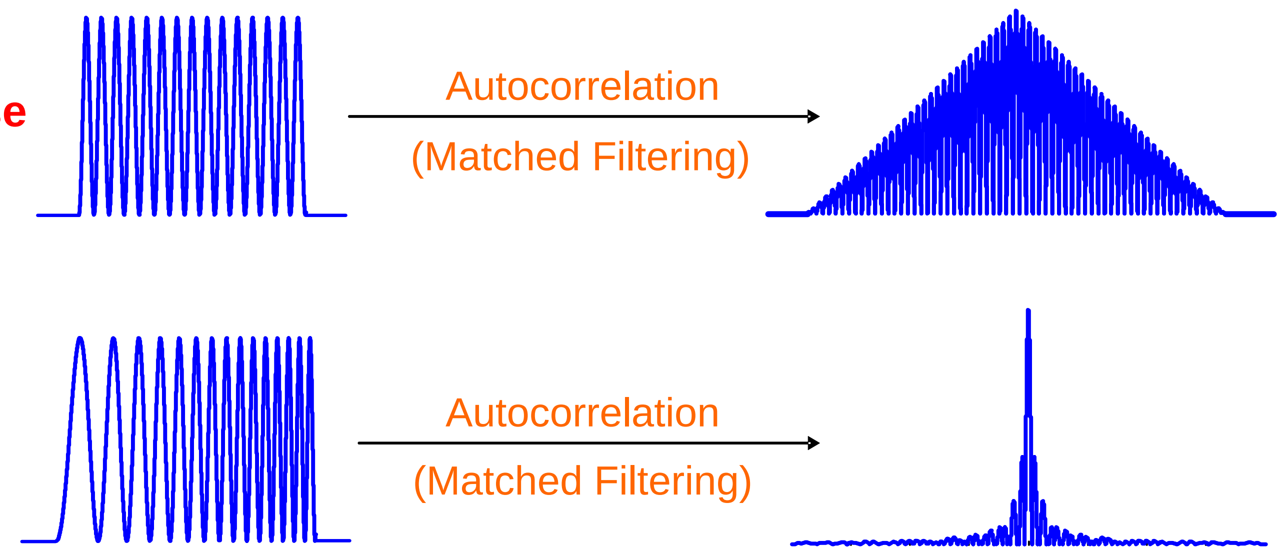

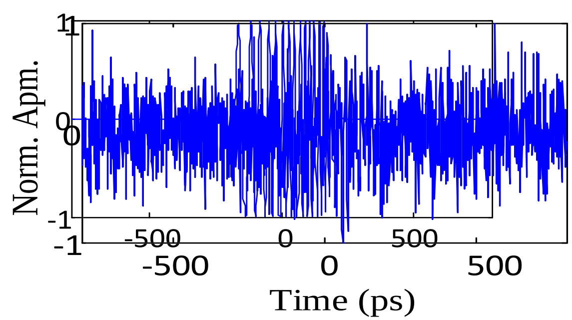

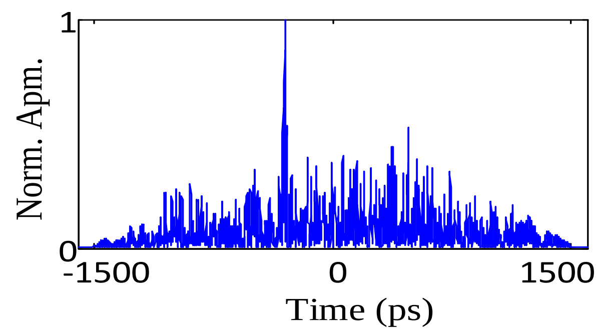

Chirped microwave pulse can be compressed by matched filtering, widely employed in Radar systems.

Photonic microwave waveform generation based on *spectral shaping and frequency-to-time mapping*

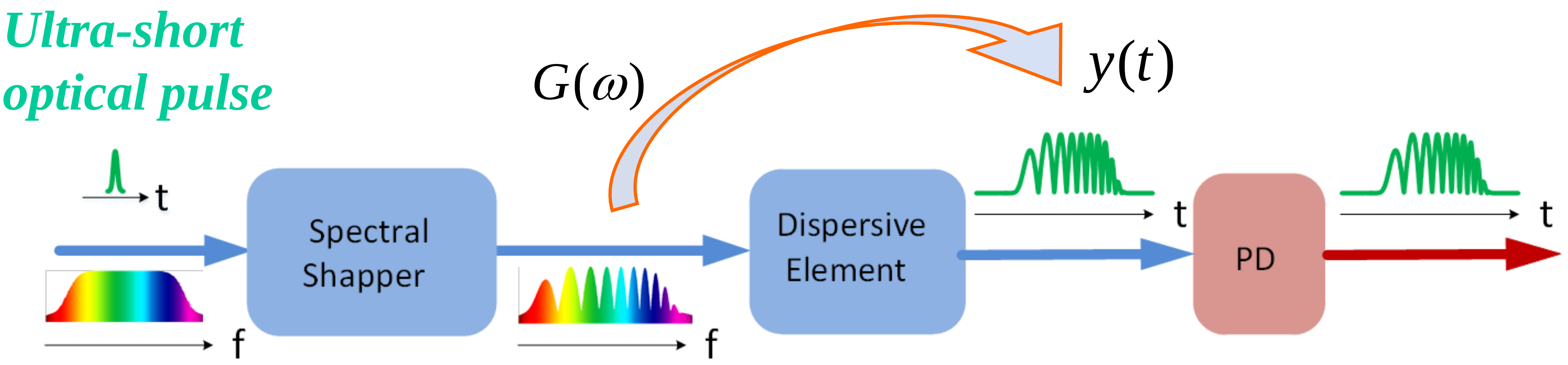

$$y(t) \propto G(\omega)\Big|_{\omega=\frac{t}{\ddot{\Phi}}}$$

J. P. Yao, *Opt. Comm.*, vol. 284, no. 15, pp. 3723-3736, Jul. 2011.

Photonic microwave waveform generation based on *spectral shaping and frequency-to-time mapping*

- **Frequency-to-time mapping**

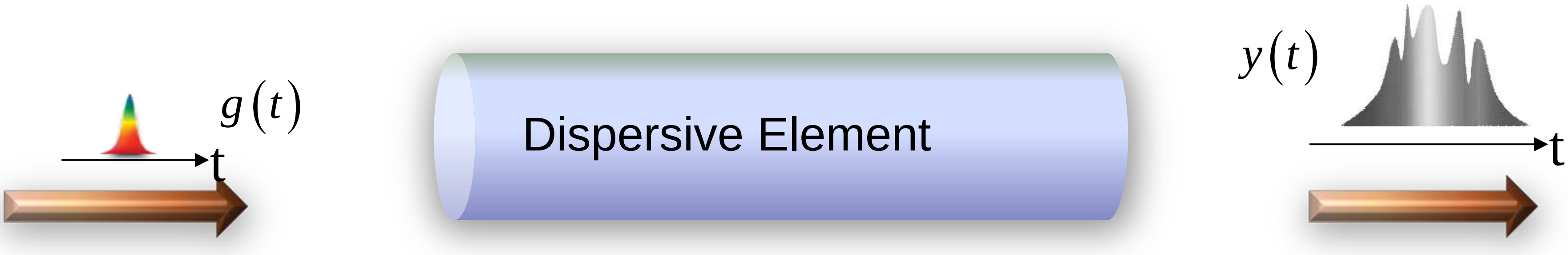

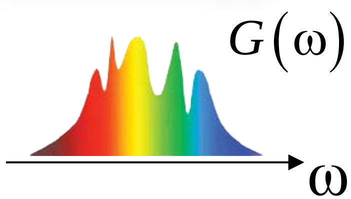

$$
\begin{aligned}
y(t) &= g(t) * \exp\left(j\frac{t^2}{2\ddot{\Phi}}\right) = \int_{-\infty}^{\infty} g(\tau) \times \exp\left[j\frac{(t-\tau)^2}{2\ddot{\Phi}}\right] d\tau \\
&= \exp\left(j\frac{t^2}{2\ddot{\Phi}}\right) \times \int_{-\infty}^{\infty} g(\tau) \times \exp\left(j\frac{\tau^2}{2\ddot{\Phi}}\right) \times \exp\left[-j\left(\frac{t}{\ddot{\Phi}}\right)\tau\right] d\tau \\
&\approx \exp\left(j\frac{t^2}{2\ddot{\Phi}}\right) \times \int_{-\infty}^{\infty} g(\tau) \times \exp\left[-j\left(\frac{t}{\ddot{\Phi}}\right)\tau\right] d\tau \\
&= \exp\left(j\frac{t^2}{2\ddot{\Phi}}\right) \times G(\omega)\Big|_{\omega=\frac{t}{\ddot{\Phi}}} \quad \approx G(\omega)\Big|_{\omega=\frac{t}{\ddot{\Phi}}}
\end{aligned}
$$

Wavelength-to-time mapping, namely dispersive Fourier transformation, is a fast and effective way to **measure optical spectrum in the time domain**.

On-chip spectral shaper incorporating multi-microring resonators

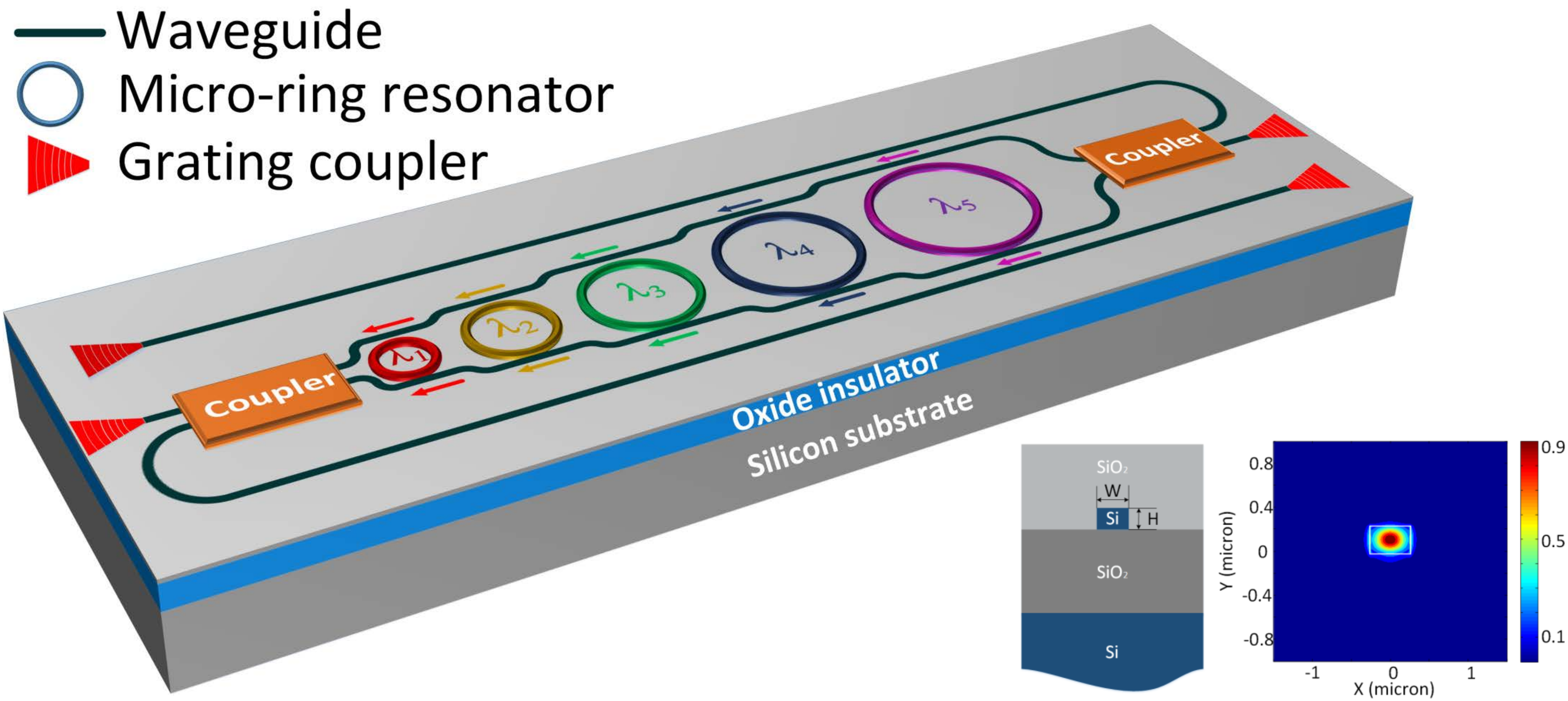

Perspective view of the proposed on-chip spectral shaper. (Inset: (left) Wire wave guide structure and (right) the simulated fundamental transverse electric (TE) mode profile of the wire waveguideat 1550 nm.

On-chip spectral shaper incorporating multi-microring resonators

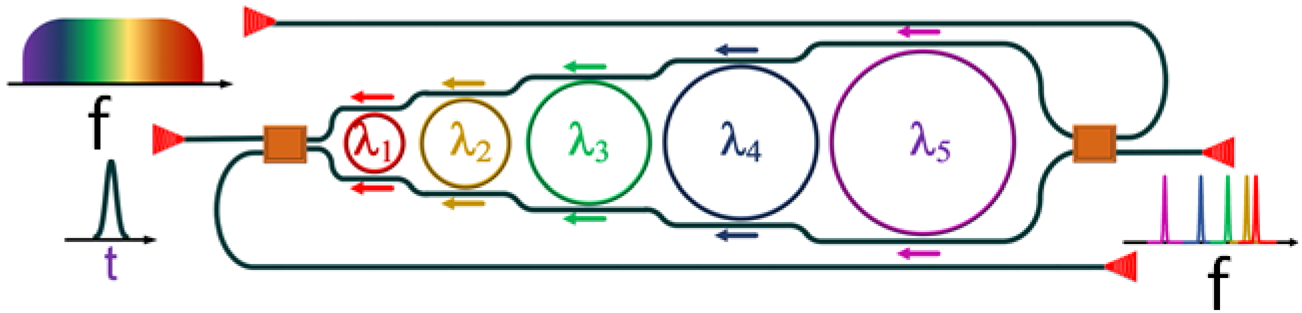

Schematic layout of the designed on-chip spectral shaper.

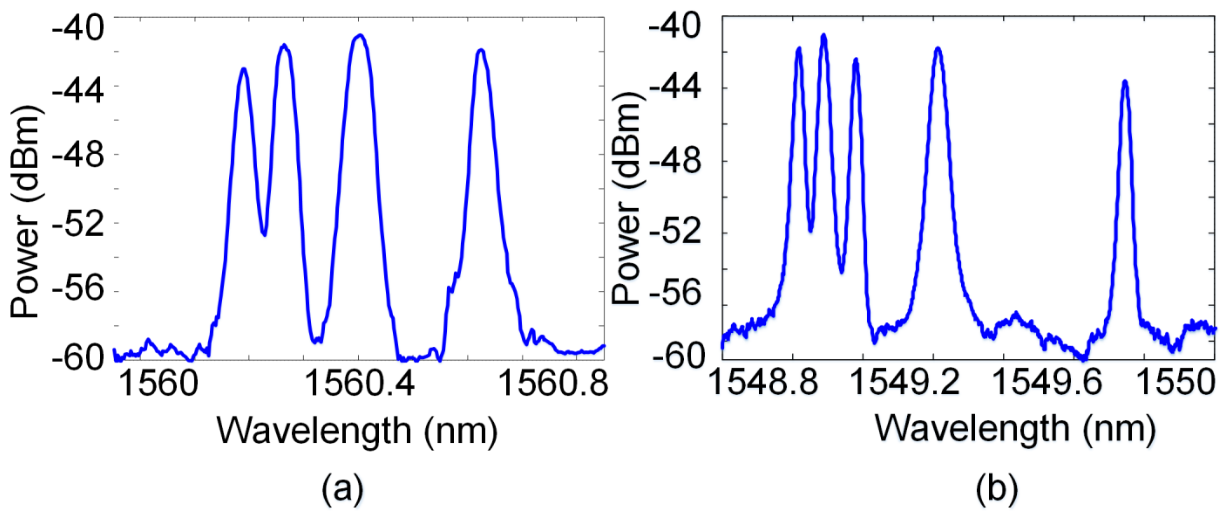

(a) Measured spectral response of an on-chip spectral shaper consisting of *four cascaded MRRs*. (b) Measured spectral response of an on-chip spectral shaper consisting of *five cascaded MRRs*.

On-chip spectral shaper incorporating multi-microring resonators

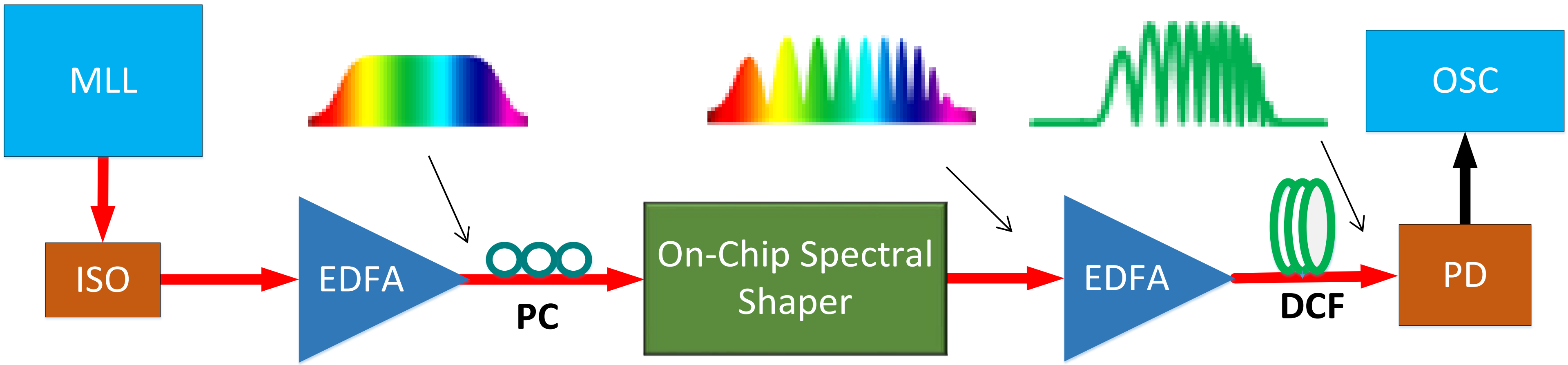

Experimental setup. MML: mode lock laser. ISO: Isolator; EDFA: erbium-doped fiber amplifier. PC: polarization controller. DCF: dispersion compensation fiber. PD: photodetector. OSC: oscilloscope.

Experimental results

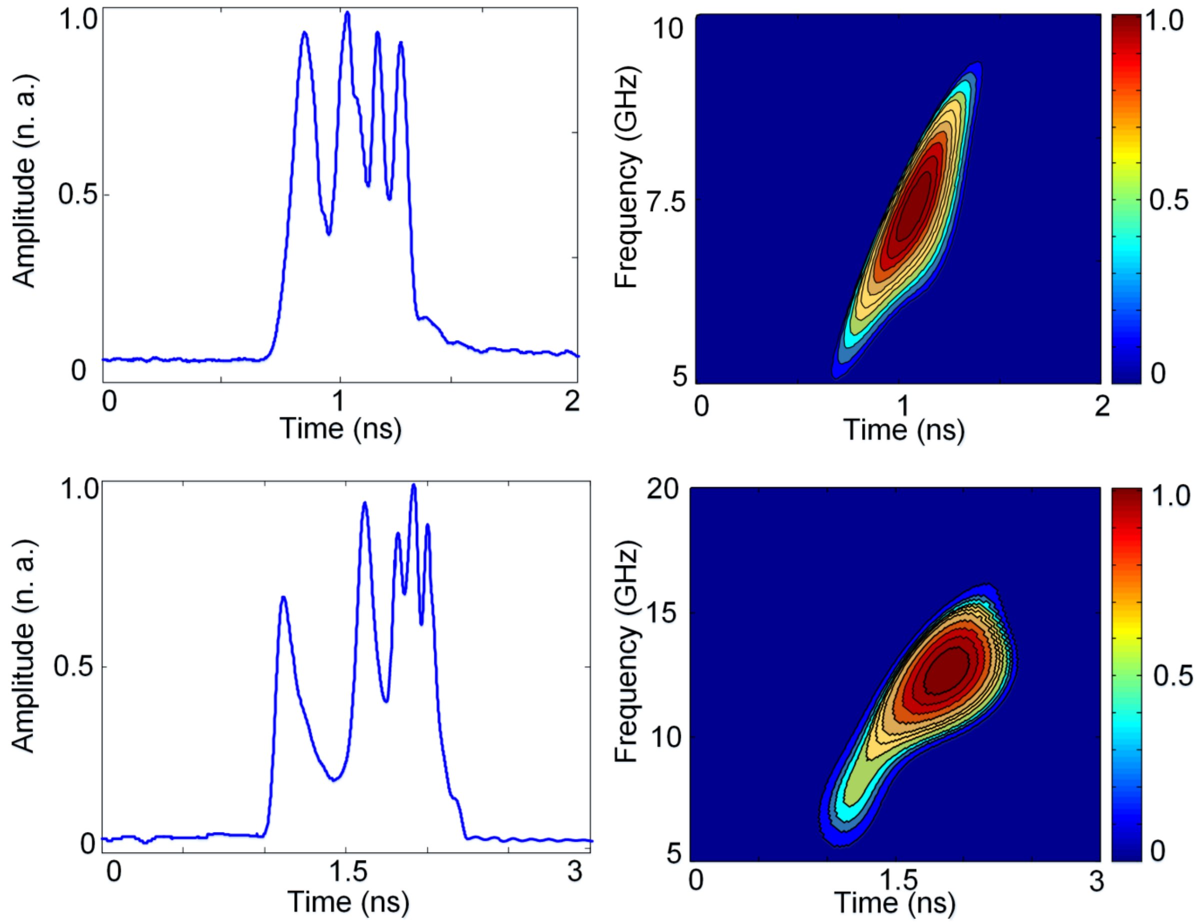

Bandwidth:8.5 GHz
Chirp rate:12.2 GHz/ns

Bandwidth:15.5 GHz
Chirp rate:17.2 GHz/ns

The generated chirped microwave waveforms and the spectrogram illustrating the time distribution of the microwave frequency components.

On-chip spectral shaper incorporating linearly chirped waveguide Bragg gratings

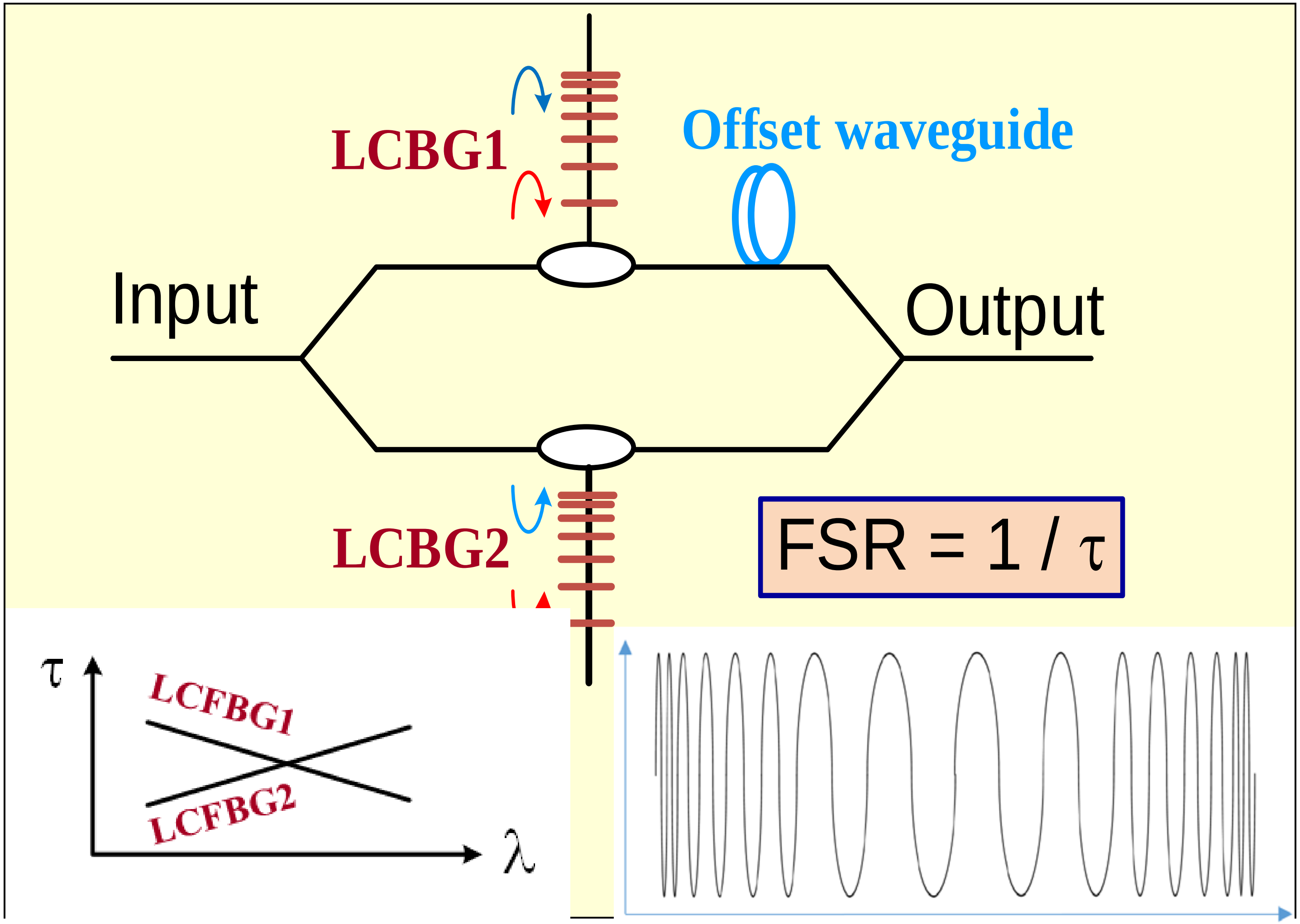

On-chip spectral shaper incorporating linearly chirped waveguide Bragg gratings

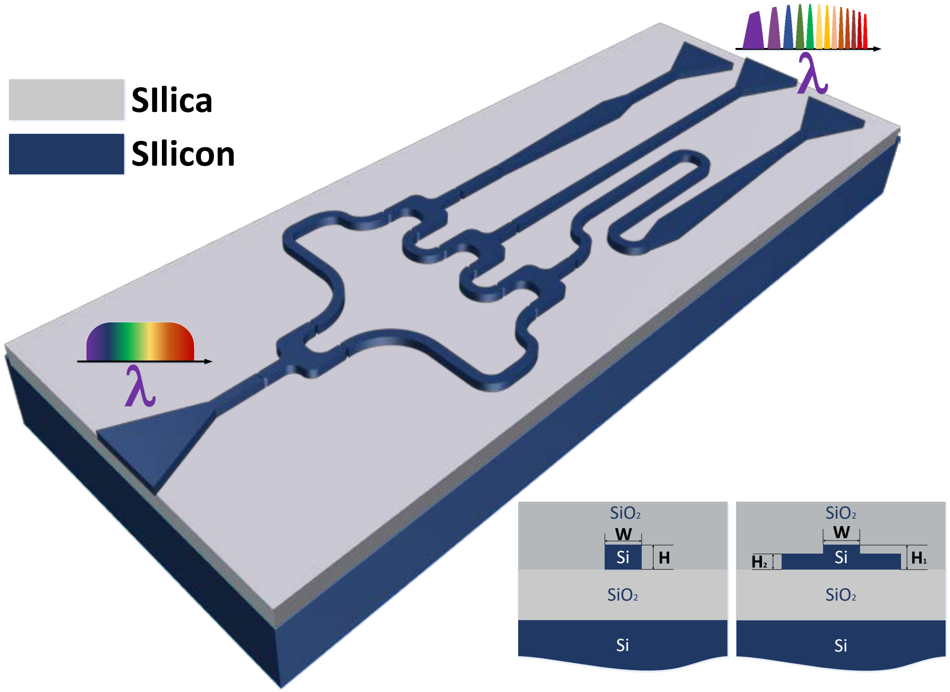

Perspective view of the proposed on-chip silicon-based optical spectral shaper. (Inset: (Left) Wire waveguide and (Right) Rib waveguide)

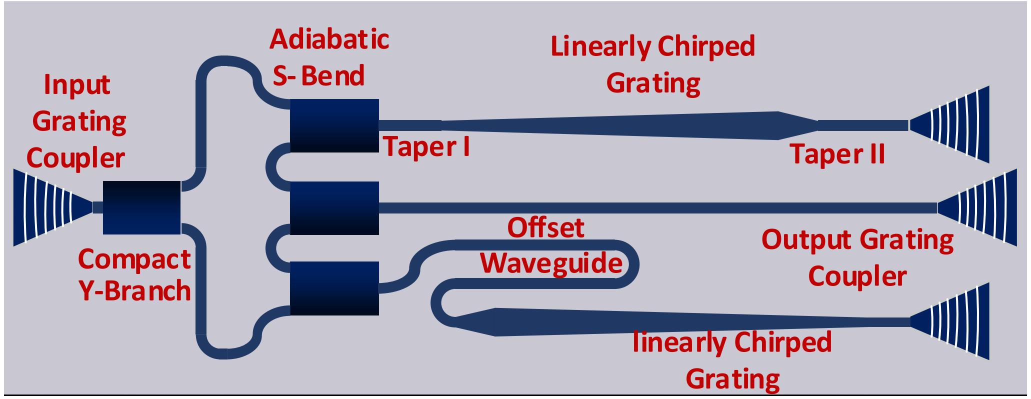

(a)

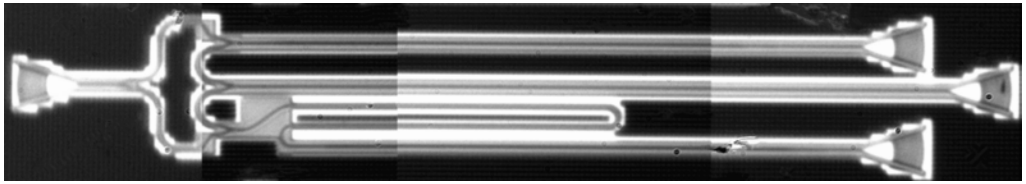

(b)

(a) Schematic layout of the designed on-chip spectral shaper; (b) Image of the fabricated spectral shaper captured by a microscope camera.

W. Zhang and J. P. Yao, "Photonic generation of linearly chirped microwave waveforms using a silicon-based on-chip spectral shaper incorporating two linearly chirped waveguide Bragg gratings," *IEEE/OSA J. Lightw. Technol.*, vo. 33, no. 24, pp. 5047-5054, Dec. 2015 .

On-chip spectral shaper incorporating linearly chirped waveguide Bragg gratings

$$\lambda_B = 2n_{eff}\Lambda$$

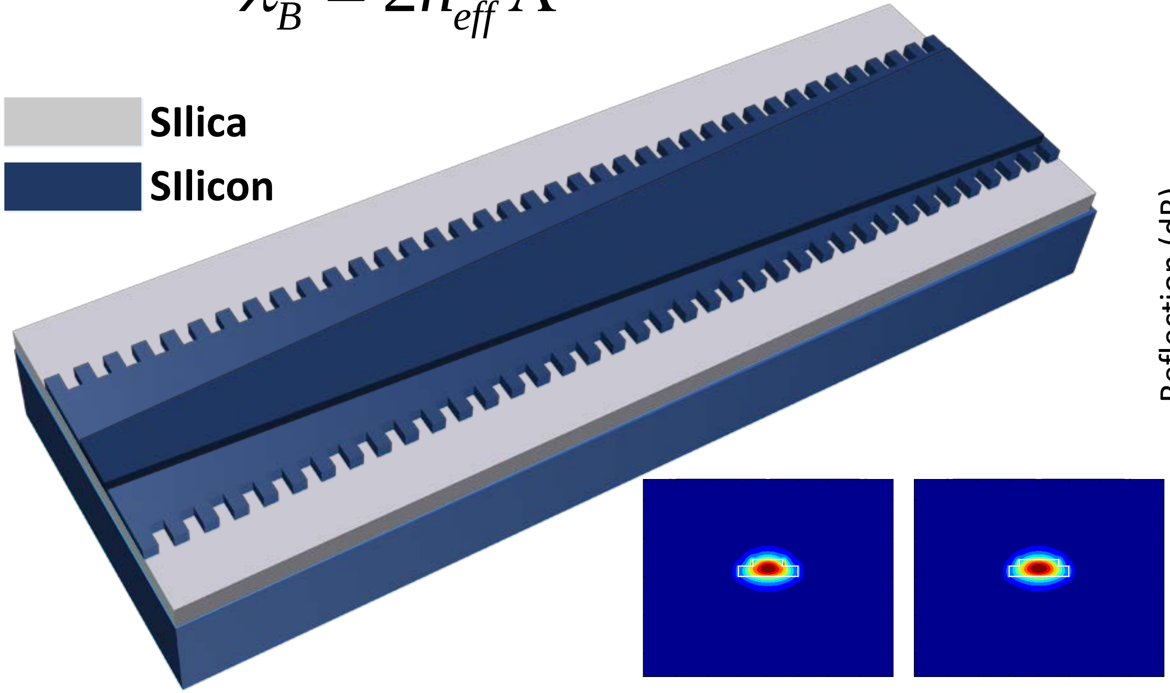

Perspective view of the proposed LC-WBG. (Inset: Simulated fundamental TE mode profile of the rib waveguide with the rib width of 500 nm (left) and 650 nm (right)).

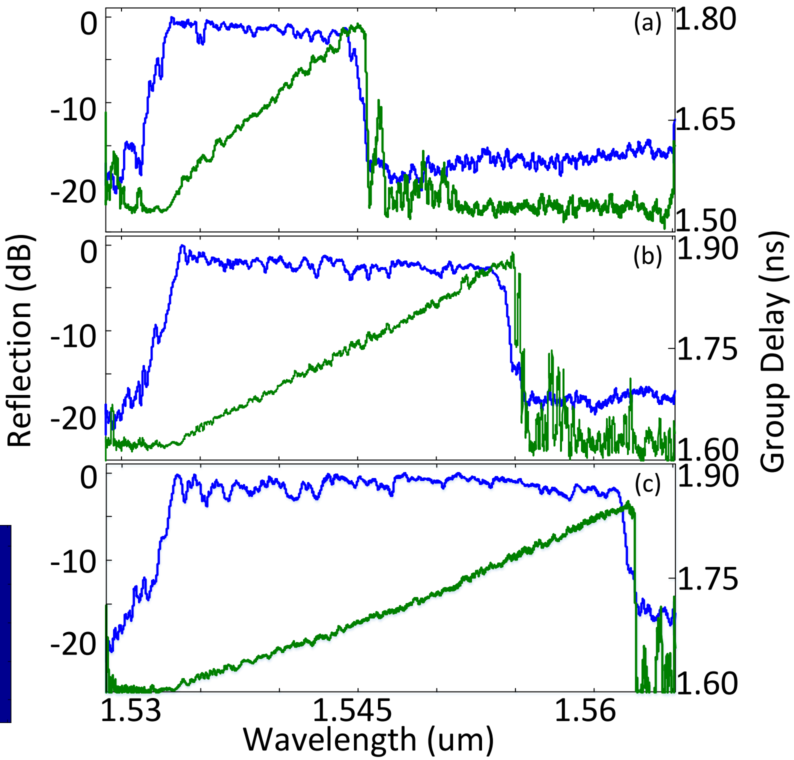

Measured spectral and group delay responses of the LC-WBG with the rib width increasing from 500 nm to (a) 550 nm, (b) 600 nm and (c) 650 nm along the gratings.

The grating is realized by introducing periodic sidewall corrugations on the slab. By keeping the grating period uniform and linearly increasing the width of the rib along the grating, a linear chirp is produced since the effective refractive index is linearly increasing as the rib width increases in a definite range.

Experimental Results

Measured spectral response of an on-chip spectral shaper when the length of the offset waveguide is (left) zero and (right) the length of the LC-WBG.

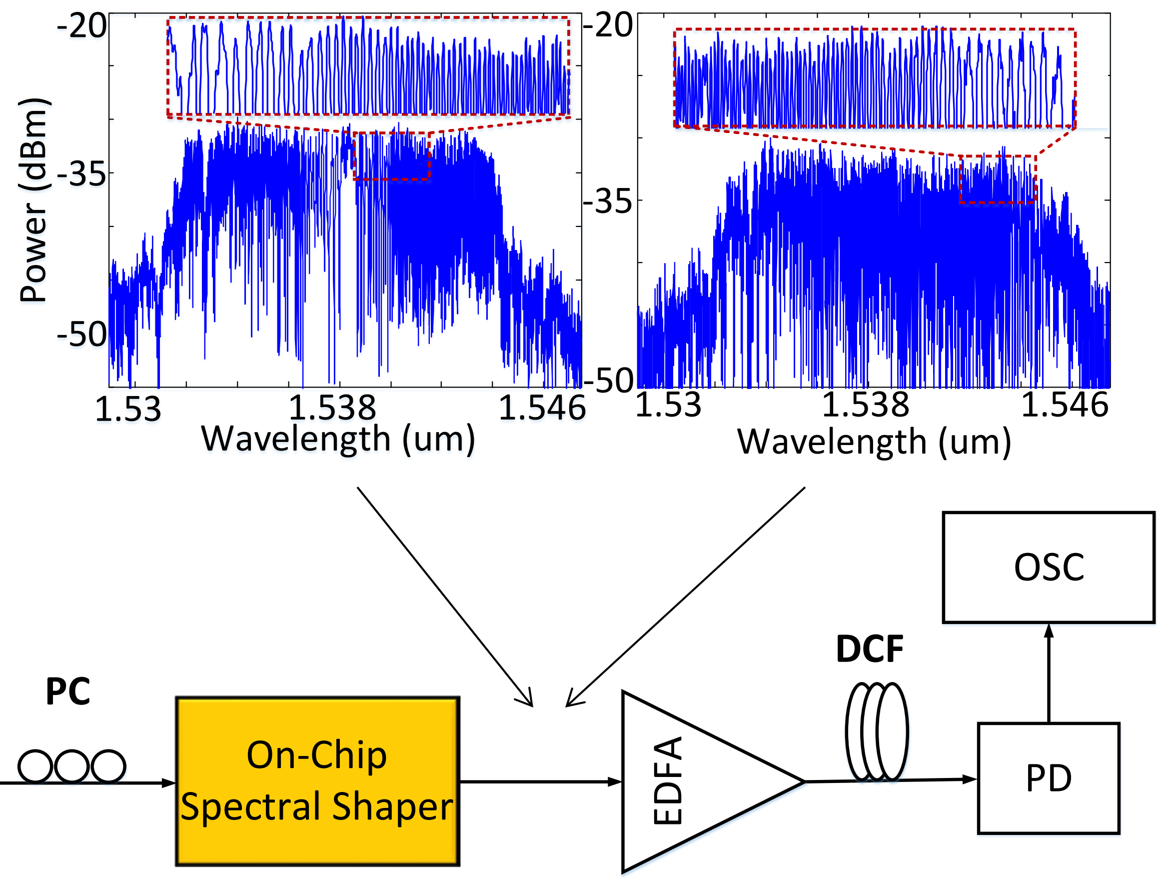

Experimental setup. TMML: tunable mode lock laser. ISO: Isolator; EDFA: erbium-doped fiber amplifier. PC: polarization controller. DCF: dispersion compensation fiber. PD: photodetector. OSC: oscilloscope.

Experimental Results

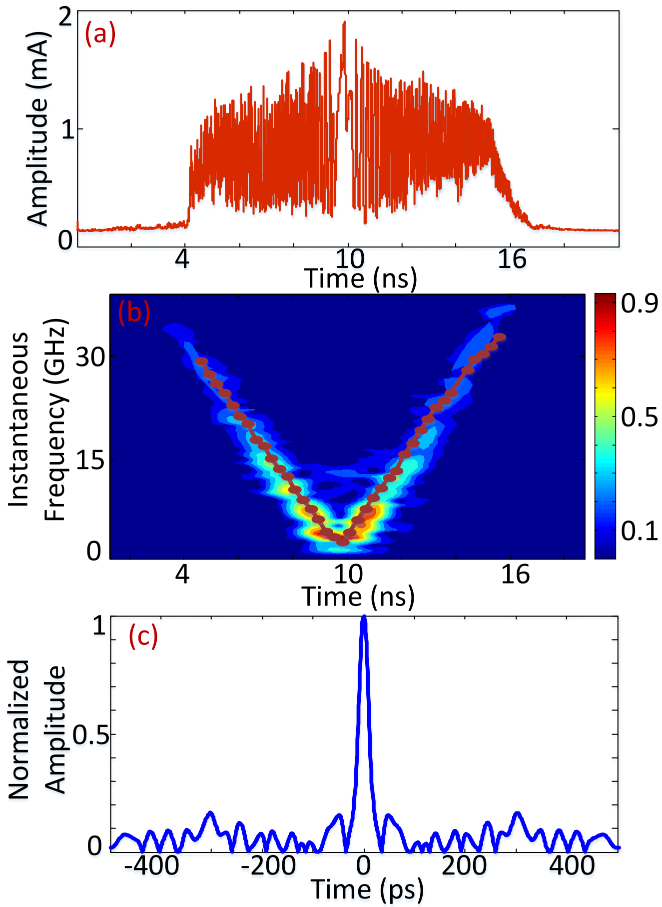

Experimental result: (a) the generated LCMW; (b) experimental spectrogram curve and numerical instantaneous frequency of the generated LCMW, and (c) compressed pulse by autocorrelation when the length of the offset waveguide equates to zero.

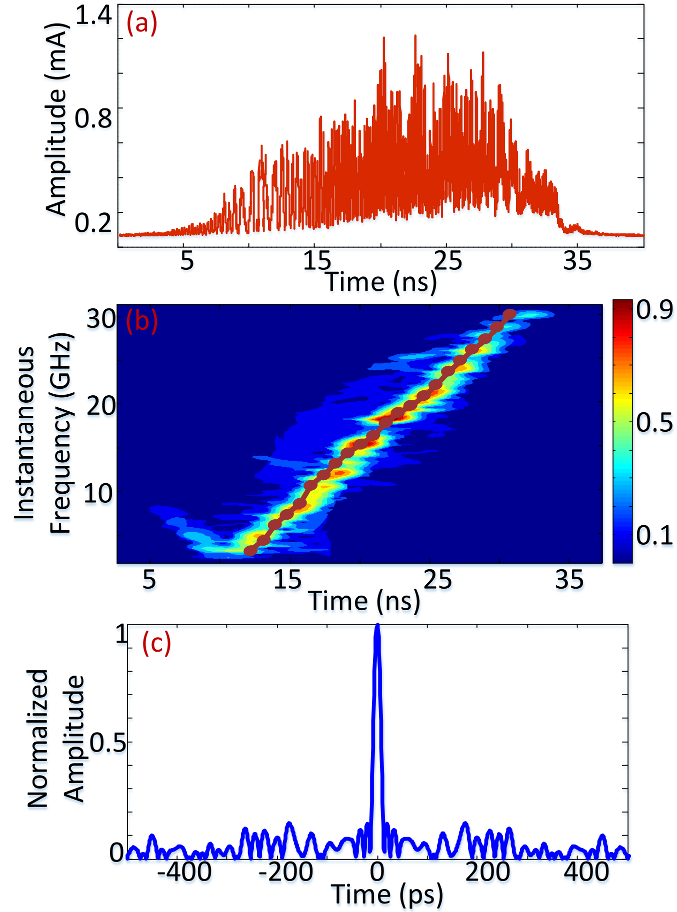

Experimental result: (a) the generated LCMW; (b) experimental spectrogram curve and numerical instantaneous frequency of the generated LCMW, and (c) compressed pulse by autocorrelation when the length of the offset waveguide equates to the length of LC-WBG.

Outline

- Introduction to Microwave Photonics (MWP)
- SiP-based MWP systems
  - Photonic generation of microwave waveforms
  - **Photonic signal processing**
  - A fully SiP integrated MWP filter
- In-P signal processing
  - A fully reconfigurable photonic signal processor
  - A fully InP integrated MWP filter
- SiN-based MWP systems
  - True time delay beamforming
  - Reconfigurable signal processor
- Conclusion

Photonic temporal differentiator

A *n*th order temporal differentiator: $y(t) = \frac{d^n x(t)}{dt^n}$

The transfer function:

$$H(\omega) = [j(\omega - \omega_0)]^n = \begin{cases} e^{jn\left(\frac{\pi}{2}\right)} \left|\omega - \omega_0\right|^n, & \omega > \omega_0 \\ e^{jn\left(-\frac{\pi}{2}\right)} \left|\omega - \omega_0\right|^n, & \omega < \omega_0 \end{cases}$$

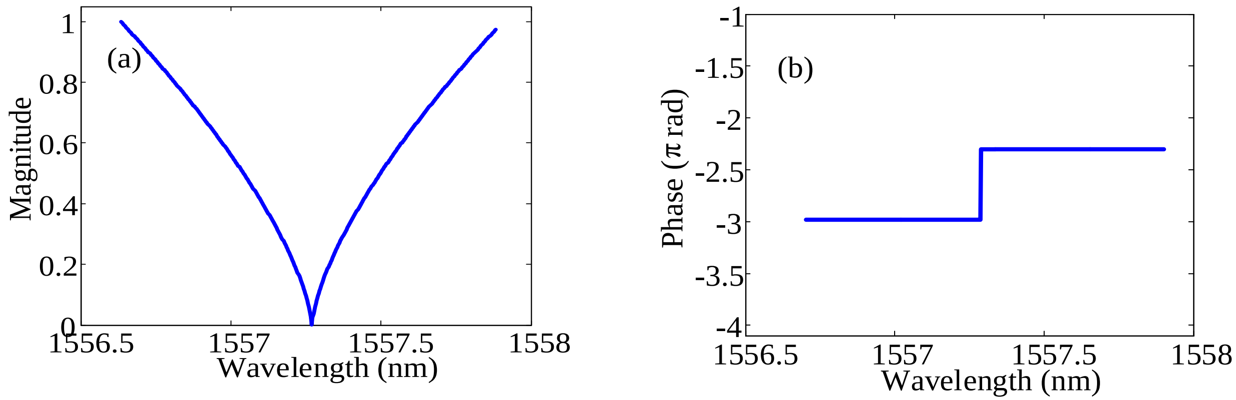

Magnitude and phase response of a differentiator.

Applications: phase to intensity conversion in an optical phase-modulated system.

Photonic microwave temporal differentiator using an integrated phase-shifted Bragg grating

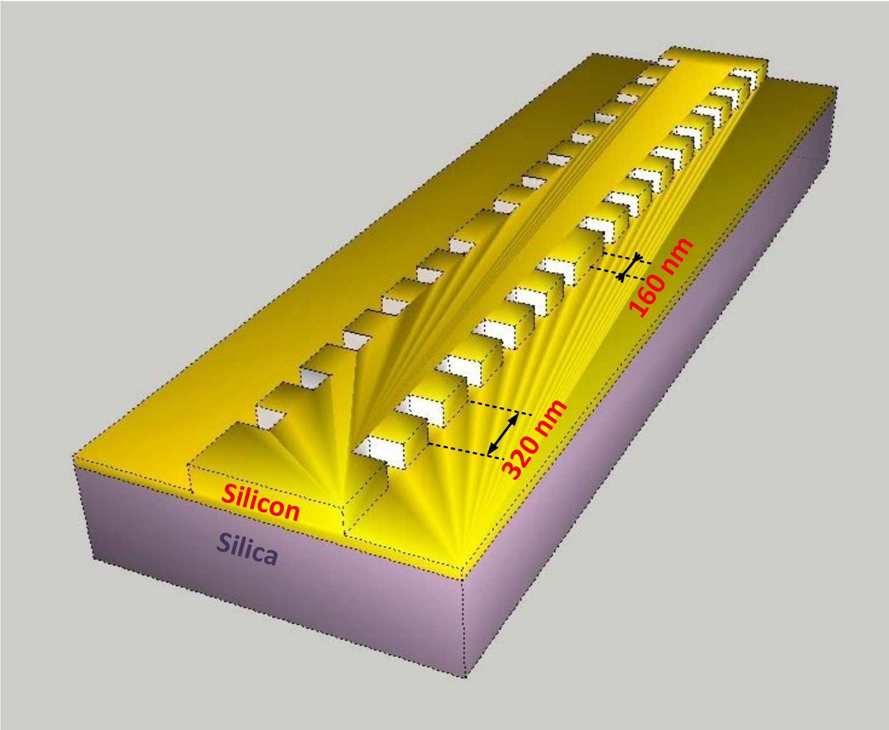

Configuration of the phase-shifted Bragg grating (PSBG) in an silicon-on-insulator ridge waveguide.

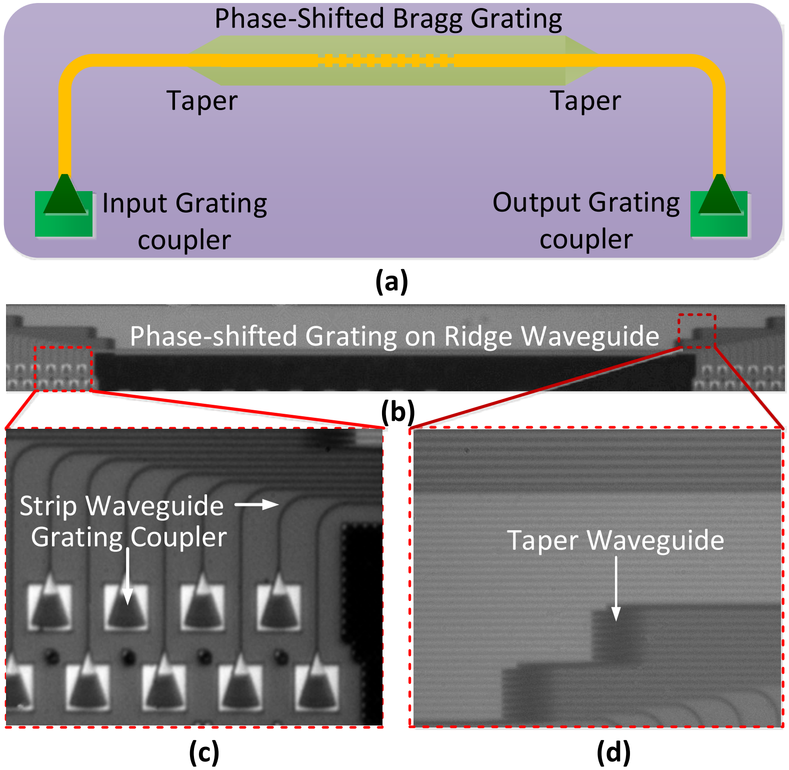

(a) Schematic layout. (b) Image of the fabricated device. (c) Image of the grating couplers and the strip waveguides. (d) Image of the taper waveguides for the transition between the strip waveguides and ridge waveguides.

W. Zhang, W. Li, and J. P. Yao, *IEEE Photon. Technol. Lett.*, vol. 26, no. 23, pp. 2383-2386, Dec. 2014.

Experimental Results

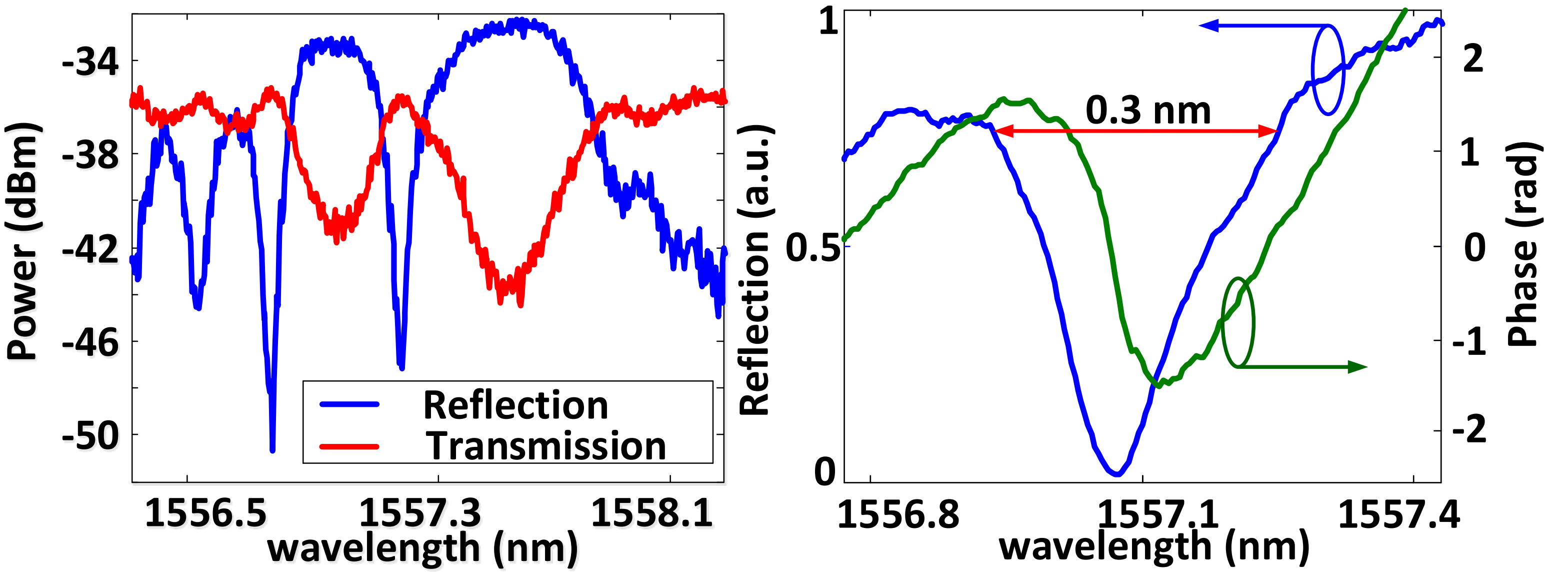

(Left) Measured reflection and transmission spectral responses of the fabricated PSBG on a ridge waveguide with a designed corrugation width of 125 nm. (Right) Zoom-in view of the reflection notch and its phase response.

Experimental Results

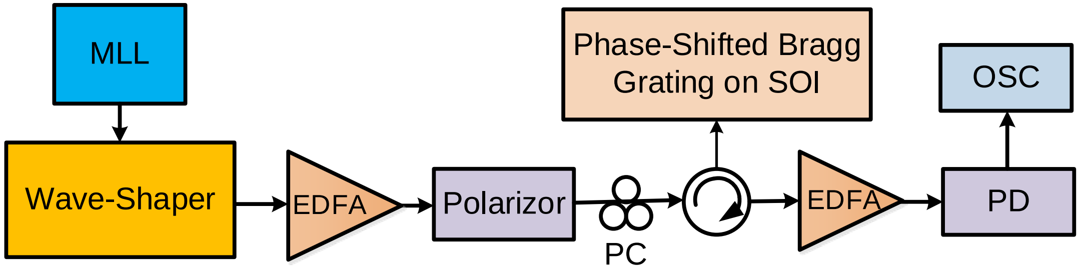

Experimental setup. MML: mode lock laser. EDFA: erbium-doped fiber amplifier. PC: polarization controller. PD: photodetector. OSC: oscilloscope.

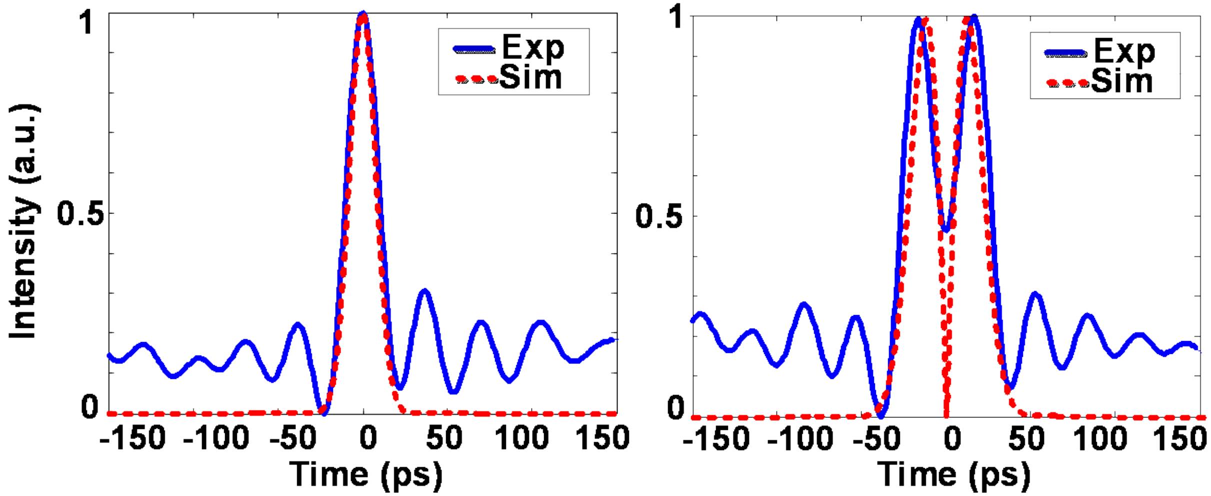

(Left) An input Gaussian pulse with an FWHM of 25 ps, and (Right) the temporally differentiated pulses by simulation and experiment.

Independently tunable *multichannel* fractional-order temporal differentiator

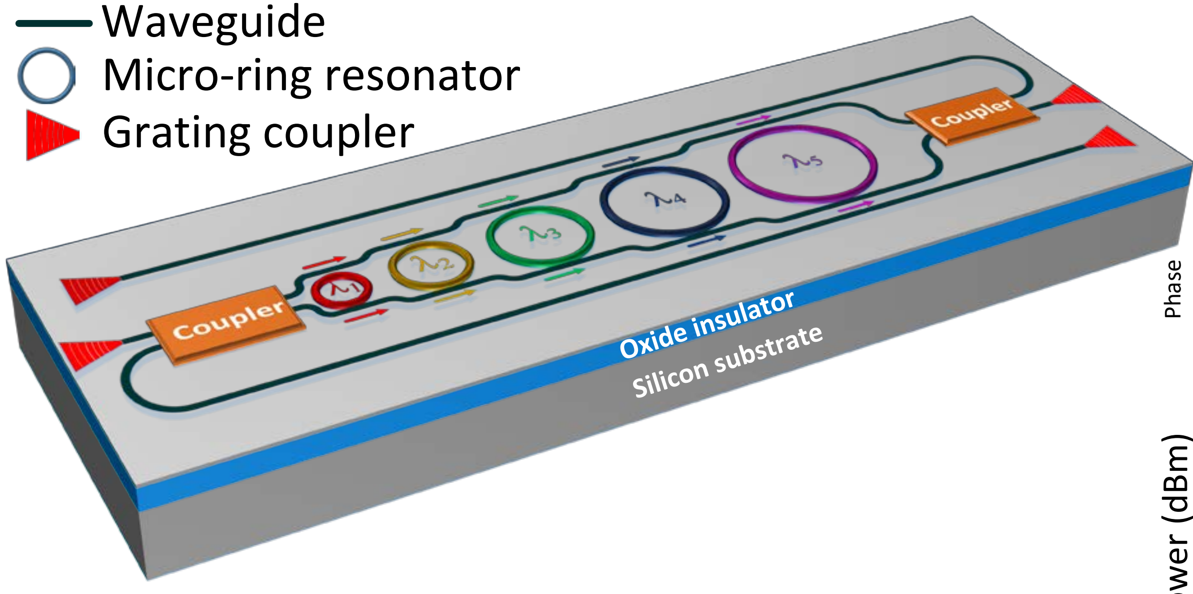

Perspective view of the proposed multi-channel fractional-order temporal differentiator.

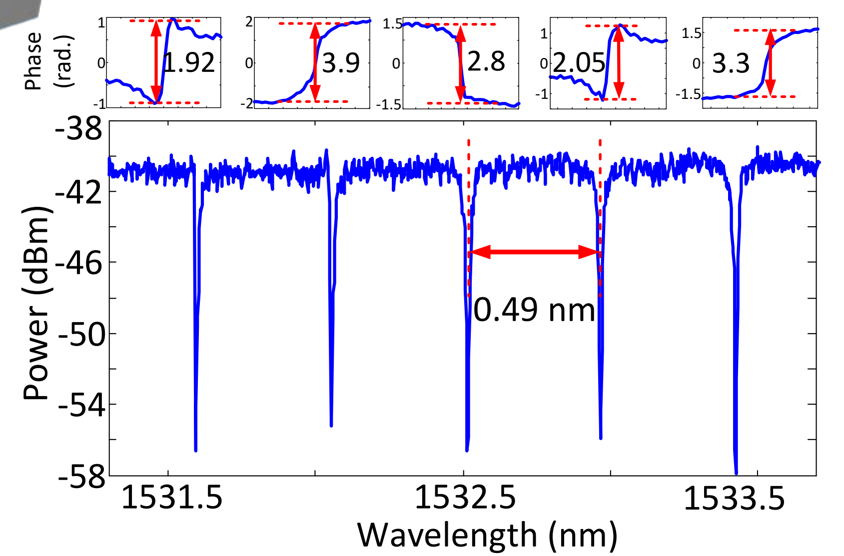

Measured spectral response of the five-channel fractional-order temporal differentiator; Inset: measured phase response of the five-channel fractional-order temporal differentiator.

Applications: phase modulation to intensity modulation conversion in a WDM optical phase-modulated system.

W. Zhang, and J. P. Yao, *IEEE/OSA J. Lightw. Technol.*, vol. 33, no. 2, pp. 361-367, Jan. 2015.

Experimental Results

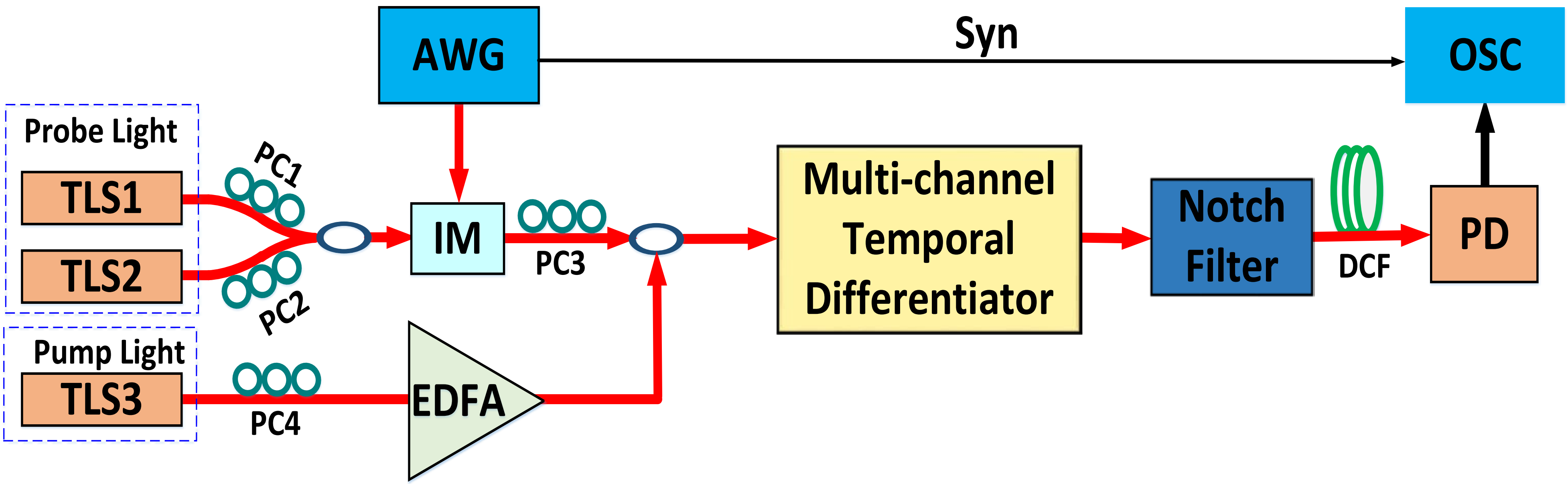

Experimental setup. TLS: tunable laser source. IM: Intensity modulator; AWG: arbitrary waveform generator. EDFA: erbium-doped fiber amplifier. PC: polarization controller. PD: photodetector. OSC: oscilloscope. DCF: dispersion compensating fiber.

Experimental Results - differentiated output pulses

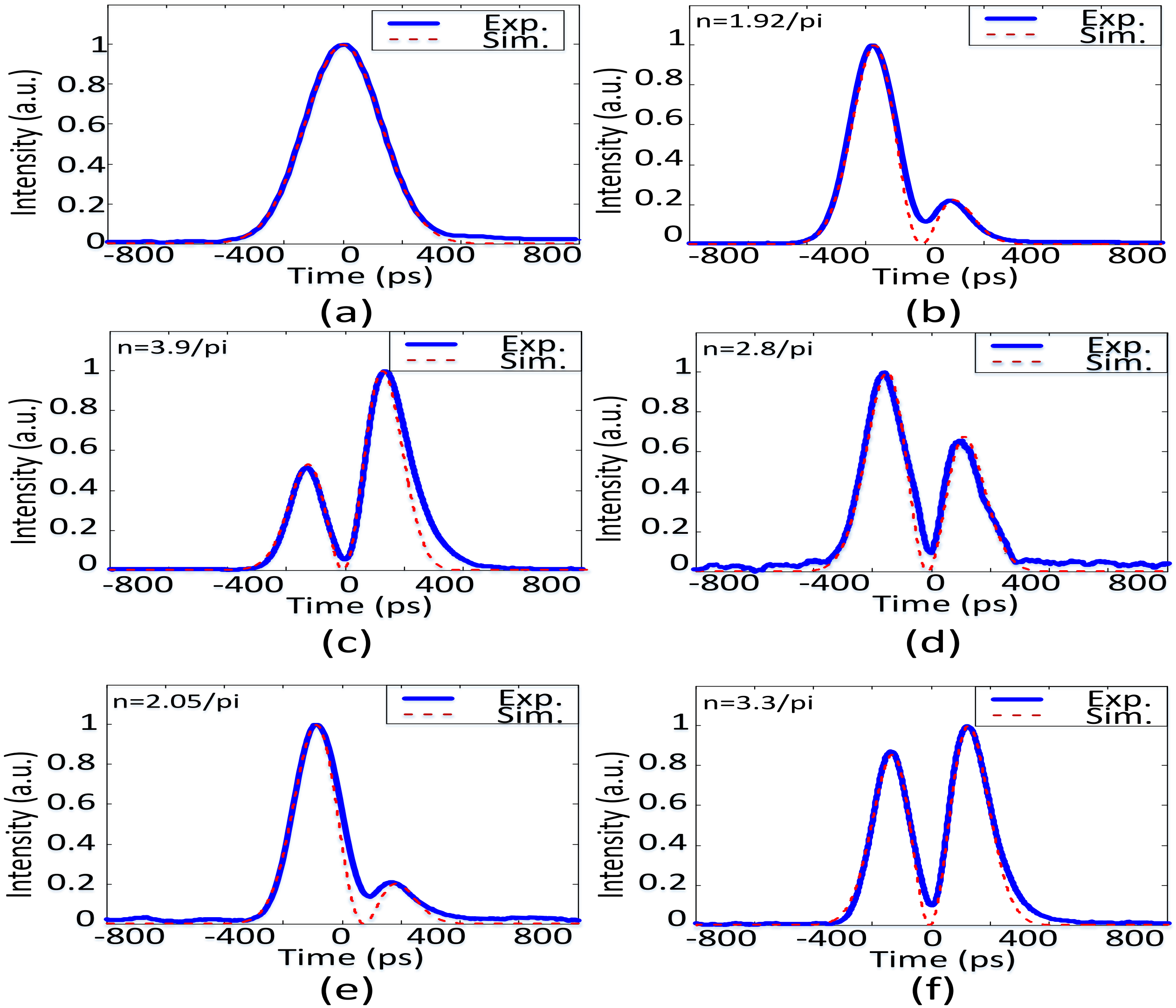

Experimental results. (a) The measured Gaussian pulse from AWG (the blue solid line) and the simulated Gaussian pulse (the red dotted line); and measured differentiated output pulses from the photonic fractional differentiator at the (b) 1^{st}, (c) 2^{nd}, (d) 3^{rd}, (e) 4^{th}, and (f) 5^{th} channel.

Experimental Results - differentiation order tuning

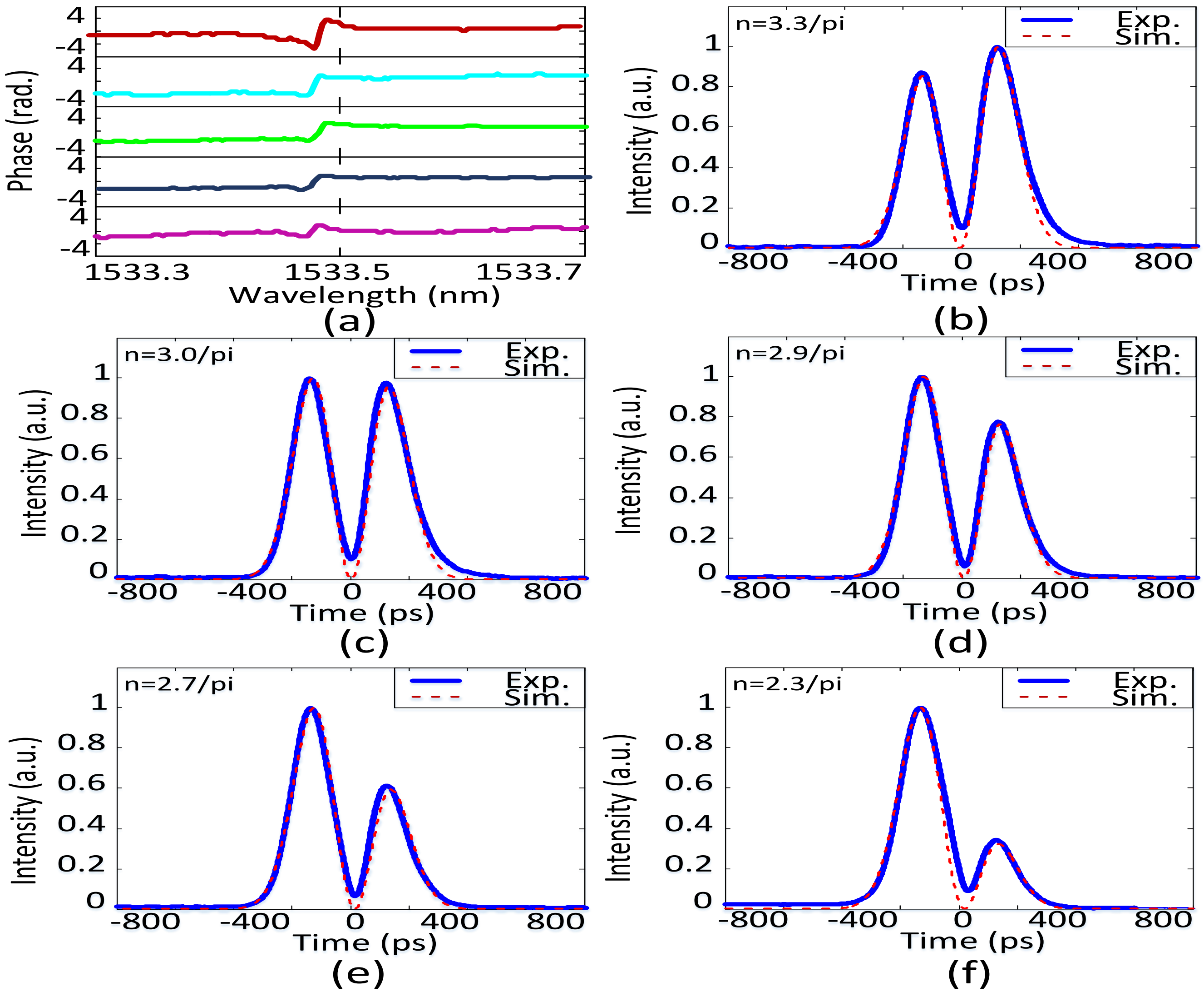

Experimental results for differentiation order tuning: (a) Measured phase response of the **second channel** with the power of the pumping light increased, and the measured differentiated output pulses from the differentiator at the **fifth channel** with the pumping power at (b) 0 dBm, (c) 21.7 dBm, (d) 25 dBm, (e) 28.7 dBm, and (f) 31 dBm.

Experimental Results - independent tunability

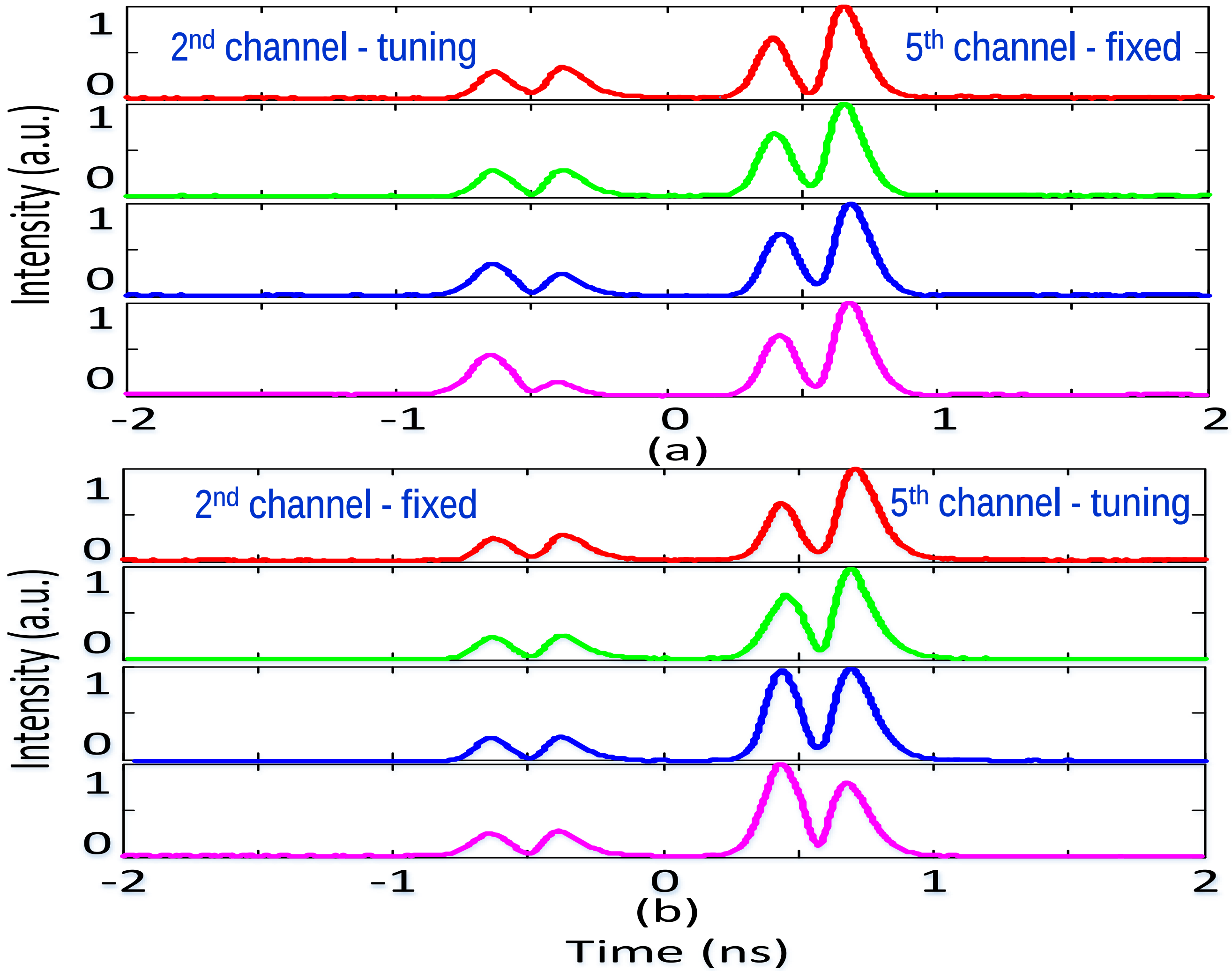

Experimental results for independent tunability. Measured differentiated output pulses from the differentiator at the **second** and the **fifth** channels with the pumping light wavelength at (a) 1537.498 nm corresponding a resonant wavelength of the fifth channel, and (b) 1535.920 nm corresponding a resonant wavelength of the second channel.

Letter Vol. 40, No. 13 / July 1 2015 / Optics Letters 3153

Optics Letters

Silicon-based on-chip electrically tunable sidewall Bragg grating Fabry–Perot filter

WEIFENG ZHANG, NASRIN EHTESHAMI, WEILIN LIU, AND JIANPING YAO*

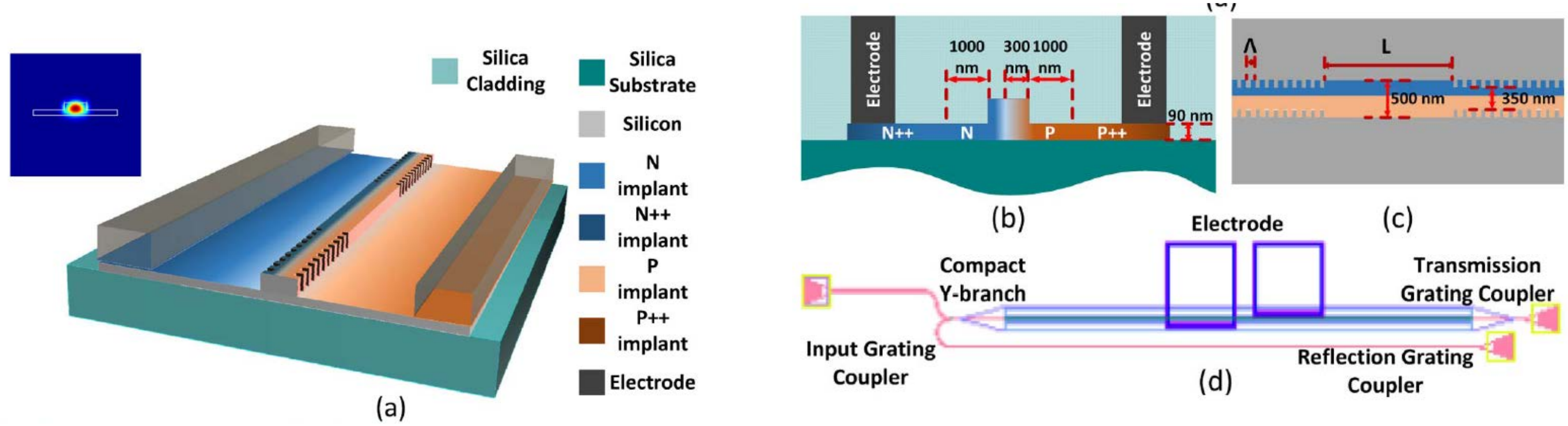

W. Zhang, N. Ehteshami, W. Liu, and J. Yao, “Silicon-based on-chip electrically tunable sidewall Bragg grating Fabry–Perot filter,” Opt. Lett., vol. 40, no. 13, pp. 3153–3156, Jun. 2015.

Silicon-based on-chip electrically tunable sidewall Bragg grating Fabry–Perot filter

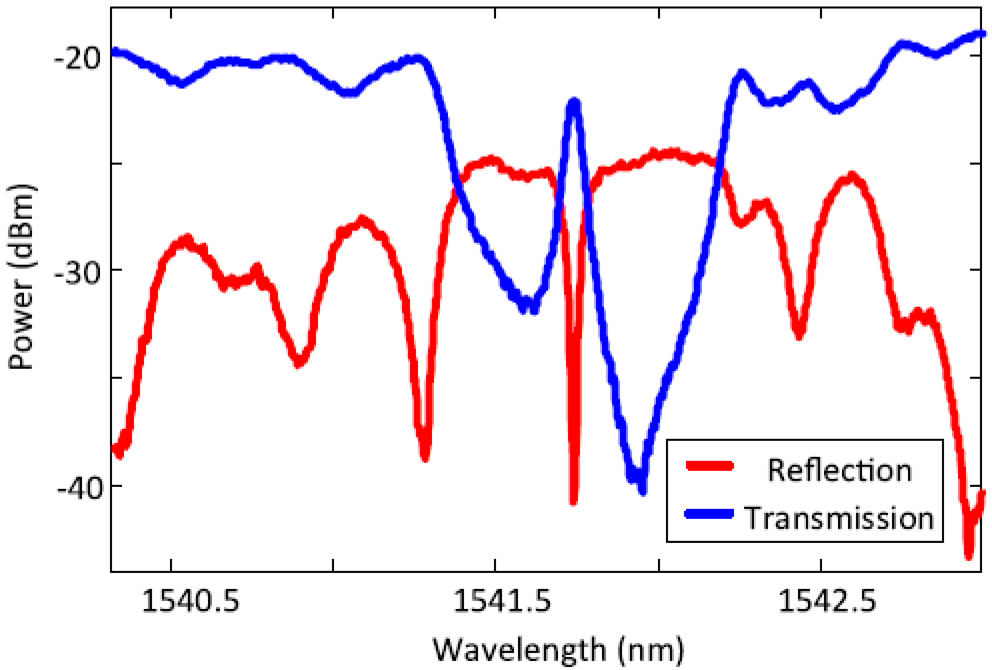

Fig. 2. Measured reflection and transmission spectra of the TBG-FPF with a zero bias voltage applied.

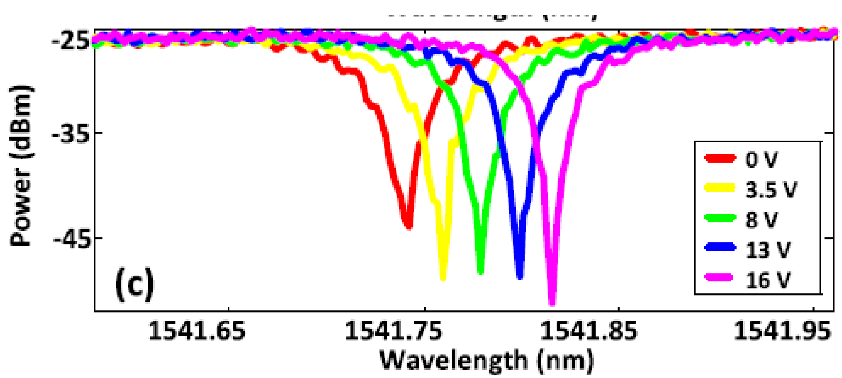

the PN junction is reverse biased. (d) Wavelength shift when the bias voltage is increasing.

Amoeba waveguide Bragg grating

Weifeng[1] Zhang and Jianping Yao[1*]

Microwave Photonic Research Laboratory, School of Electrical Engineering and Computer

University of Ottawa, 25 Templeton Street, Ottawa, Ontario, Canada K1N 6N5

*email: jpyao@eecs.uottawa.ca

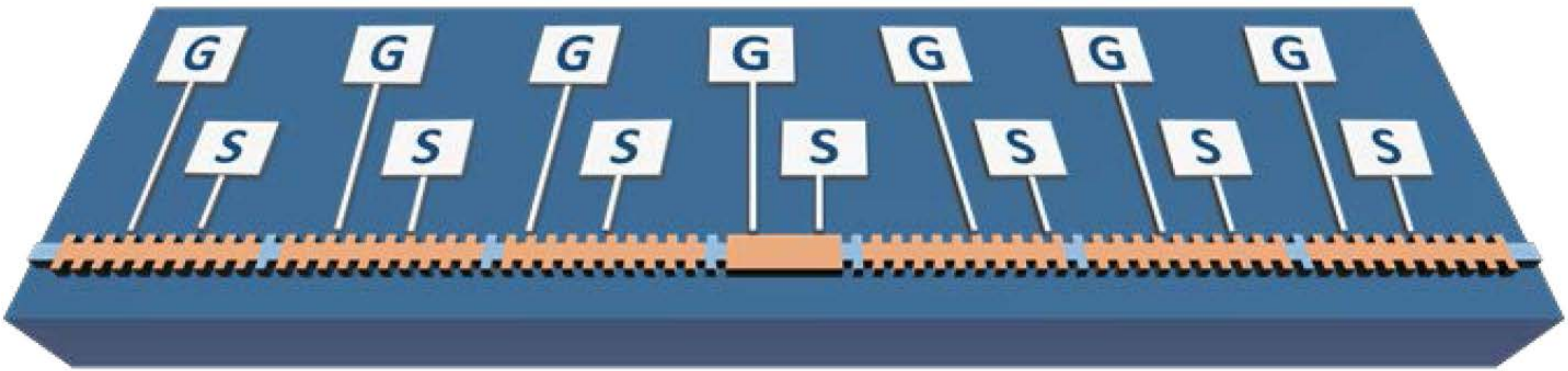

Figure 1. Perspective view. An ultrafast and fully reconfigurable amoeba waveguide Bragg grating in an SOI platform.

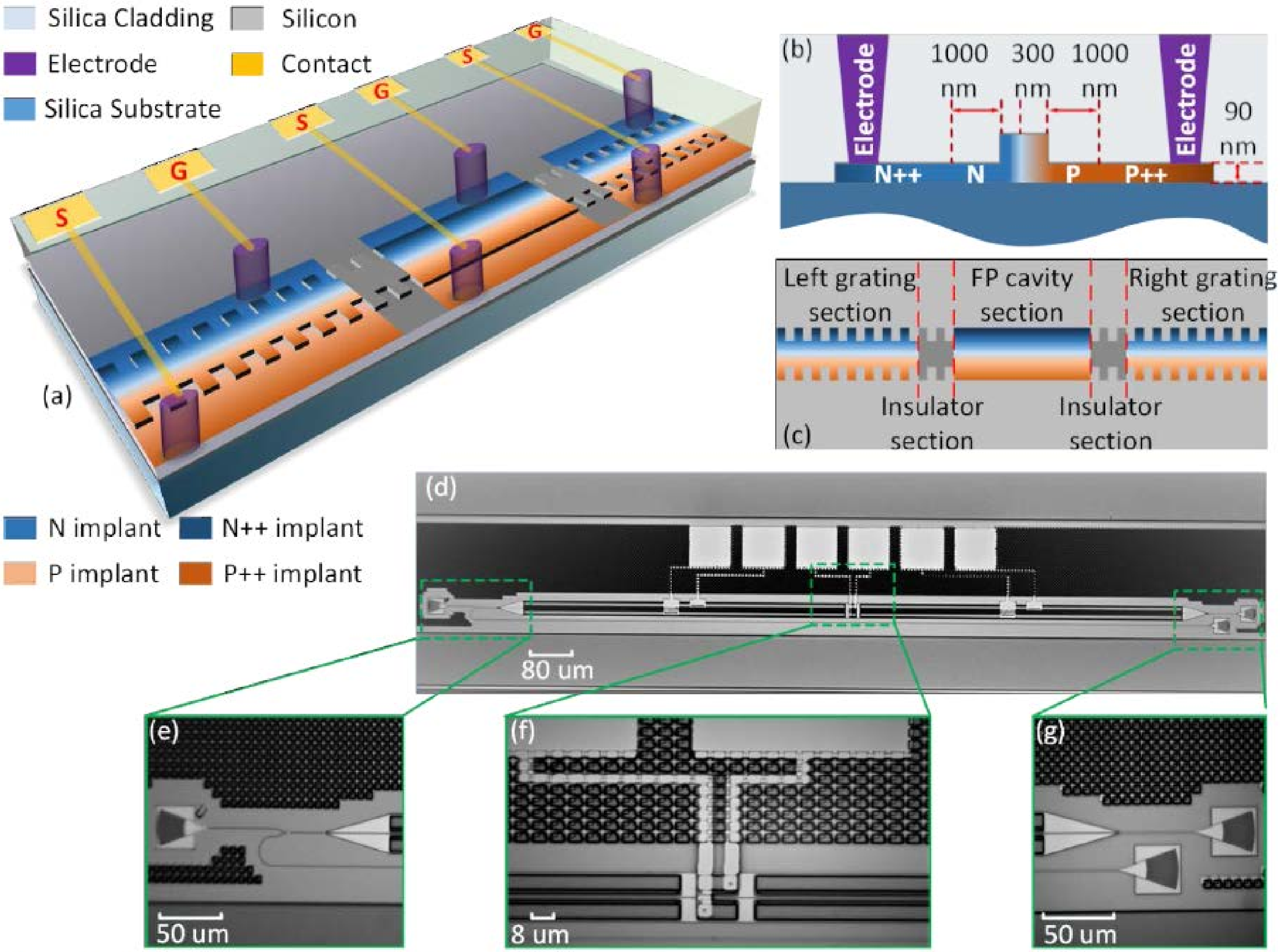

Figure 2. The schematics of the designed amoeba grating. (a) Perspective view of an amoeba grating on a silicon chip; (b) cross-sectional view of the rib waveguide of the amoeba grating; (c) top-view of an amoeba grating; (d) image of the fabricated grating; zoom-in view of (e) the input grating coupler and compact Y-branch, (f) the FP cavity section and (g) the transmission and reflection grating couplers.

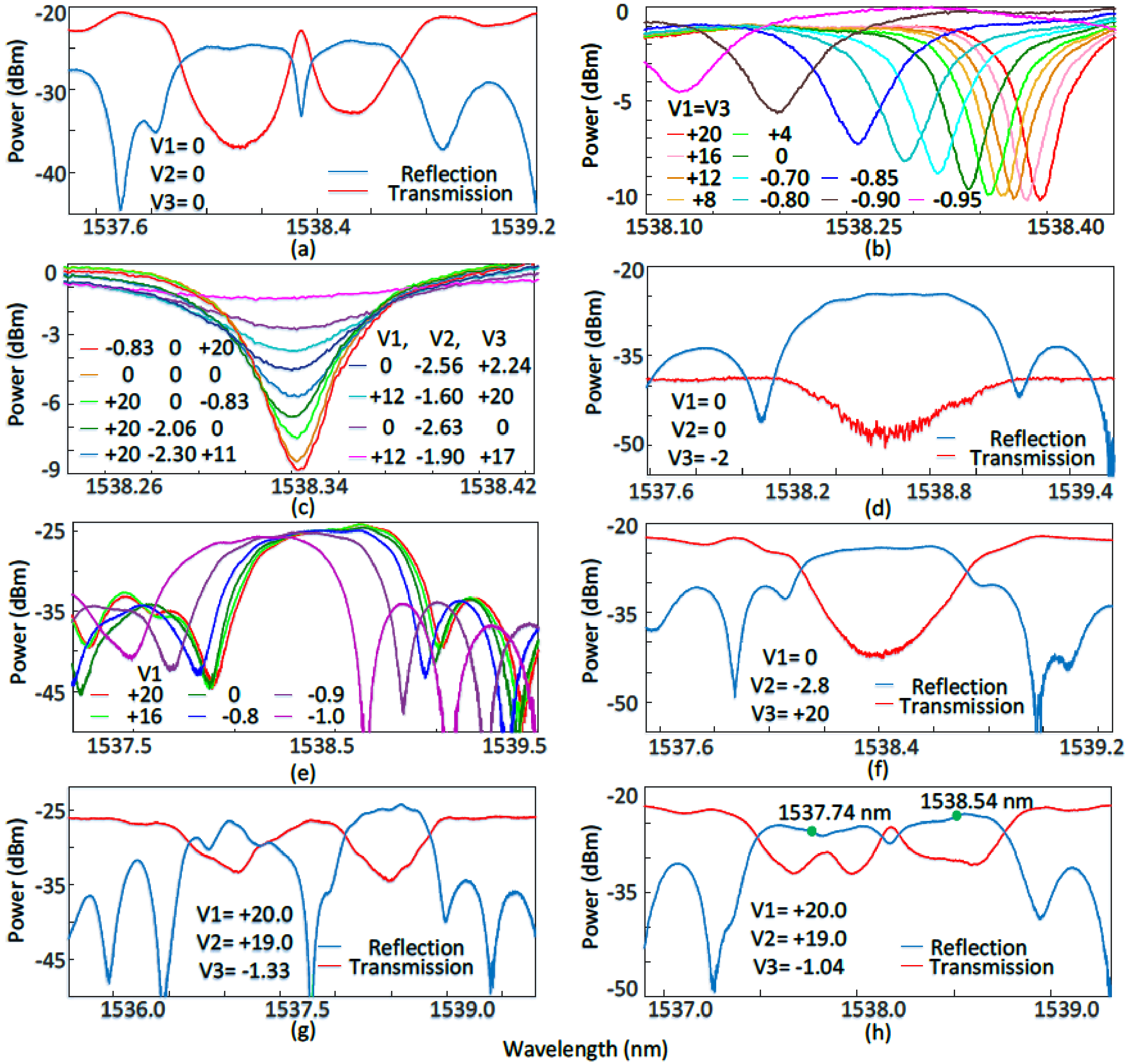

Figure 3 Measured reflection and transmission spectrums.

(a) Reflection and transmission spectrum of the fabricated grating in the static state;
(b) notch wavelength shift when the bias voltages applied to the left and right sub-gratings vary synchronously;
(c) extinction ratio tuning while the notch wavelength is kept unchanged;
(d) reflection and transmission spectrums when the grating is reconfigured to be a uniform grating;
(e) wavelength tuning of the uniform grating;
(f) reflection and transmission spectrums when the device is reconfigured to be a uniform grating by increasing the cavity loss;
(g) reflection and transmission spectrums when the device is reconfigured to be two independent uniform sub-gratings; and
(h) reflection and transmission spectrums when the device is reconfigured to be a chirped grating.

A Silicon Photonic Integrated Frequency-Tunable Microwave Photonic Bandpass Filter

Weifeng Zhang and Jianping Yao
Microwave Photonics Research Laboratory
School of Electrical Engineering and Computer Science, University of Ottawa
Ottawa, ON K1N 6N5, Canada
jpyao@eecs.uottawa.ca

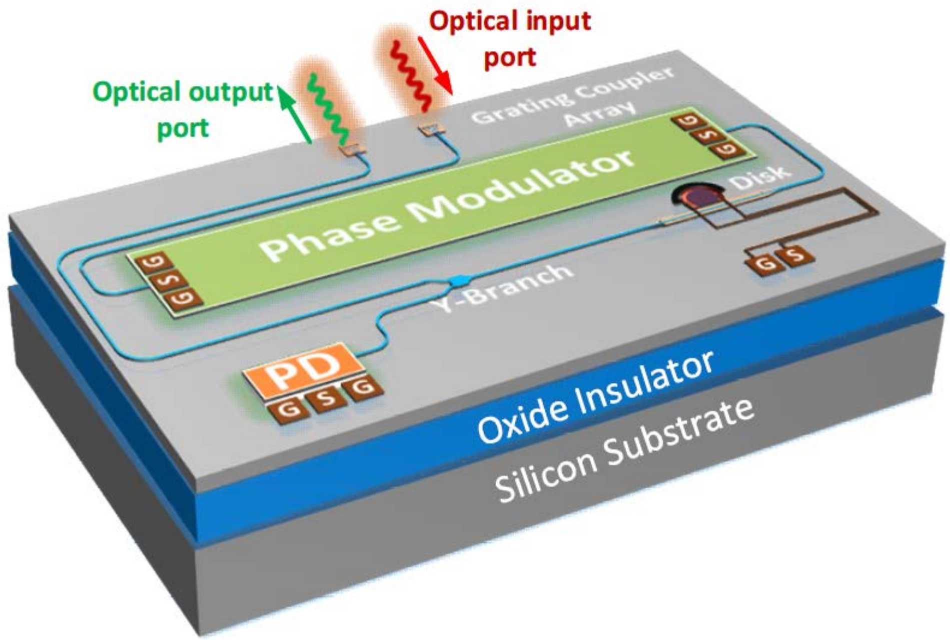

Fig. 1. Perspective view of the proposed IMPF on a silicon photonic chip

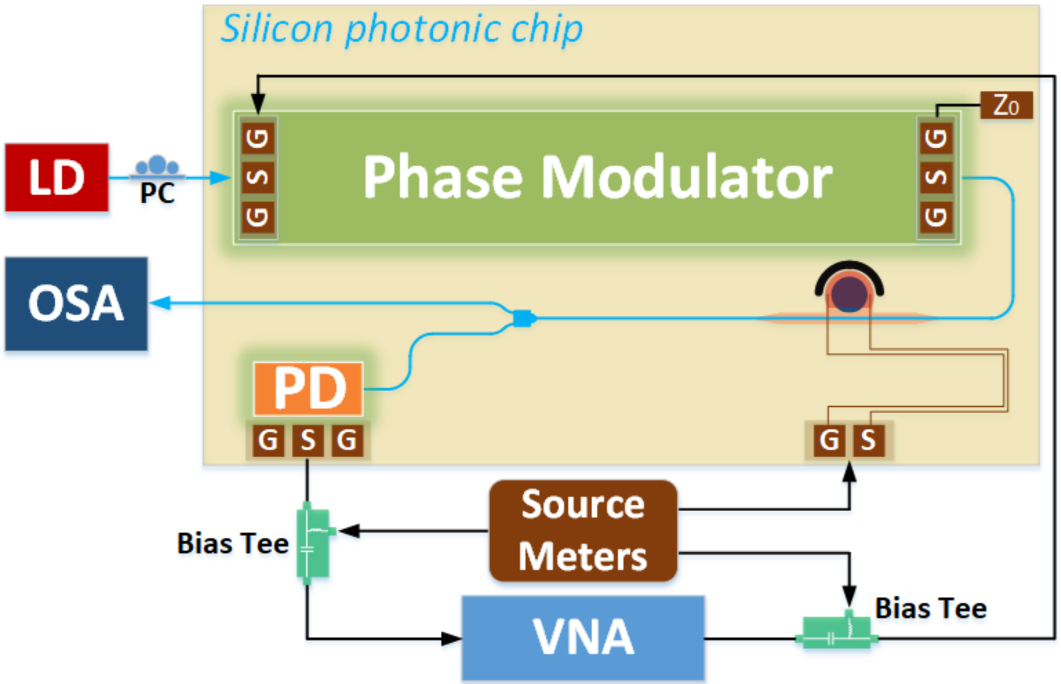

Experimental set-up

To be presented at MWP2017, Beijing

Frequency-tunable photonic microwave filter — Principle

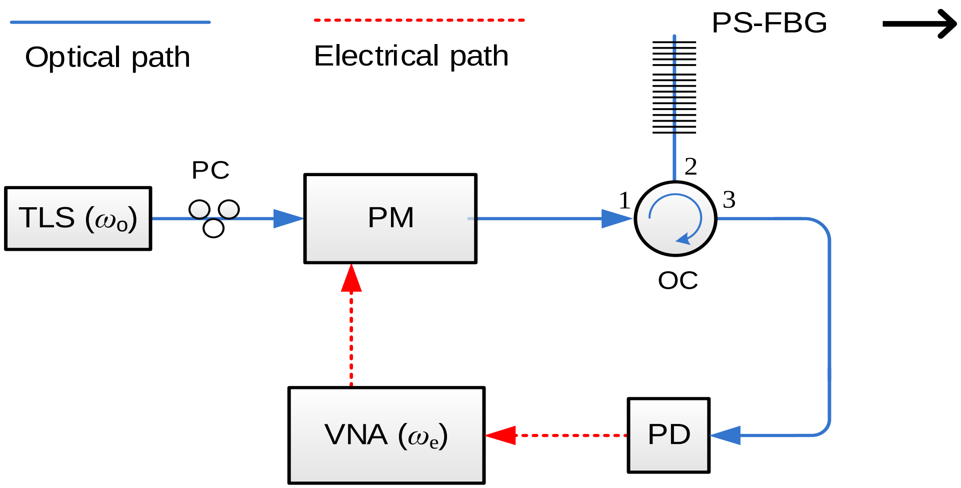

Phase modulation to intensity modulation conversion

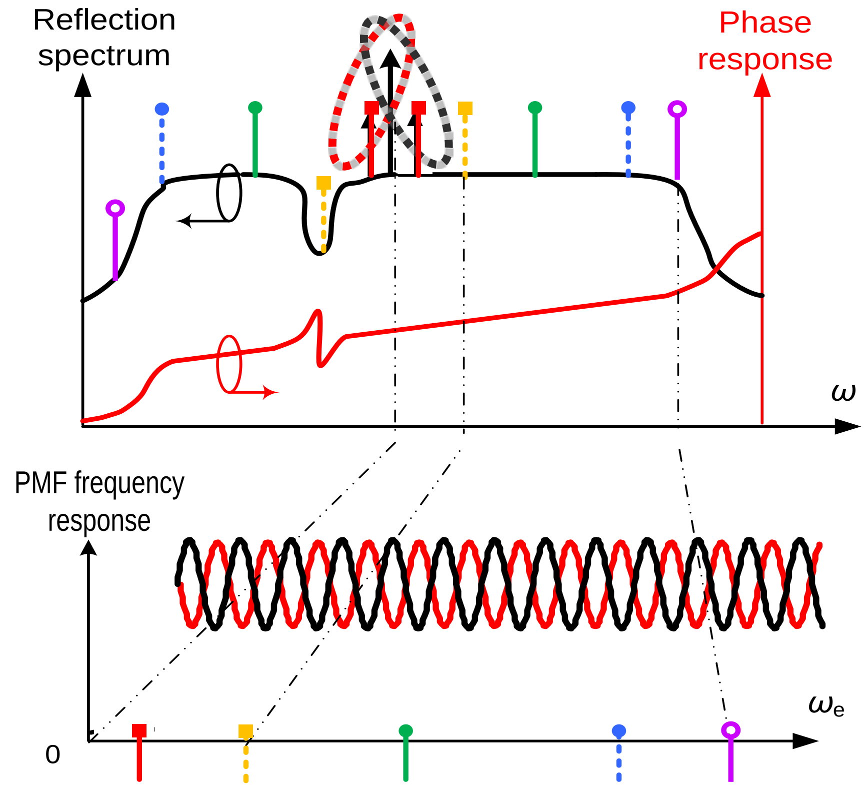

- **Central frequency of the PMF ← the wavelength of the TLS;**
- **Tuning range ← the reflection band of the PS-FBG;**
- **The 3-dB bandwidth of the PMF ←the transmission bandwidth of the PS-FBG**

W. Li, M. Li, and J. P. Yao, *IEEE Trans. Microw. Theory Tech.*, 60(5) 1287, 2012.

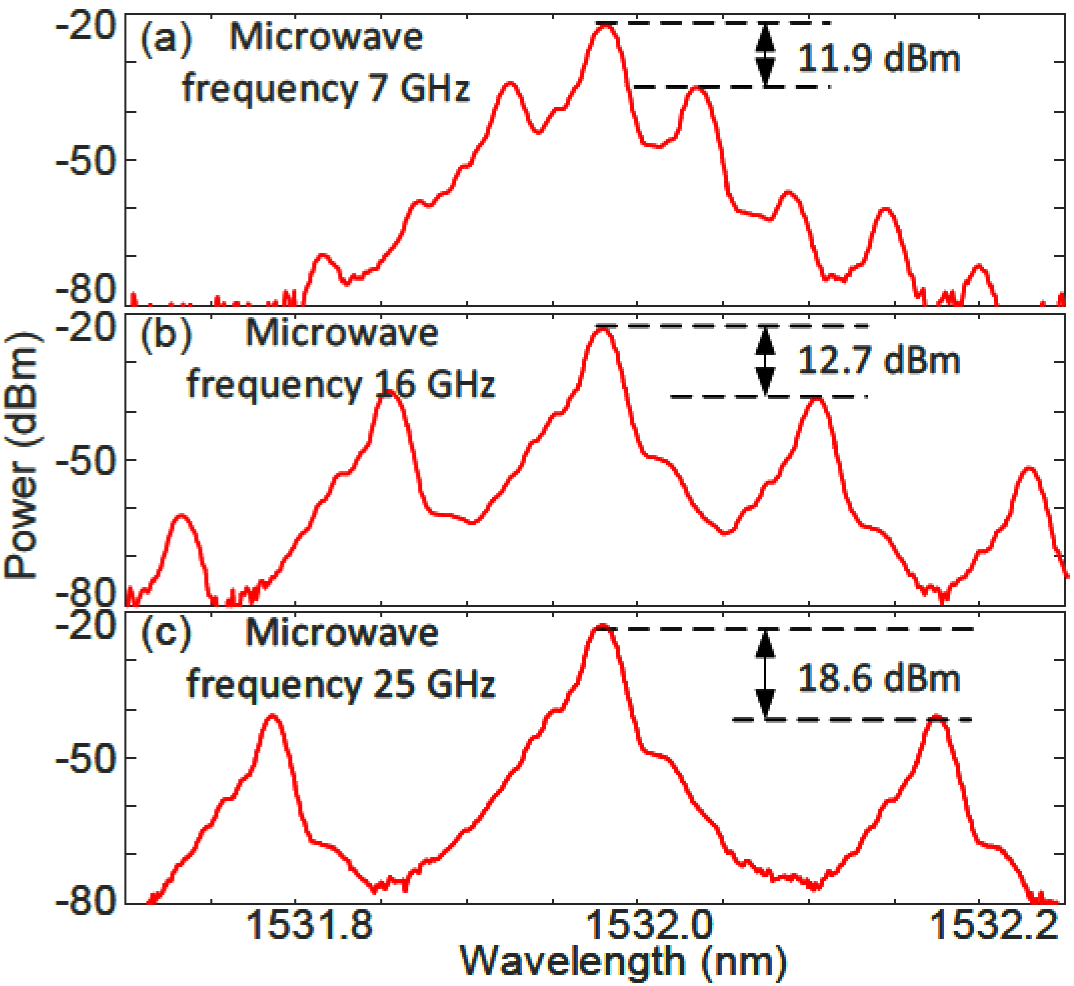

Fig. 3 Optical spectrums of the modulated optical signal using the on-chip high-speed PM when the microwave signal applied to the PM has a frequency of (a) 7, (b) 16 and (c) 25 GHz.

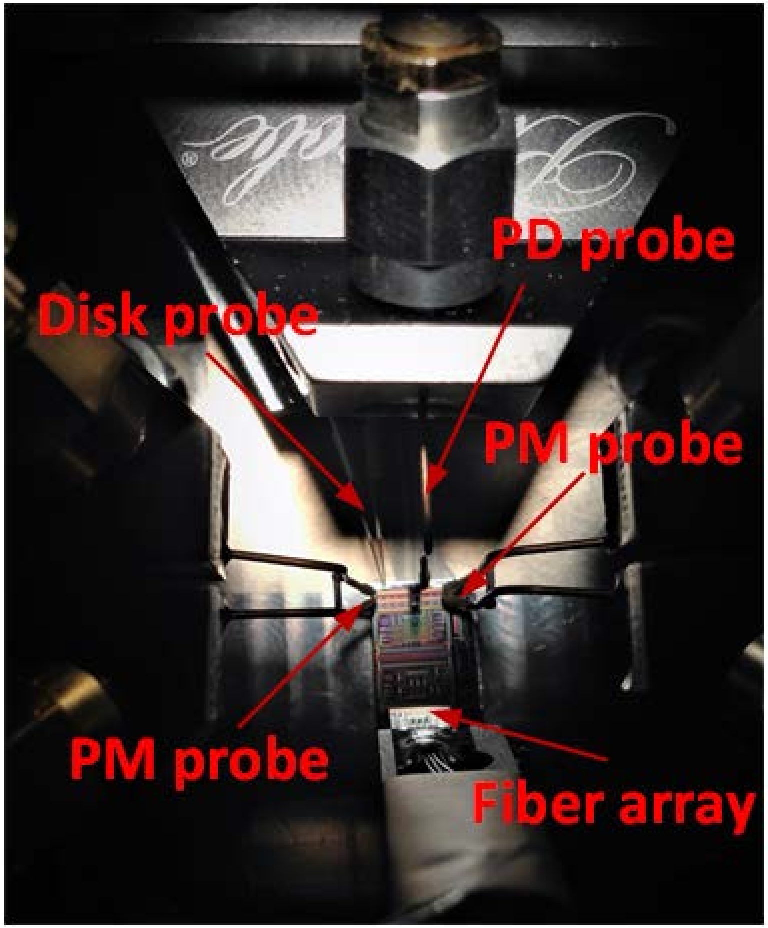

Image of the experimental set-up captured by a camera.

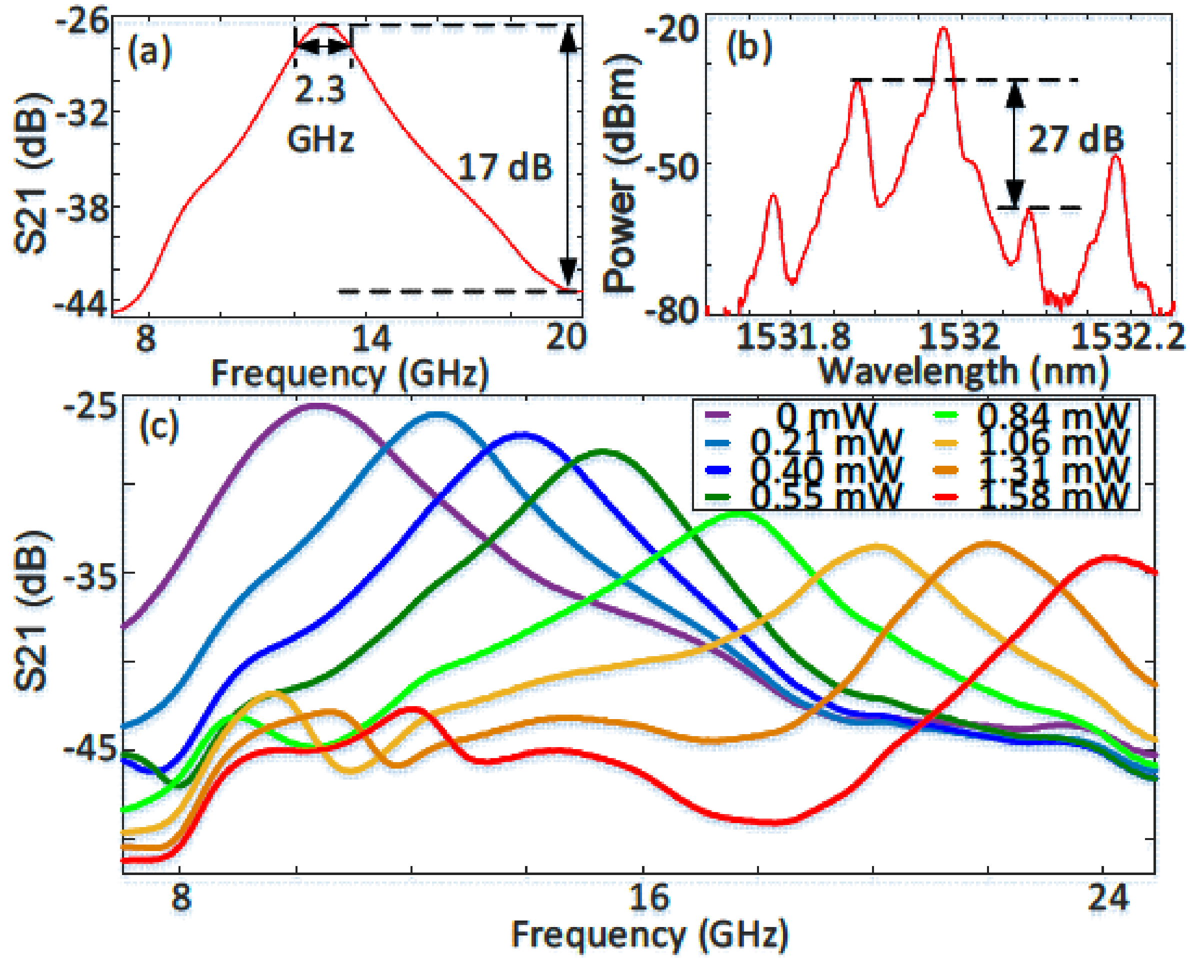

Fig. 7 Experimental result: (a) frequency response of the filter with a center frequency of 13 GHz; (b) optical spectrum of the modulated optical signal when the microwave signal frequency is 13 GHz; (c) measured frequency responses of the filter with the center frequency tuned from 7 to 25 GHz.

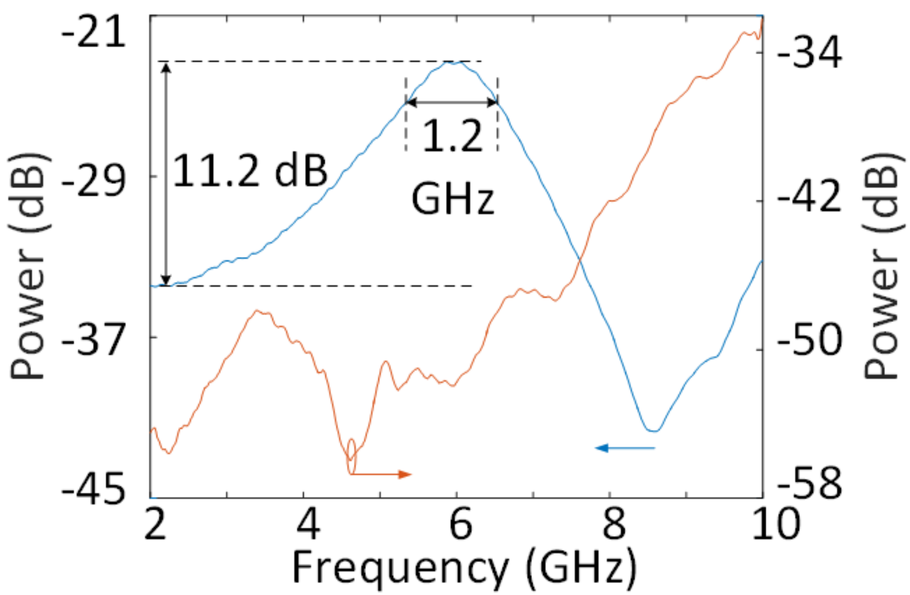

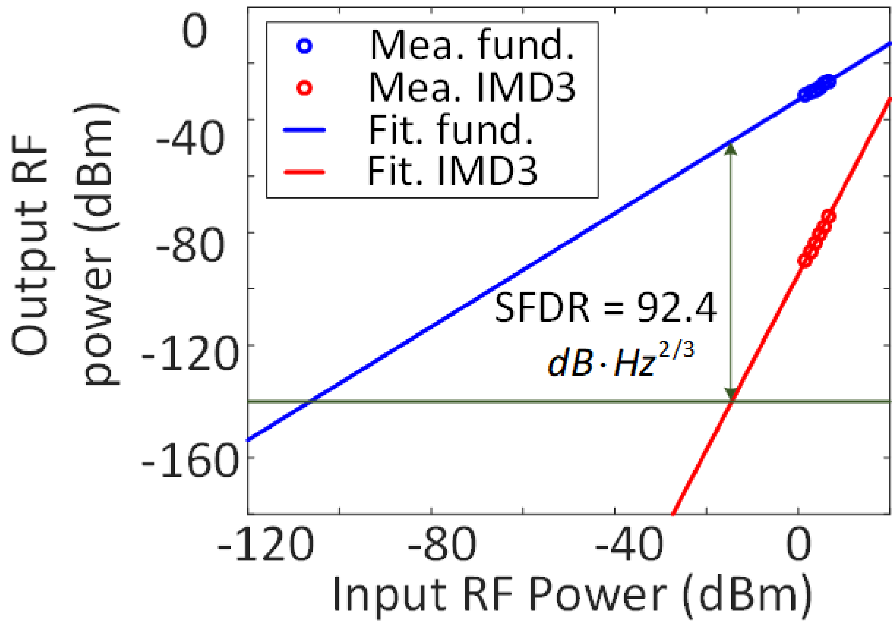

Frequency response of the filter (in blue) with a center frequency of 6 GHz and measured frequency response (in red) when no optical signal is coupled into the chip (to show the EMI)

Measurements of the fundamental signal power and that of the IMD3. Given a noise floor of -140 dBm/Hz, the measured spurious-free dynamic range (SFDR) of the filter are 92.4 dB·$Hz^{2/3}$.

Outline

- Introduction to Microwave Photonics (MWP)
- SiP-based MWP systems
  - Photonic generation of microwave waveforms
  - Photonic processing of microwave signals
  - A fully SiP integrated MWP filter
- InP-based signal processing
  - **A fully reconfigurable photonic signal processor**
  - A fully InP integrated MWP filter
- SiN-based MWP systems
  - True time delay beamforming
  - Reconfigurable signal processor
- Conclusion

ARTICLES
PUBLISHED ONLINE: 15 FEBRUARY 2016 | DOI: 10.1038/NPHOTON.2015.281
nature photonics

A fully reconfigurable photonic integrated signal processor

Weilin Liu[1‡], Ming Li[1†‡], Robert S. Guzzon[2‡], Erik J. Norberg[2], John S. Parker[2], Mingzhi Lu[2], Larry A. Coldren[2] and Jianping Yao[1*]

The signal processor can be reconfigured to operate as a

- Temporal integrator
- Temporal differentiator
- Hilbert transformer
- Microwave generator

Temporal Integrator

Data storage

Bit counting

Optical memory

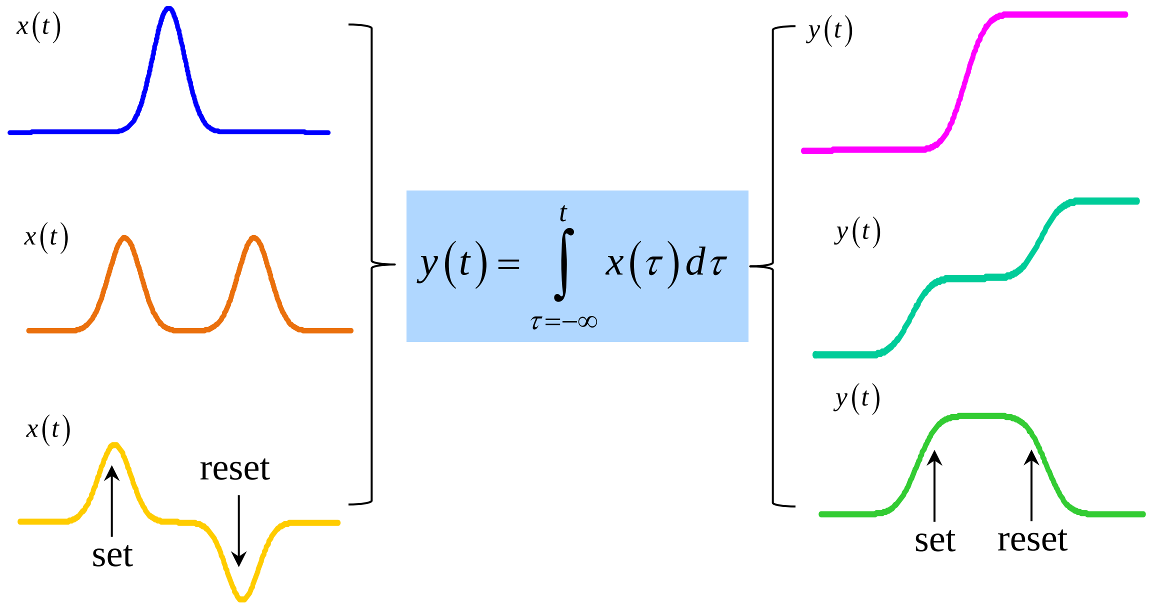

Optical computing
(Linear Differential Equation)

$$\frac{dy(t)}{dt} + ky(t) = x(t)$$

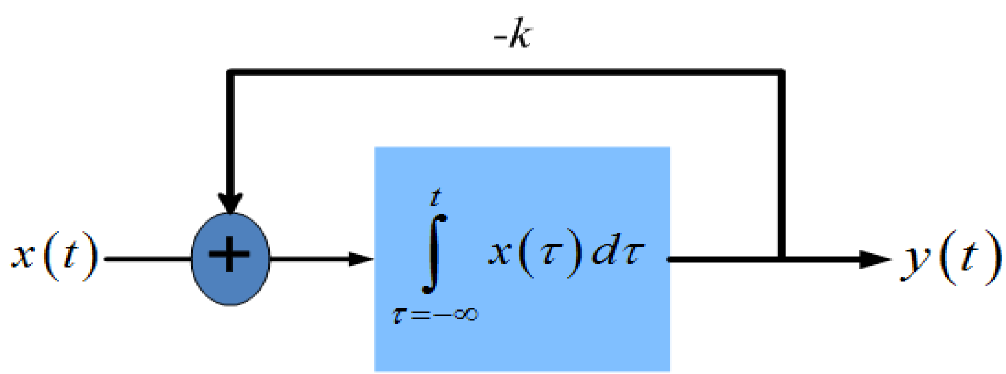

M. Ferrera, Y. Park, L. Razzari, B. E. Little, S. T. Chu, R. Morandotti, D. J. Moss, and J. Azaña, "On-chip CMOS-compatible all-optical integrator," Nature Commun., vol. 1, 2010, Article 29.

Photonic implementation of a temporal integrator

Mathematically, a temporal integrator can be implemented using a linear filtering device with a transfer function given by

$$H(\omega) = \frac{1}{j(\omega - \omega_0)}$$

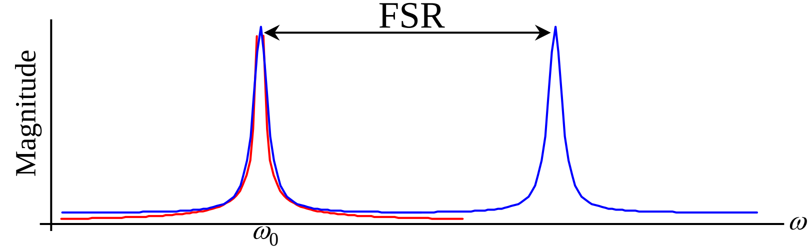

A photonic temporal integrator can be implemented using a fiber Bragg grating (FBG) or a microring resonator.

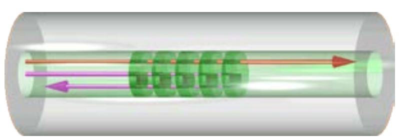

Apodized uniform FBG

Reflection Spectra

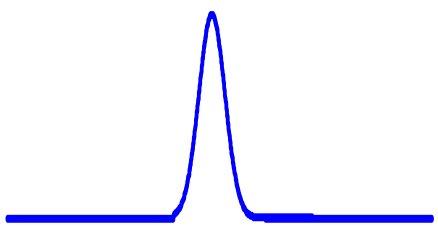

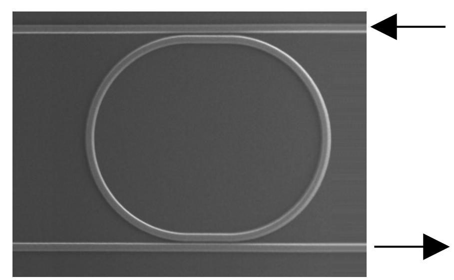

Micro-ring resonator

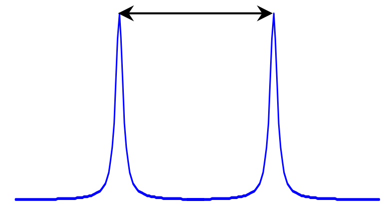

Temporal Differentiator

$$y(t)=\frac{d^n x(t)}{dt^n}$$

$$H(\omega)=\left[j(\omega-\omega_0)\right]^n=\begin{cases} e^{jn\frac{\pi}{2}}\left|\omega-\omega_0\right|^n & \omega>\omega_0 \\ e^{-jn\frac{\pi}{2}}\left|\omega-\omega_0\right|^n & \omega<\omega_0 \end{cases}$$

where n is the order of differentiation, and n can be a fractional order. When n=1, it is the first order differentiation.

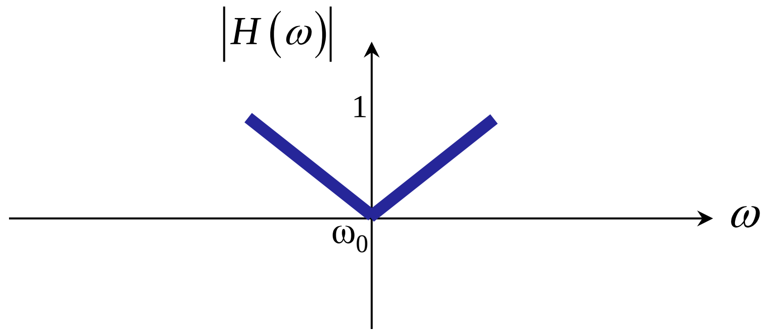

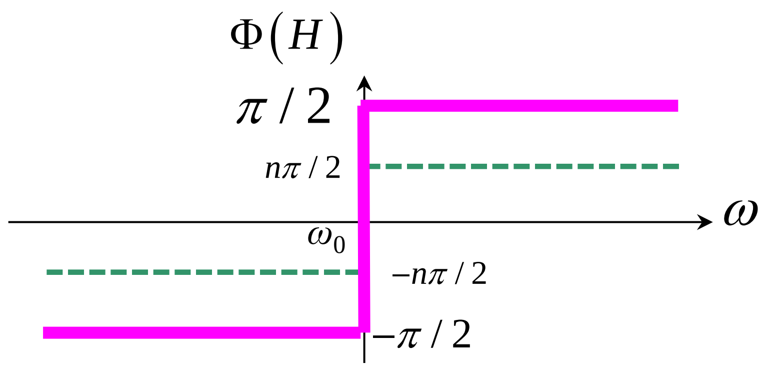

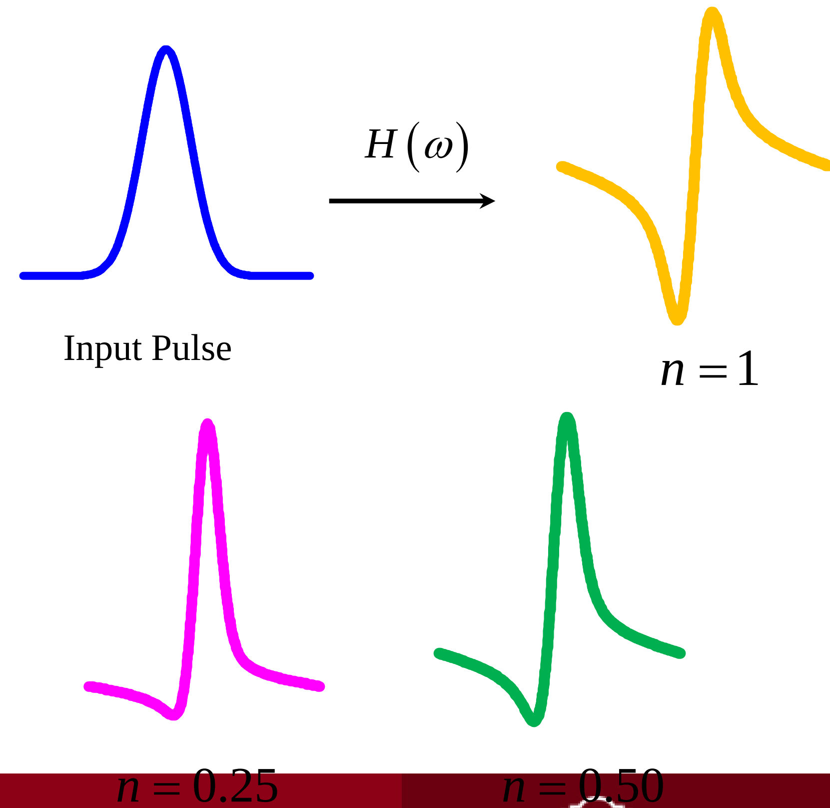

Temporal Differentiator

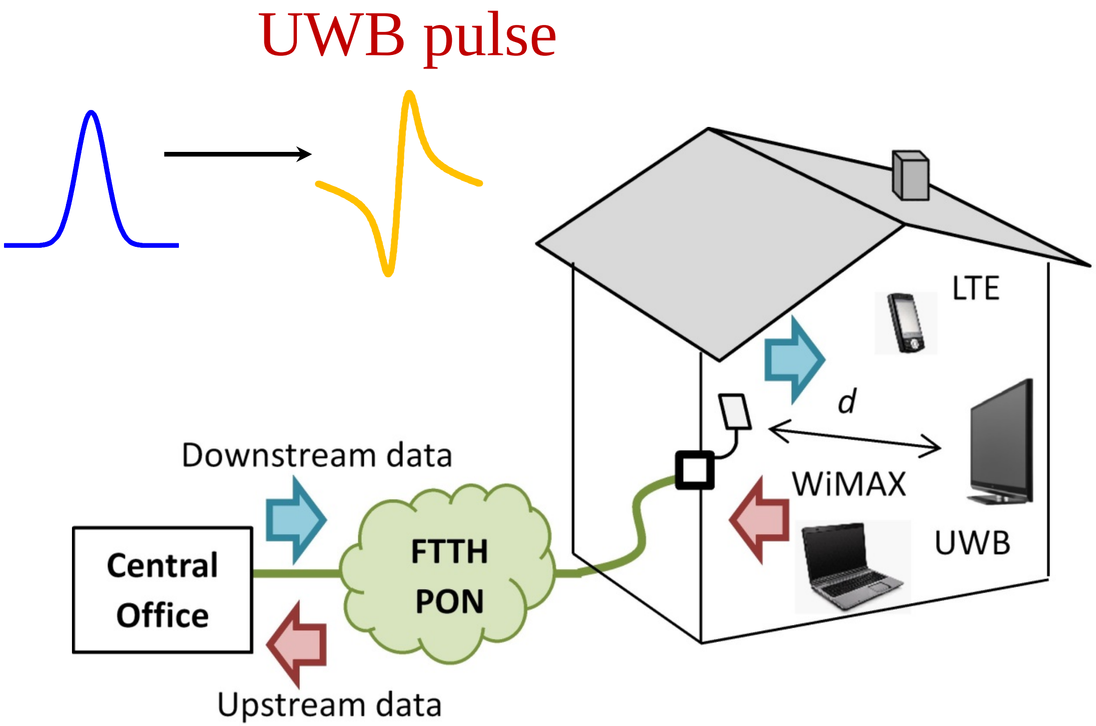

UWB pulse generation for wireless access

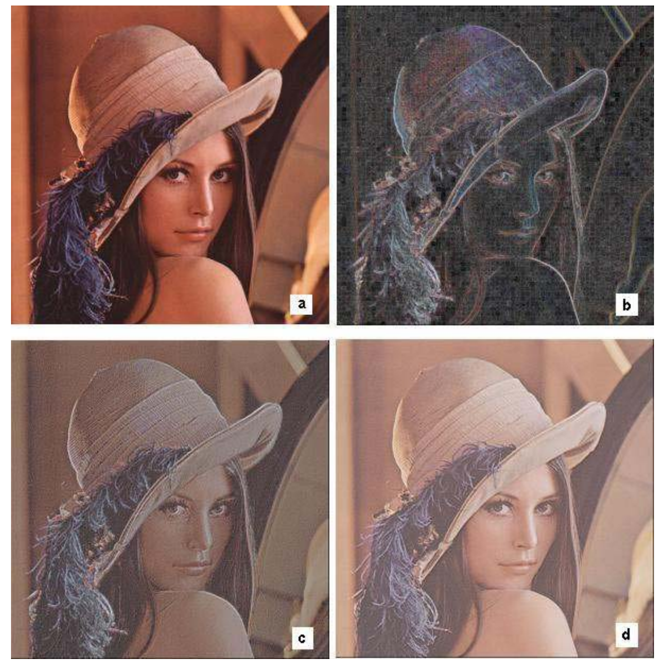

Tunable Image Enhancement

A. C. Sparavigna, "Fractional differentiation based image processing," arXiv.

Implementation of a Photonic Temporal Differentiator

Practically, a temporal differentiator can be implemented using an optical interferometer, such as a Michelson interferometer, a Mach-Zehnder interferometer (MZI).

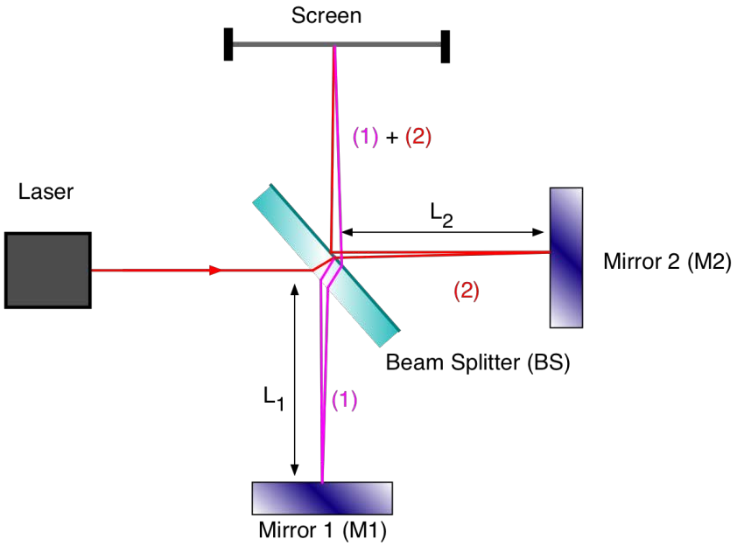

Michelson Interferometer

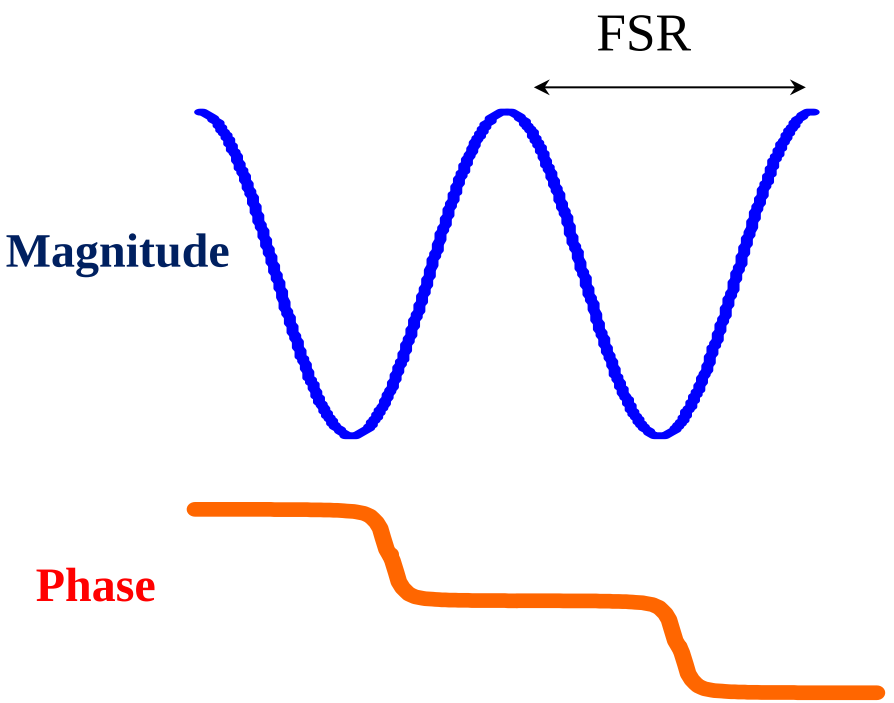

Hilbert Transformer

$$H^{(1)}(\omega)=\begin{cases} e^{j\frac{\pi}{2}} & \omega>0 \\ 0 & \omega=0 \\ e^{-j\frac{\pi}{2}} & \omega<0 \end{cases}$$

where $\varphi = P\pi/2$, and P indicates the fractional order. When P = 1, it becomes the conventional Hilbert transform.

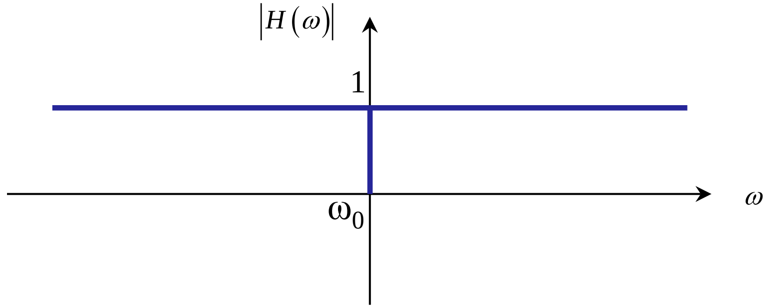

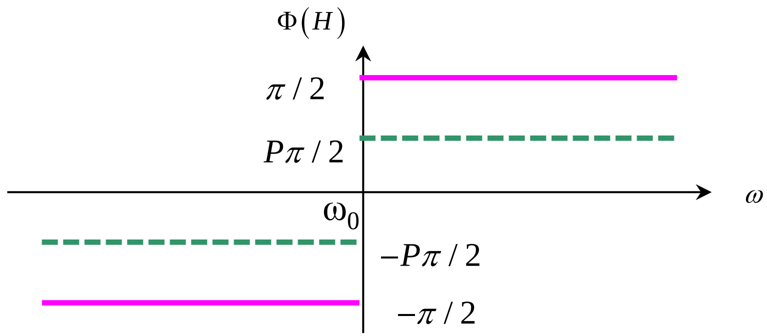

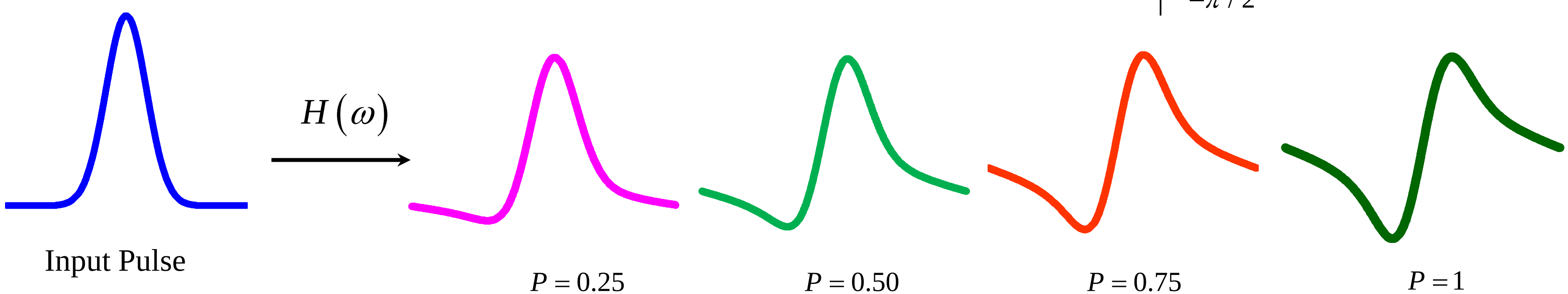

Temporal Hilbert Transformer

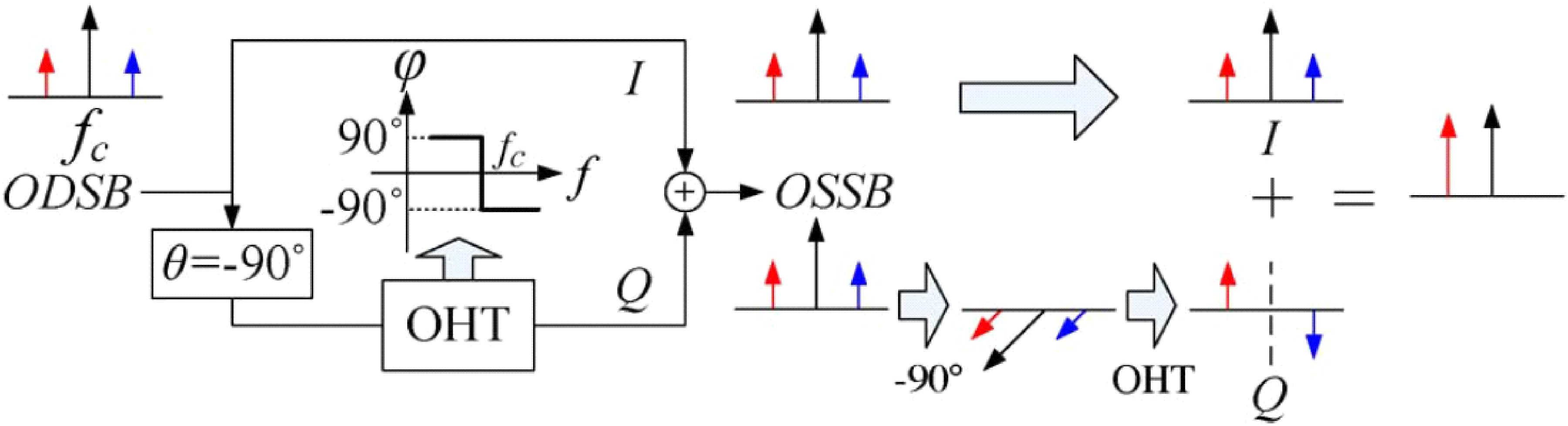

Single Sideband Modulation

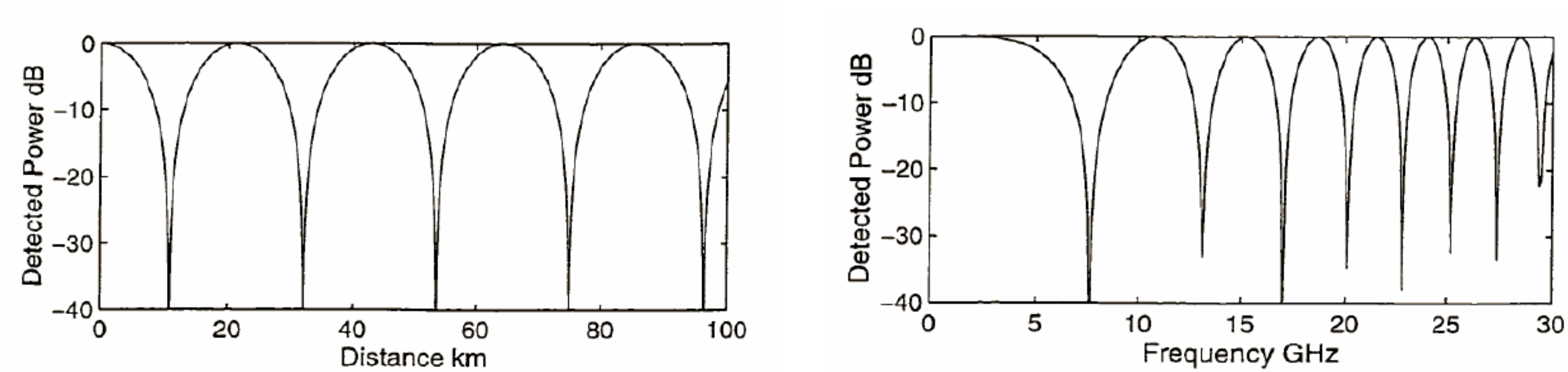

Power fading due to chromatic dispersion

S. L. Hahn, *Transforms and Applications Handbook*, A. D. Poularikas, Ed., 3rd ed. Boca Raton, FL: CRC Press, 2010, ch. 7.

Implementation of a Photonic Hilbert Transformer

Practically, a Hilbert transformer can be implemented using a linear filtering device with a narrow notch.

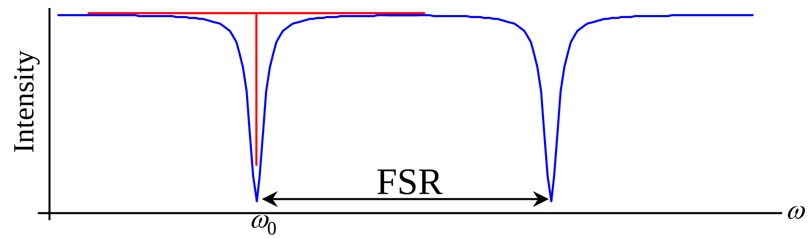

A photonic Hilbert transformer can be implemented using a phase shifted fiber Bragg grating (FBG) or a microring resonator.

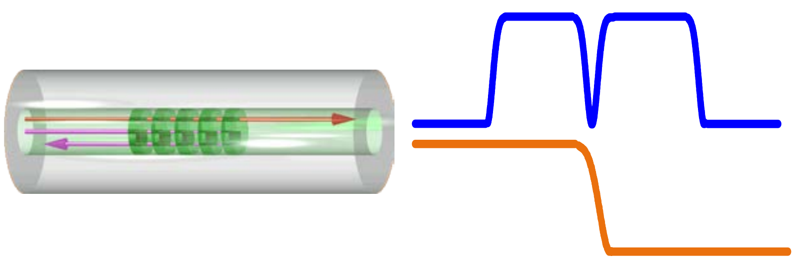

Reflection Spectra

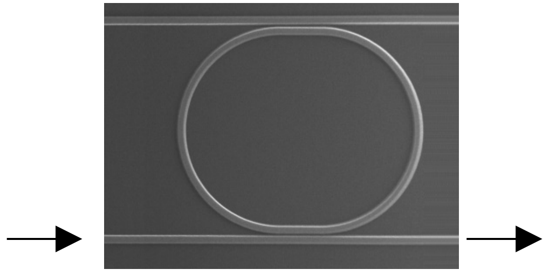

Phase Shifted FBG

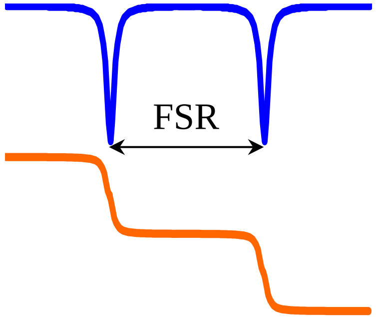

Micro-ring resonator

Reconfigurable Photonic Signal Processor - Configuration

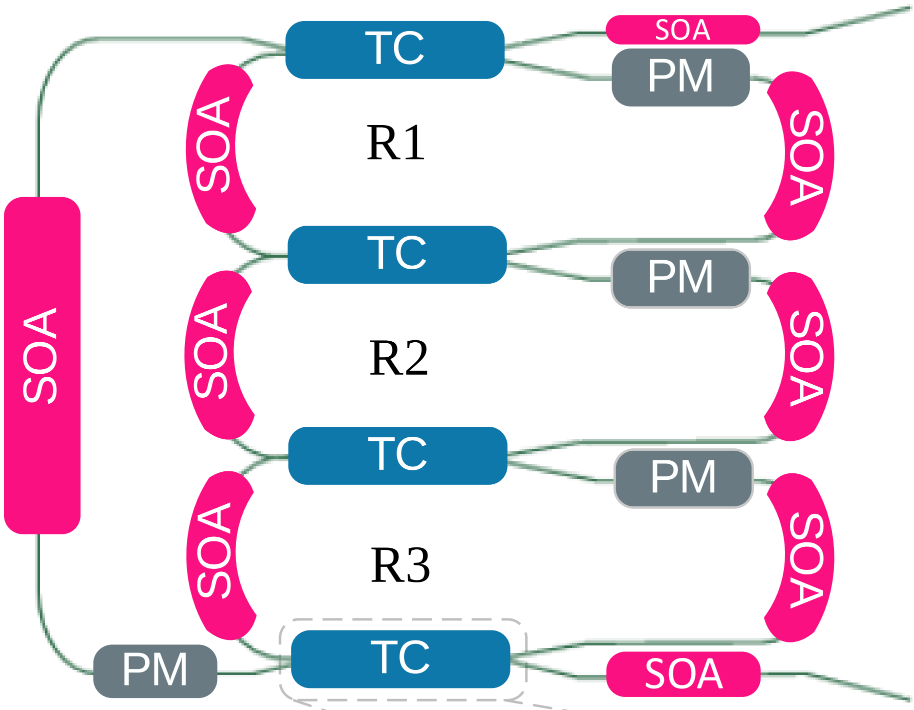

Reconfigurable - The reconfigurability is achieved by tuning the injection currents to the semiconductor optical amplifiers (9 **SOA**s) and current injection phase modulators (3 **PM**s) in the design.

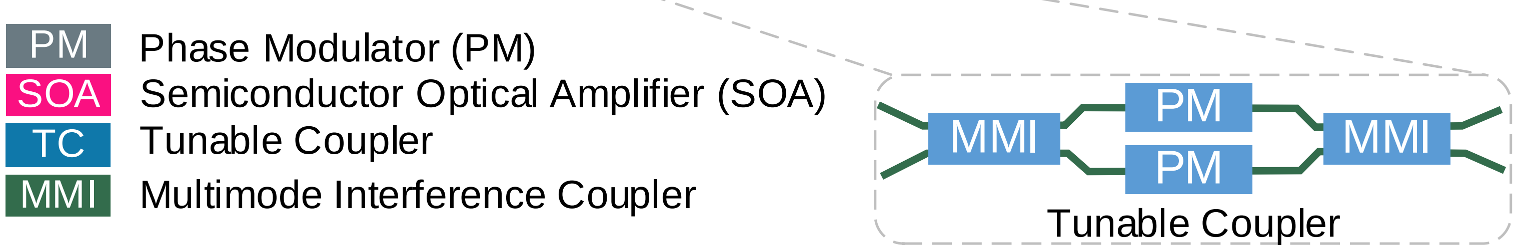

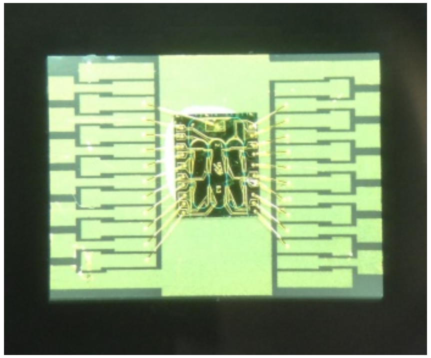

W. Liu, M. Li, R. S. Guzzon, E. J. Norberg, J. S. Parker, M. Lu, L. A. Coldren, and J. P. Yao, "A fully reconfigurable photonic integrated signal processor," *Nature Photon.*, vol. 10, no. 3, pp. 190-195, Mar. 2016.

Photonic Signal Processor - SEM images

Low loss deeply etched waveguide (1.7 cm^{-1})

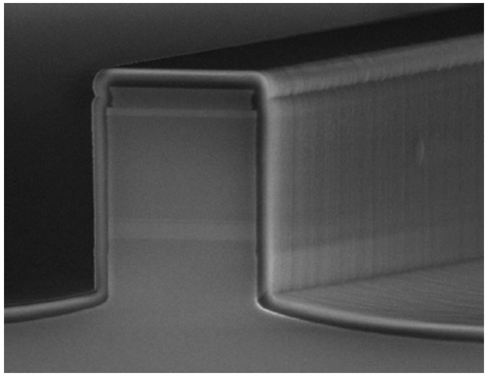

2×2 Multi-mode interference (MMI) coupler

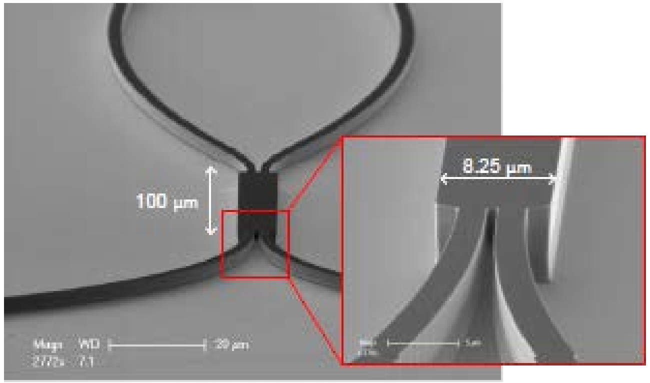

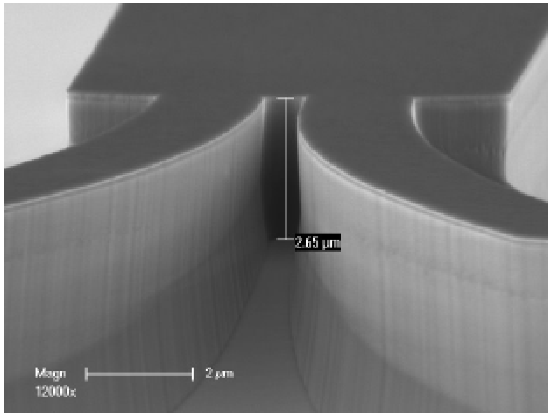

Transaction between an active and passive region (PM loss: 1.56 dB at 2π phase shift)

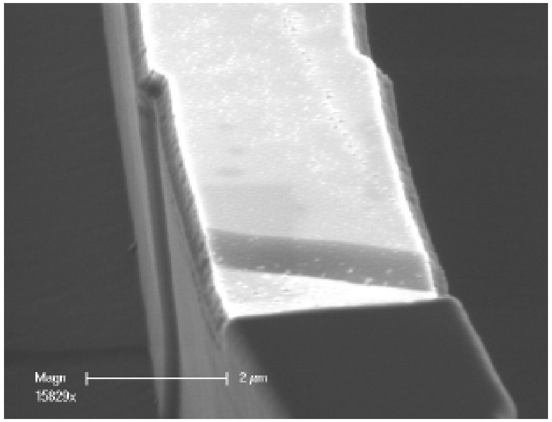

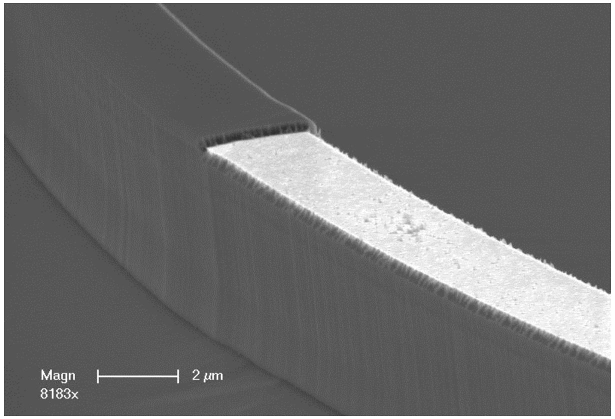

Tunable MMI Mach-Zehnder interferometer coupler

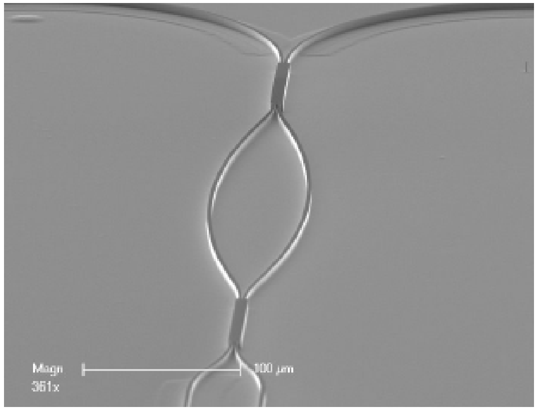

Photonic Signal Processor – pictures of the chip

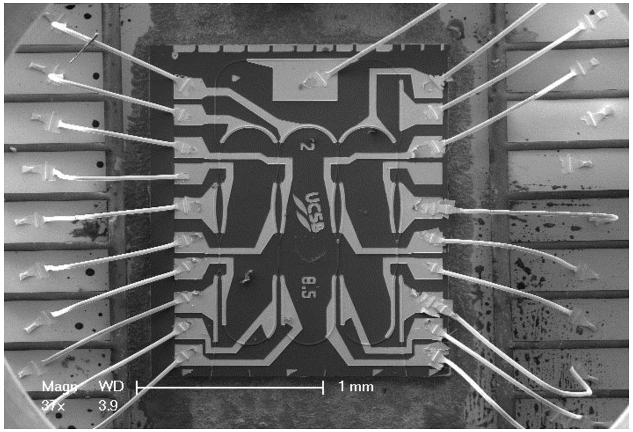

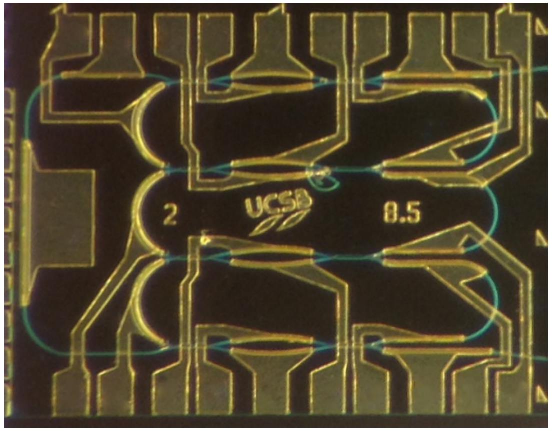

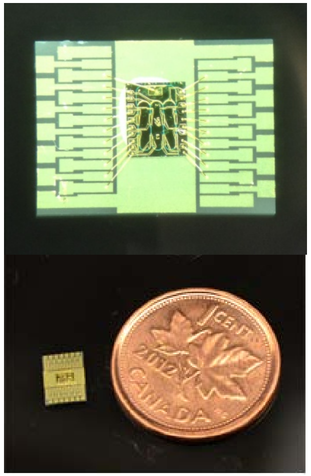

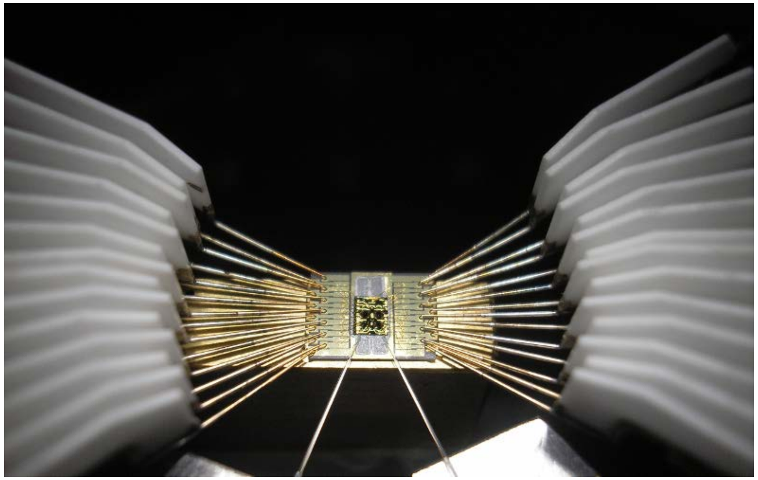

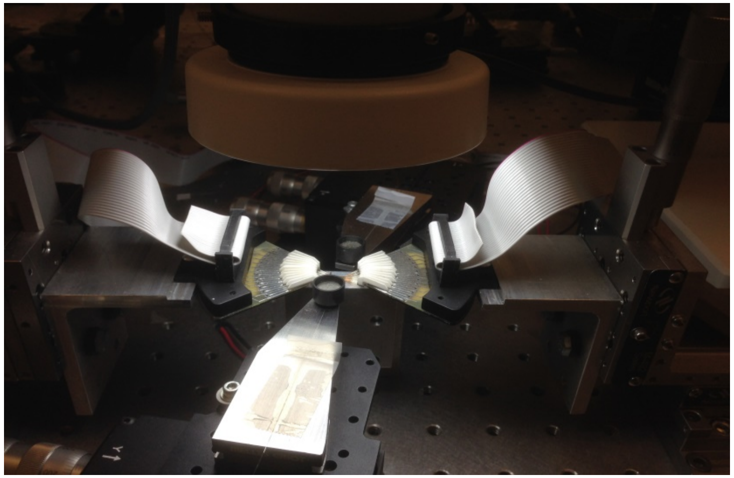

Photonic Signal Processor – experimental results

400 μm SOA: Large Signal Gain

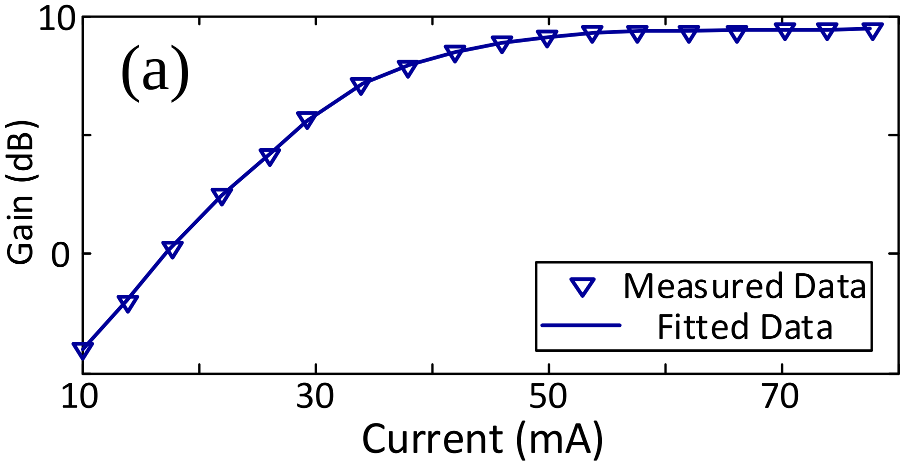

(a) The measured gain profile of an SOA as a function of the injection current. (peak gain at 240 dB/cm, saturation power 12.8 dBm)

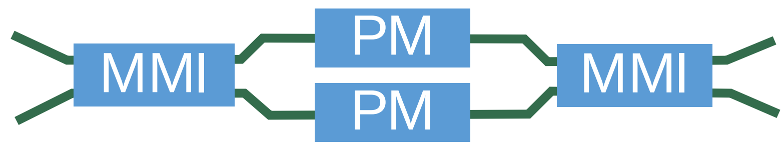

Tunable Coupler

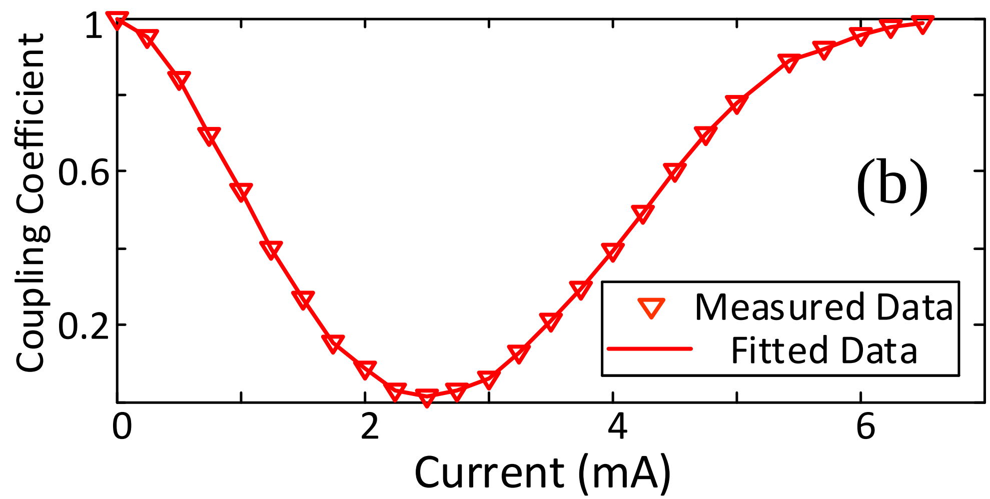

(b) Tunable coupling coefficient of an MMI MZI coupler at different injection current of one PM on one of the two arms.

Photonic Temporal Integrator

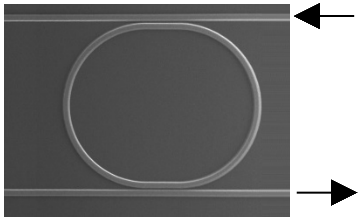

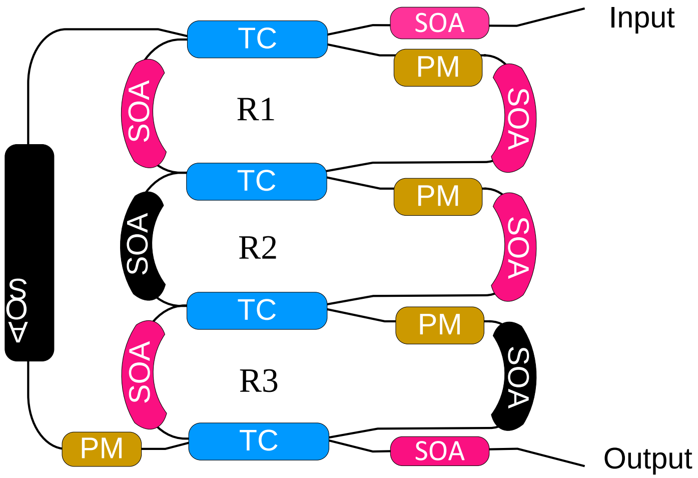

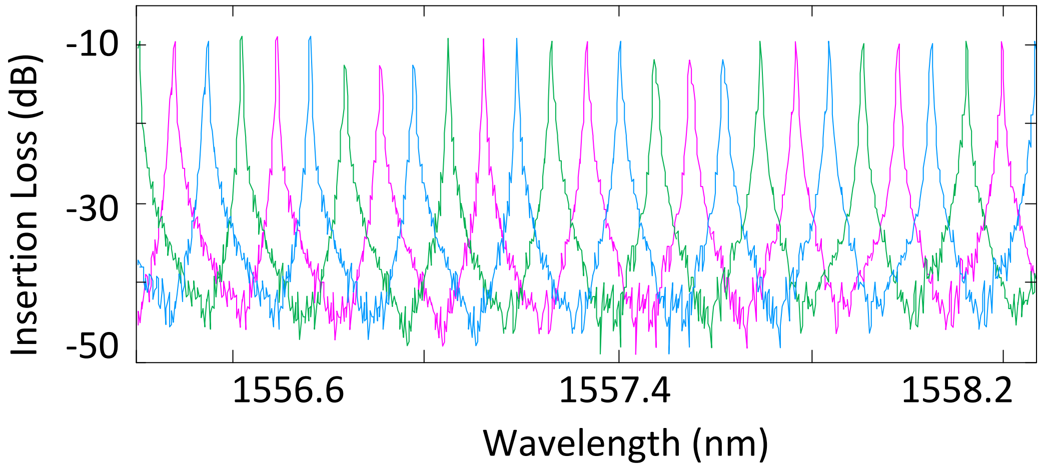

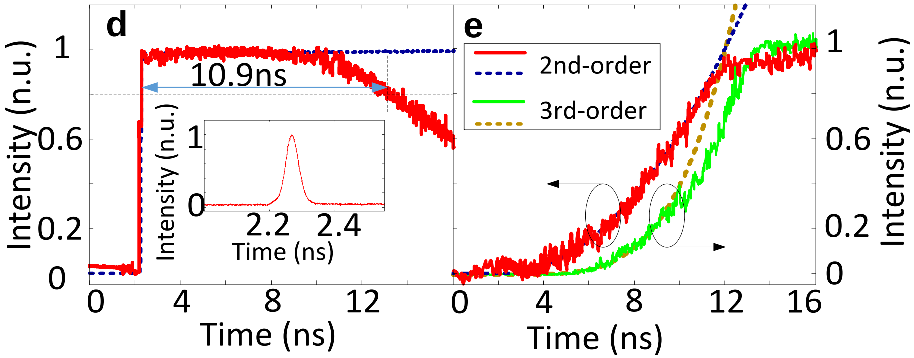

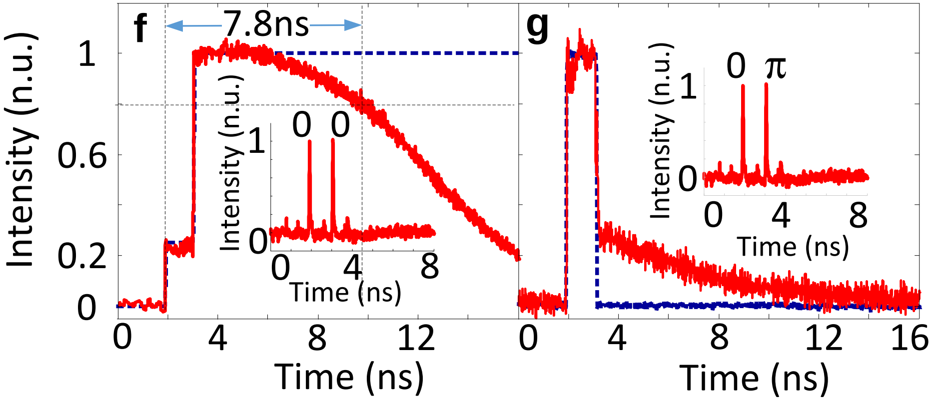

Photonic Temporal Differentiator

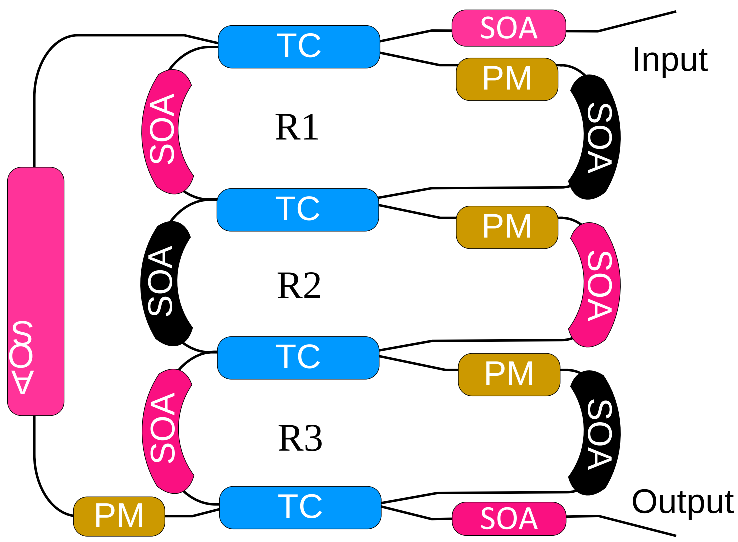

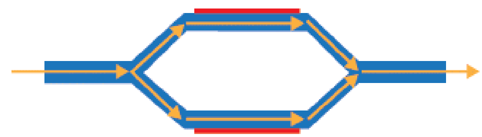

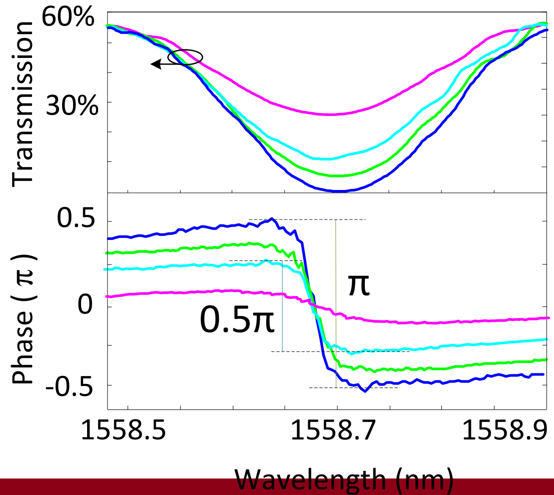

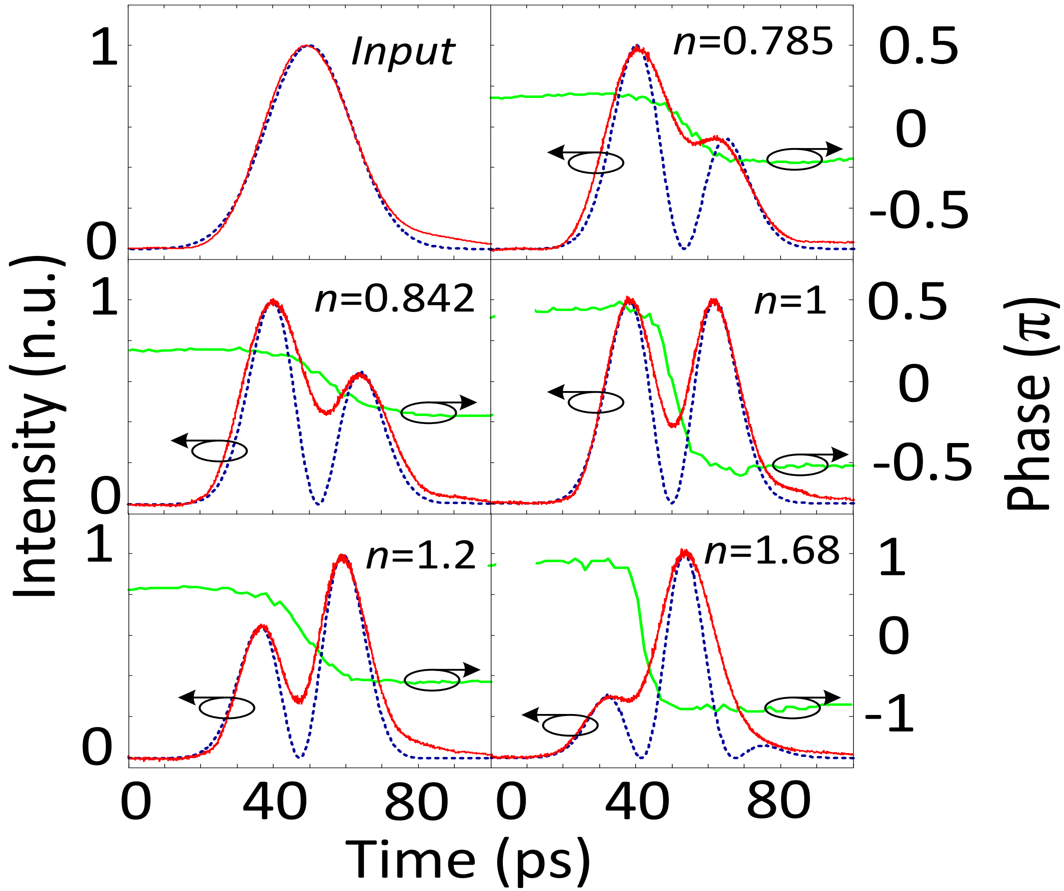

Photonic Hilbert Transformer

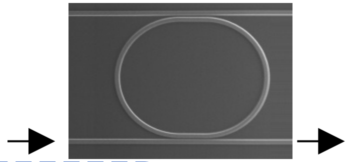

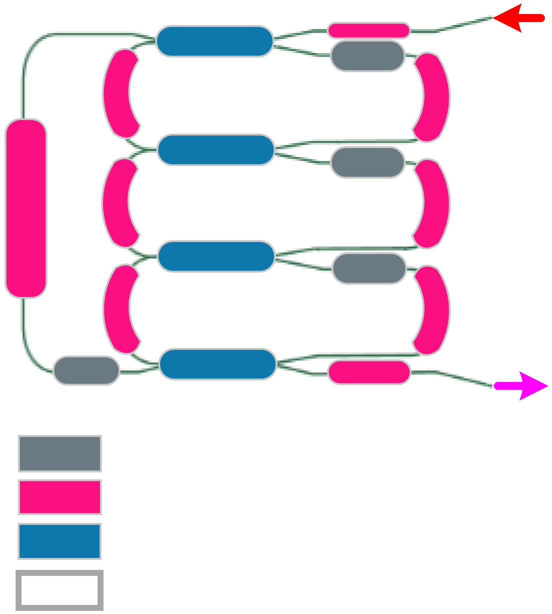

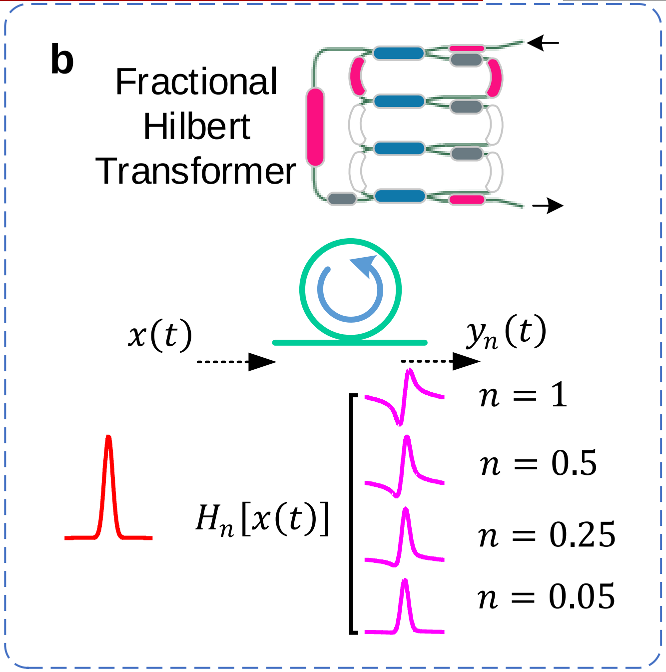

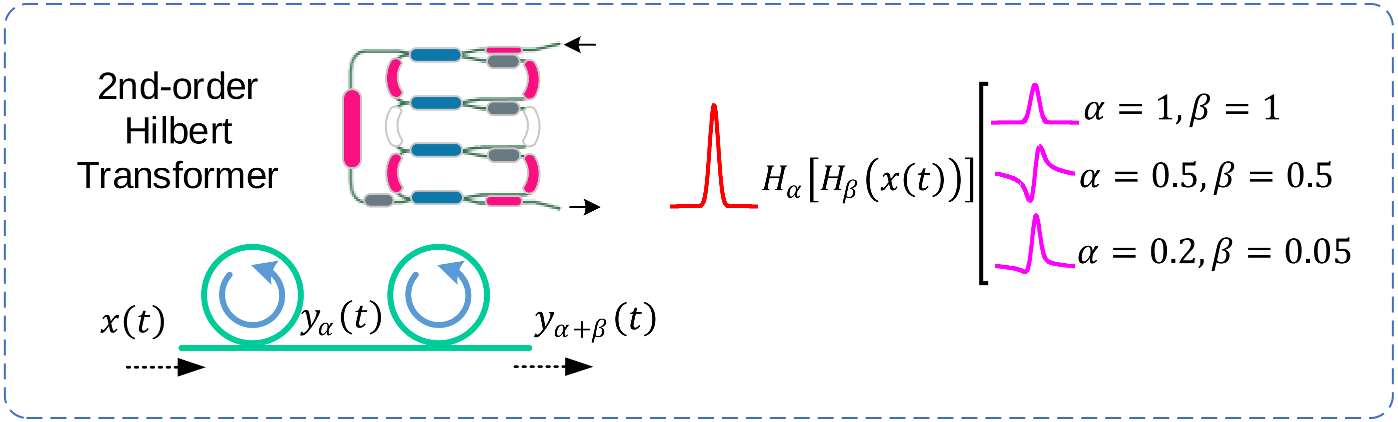

Photonic Temporal Hilbert Transformation

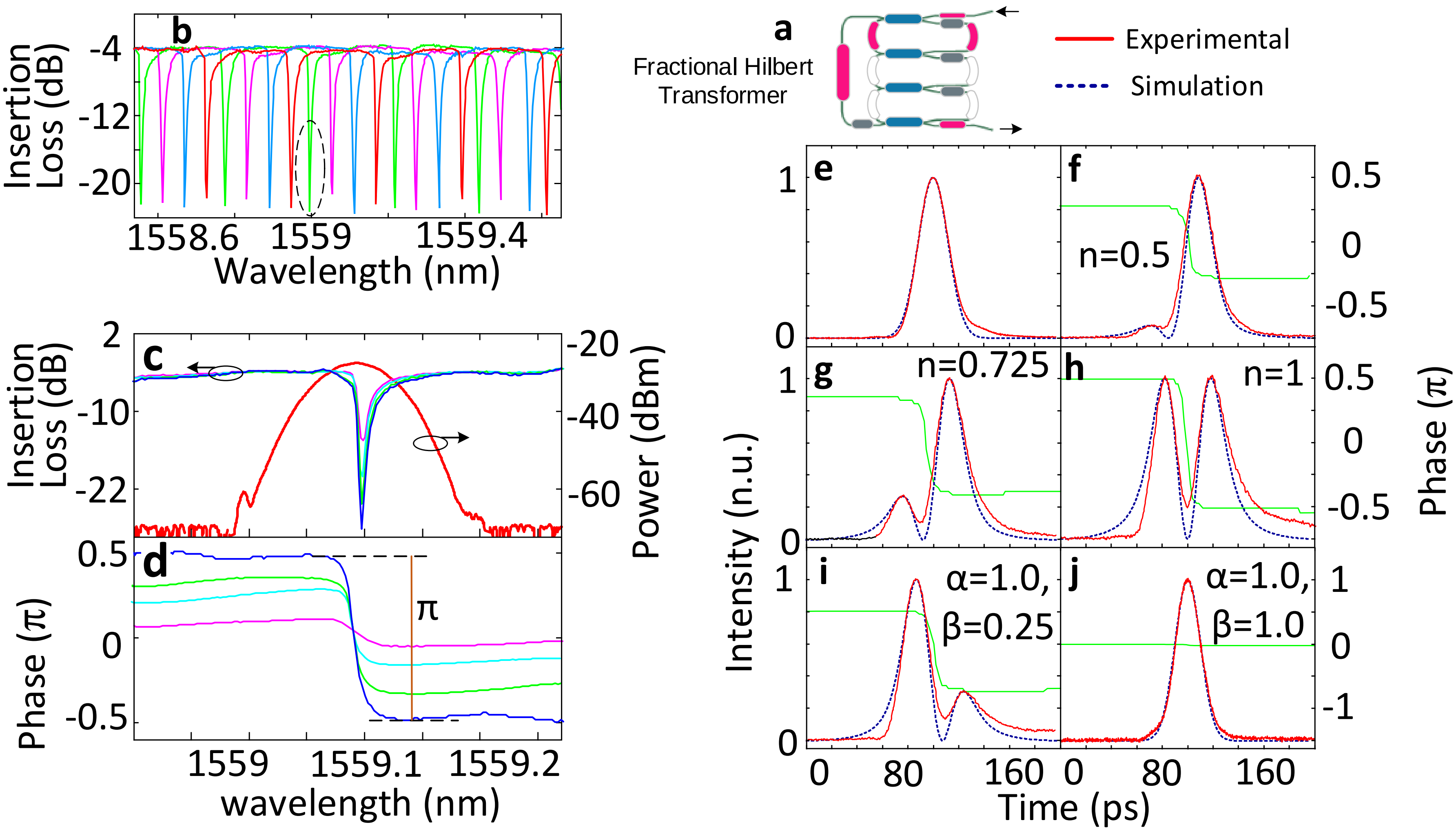

Application Examples

Image processing using the signal processor

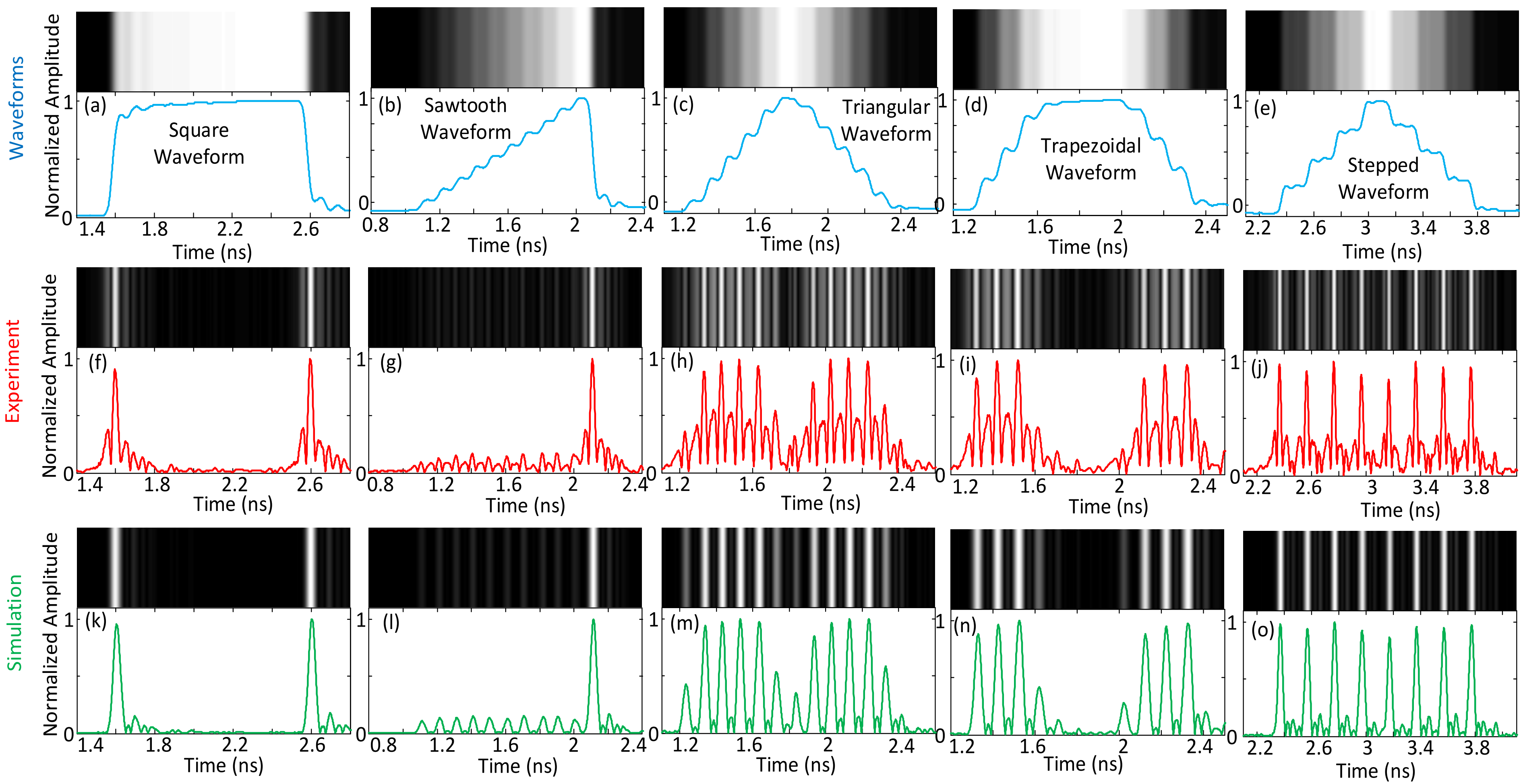

Application Examples

Single sideband modulation

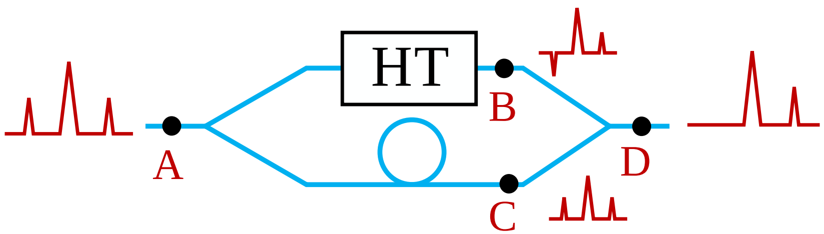

Single Sideband modulation is important in a radio over fiber (RoF) link to avoid dispersion-induced power penalty

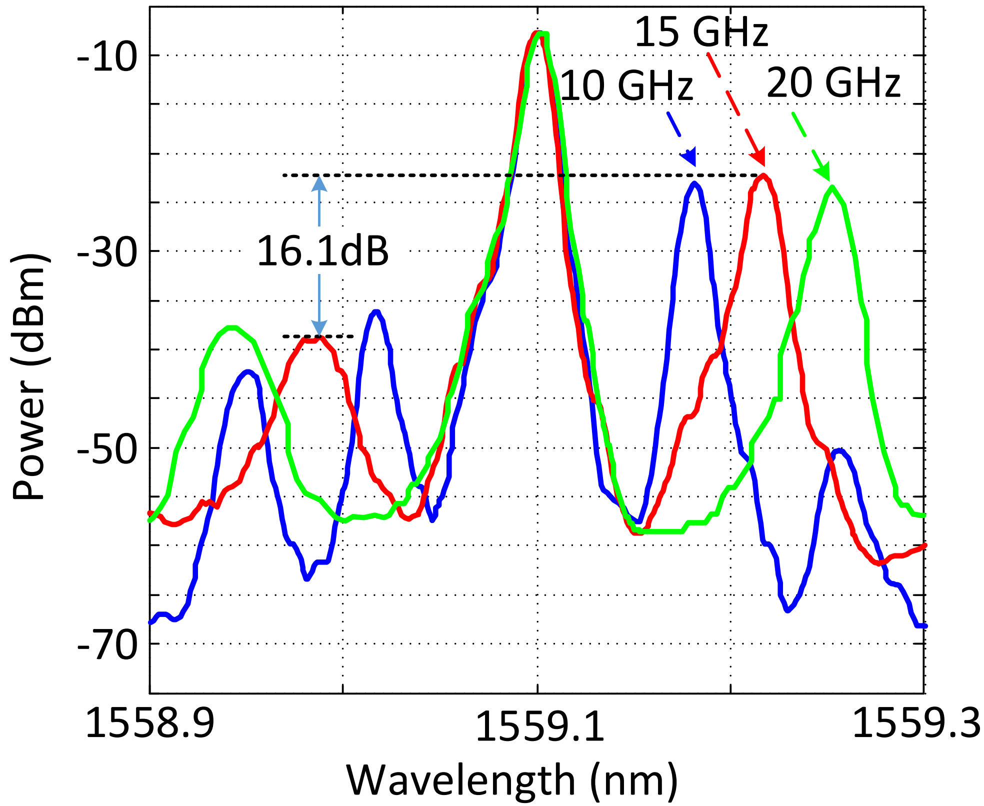

The spectrum of the experimentally generated SSB modulated optical signal.

Photonic Microwave Signal Generator

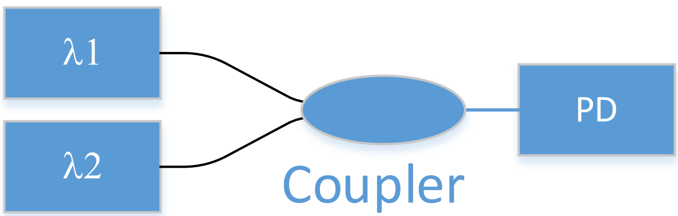

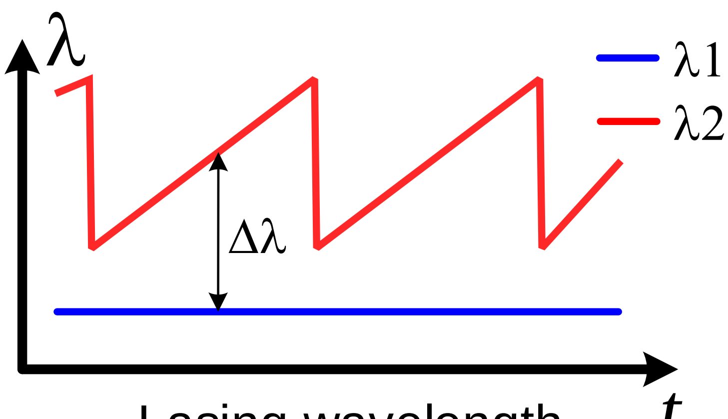

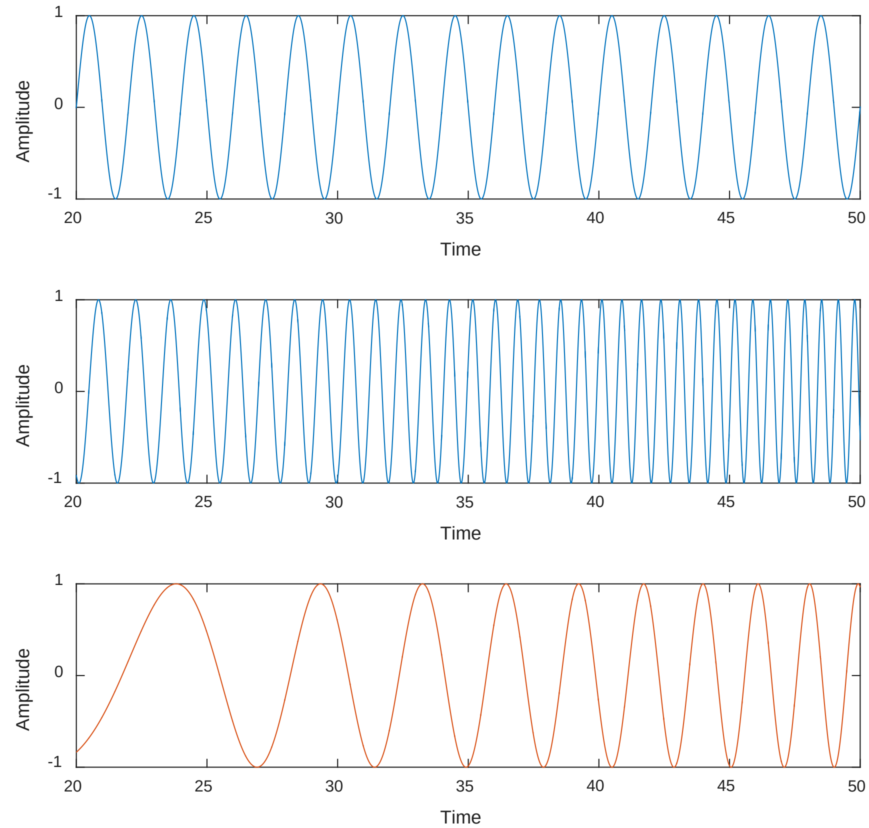

Photonic Microwave Signal Generator

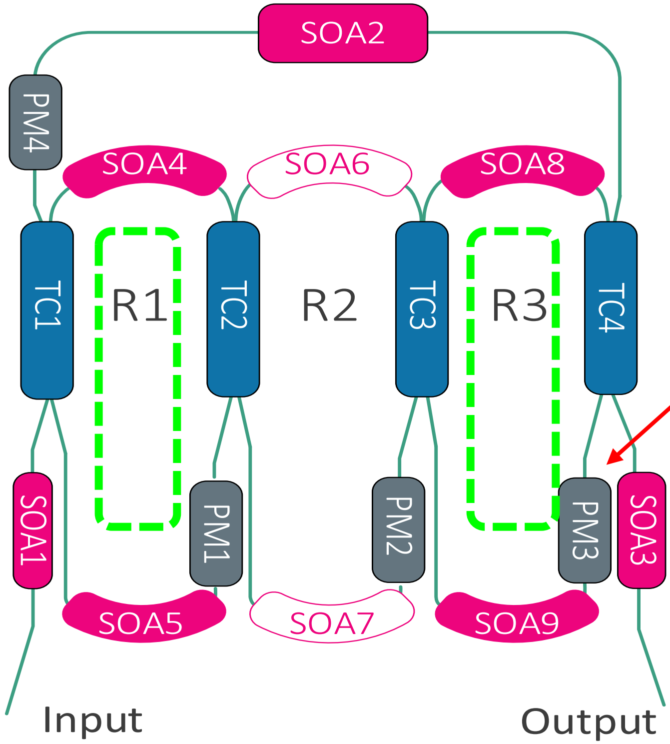

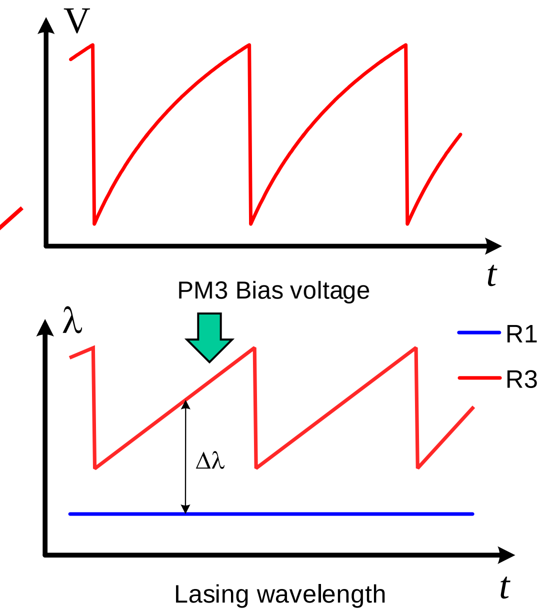

$$\Delta f = \frac{d\phi}{dt} = At \quad \left(if \quad \phi(t) = \frac{A}{2}t^2 \right)$$

- The signal processor is reconfigured to operate as a microwave generator consisting of two ring lasers.
- A changing driving voltage is applied to PM3 in R3 to generate a chirped optical light.

J. Zhang and J. P. Yao, "A photonic integrated microwave waveform generator for linearly chirped microwave waveform generation," MWP2016, Long Beach, California, USA, Oct. 2016.

Photonic Microwave Signal Generator

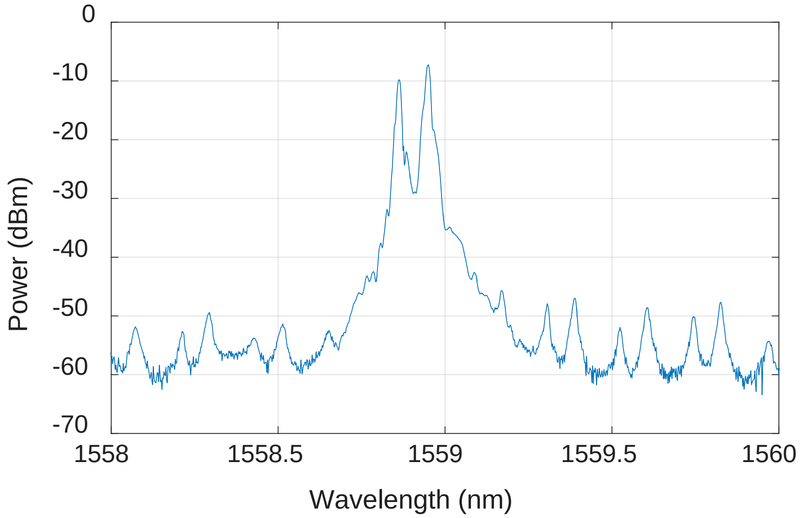

The optical spectrum measured at the output port of the chip. Two wavelengths with a wavelength spacing of 85 pm.

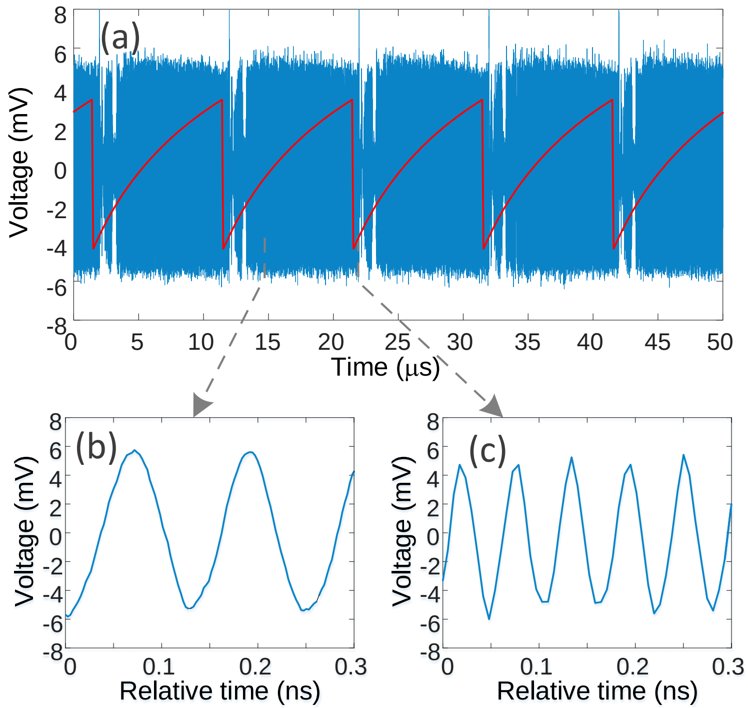

(a) The driving voltage applied to the PM3 (red) and the generated high frequency microwave waveform (blue); (b) and (c) the zoom-in view of the generated waveform at different locations within a period of the driving voltage.

Photonic Microwave Signal Generator

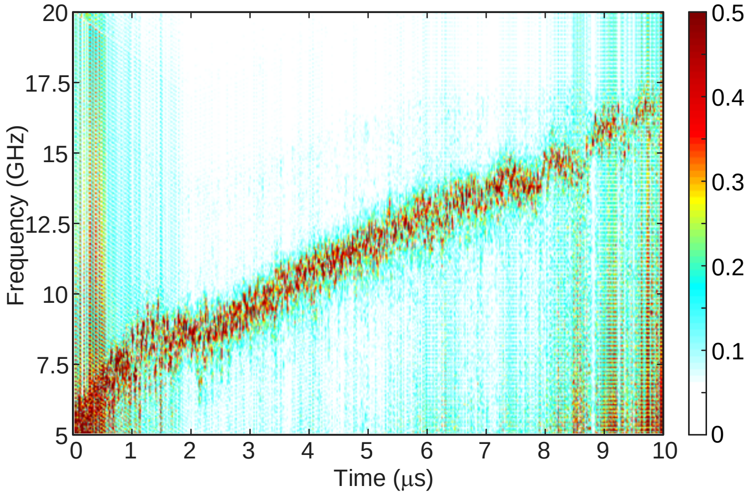

Spectrogram of the generated LCMW. The color scale represents the normalized amplitude of the instantaneous spectrum.

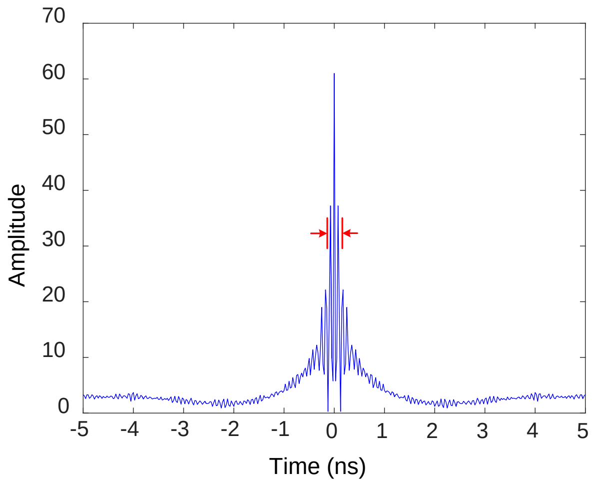

Calculated auto-correlation between two generated LCMWs. A correlation peak of 250 ps is achieved.

- Within the temporal duration of the 10 μs, the frequency increases from 5 to 17 GHz, corresponding to a TBWP of $\mathbf{1.2 \times 10^5}$.
- A compressed pulse with a temporal width of 200 ps is achieved from the autocorrelation of the generated waveform. The pulse compression ratio is calculated to be $\mathbf{5 \times 10^4}$.

Outline

- Introduction to Microwave Photonics (MWP)
- SiP-based MWP systems
  - Photonic generation of microwave waveforms
  - Photonic processing of microwave signals
  - A fully SiP integrated MWP filter
- InP-based signal processing
  - A fully reconfigurable photonic signal processor
  - **A fully InP integrated MWP filter**
- SiN-based MWP systems
  - True time delay beamforming
  - Reconfigurable signal processor
- Conclusion

ARTICLES
PUBLISHED ONLINE: 5 DECEMBER 2016 | DOI: 10.1038/NPHOTON.2016.233
nature photonics

A monolithic integrated photonic microwave filter

Javier S. Fandiño[1], Pascual Muñoz[1,2], David Doménech[2] and José Capmany[1]*

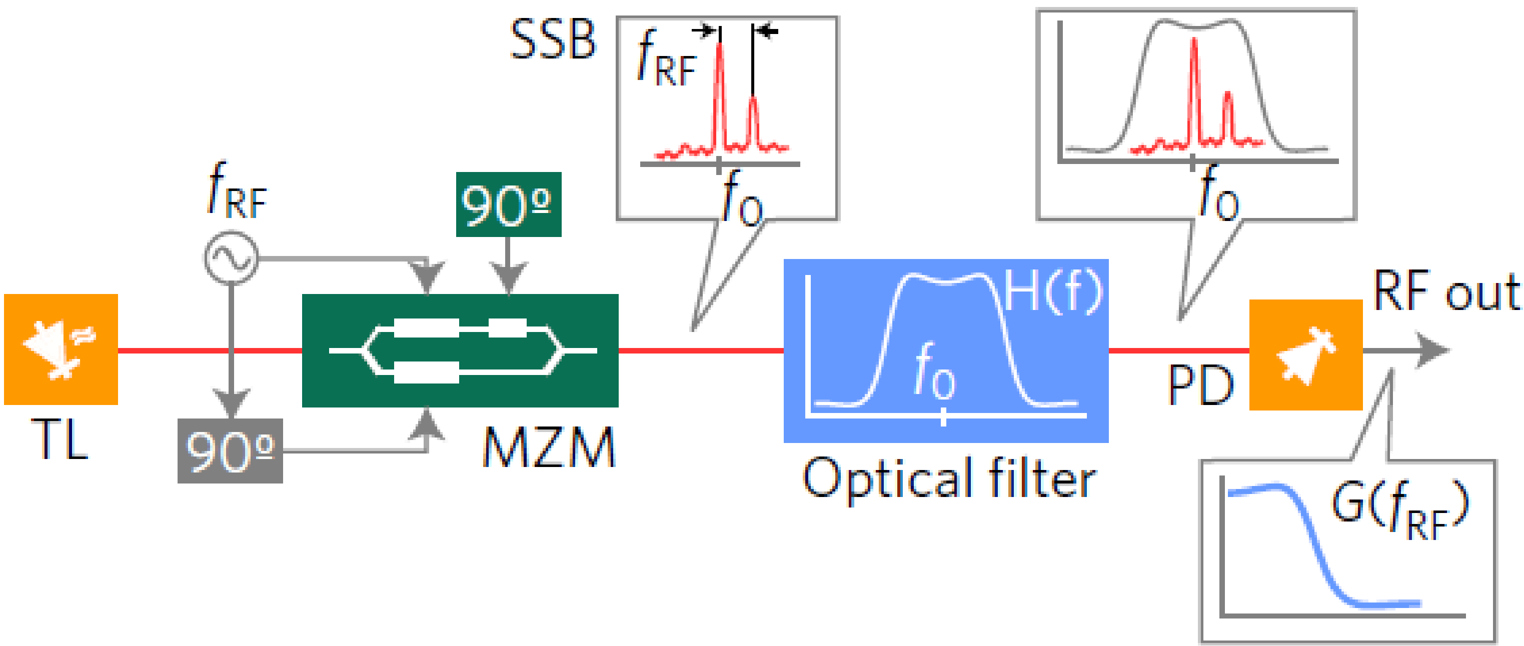

ARTICLES
PUBLISHED ONLINE: 5 DECEMBER 2016 | DOI: 10.1038/NPHOTON.2016.233
nature photonics

A monolithic integrated photonic microwave filter

Javier S. Fandiño[1], Pascual Muñoz[1,2], David Doménech[2] and José Capmany[1]*

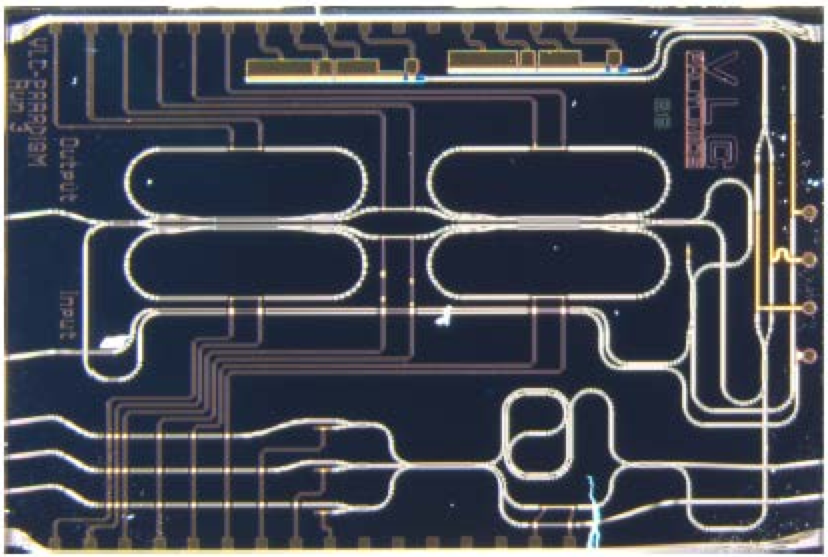

Image of a fabricated die

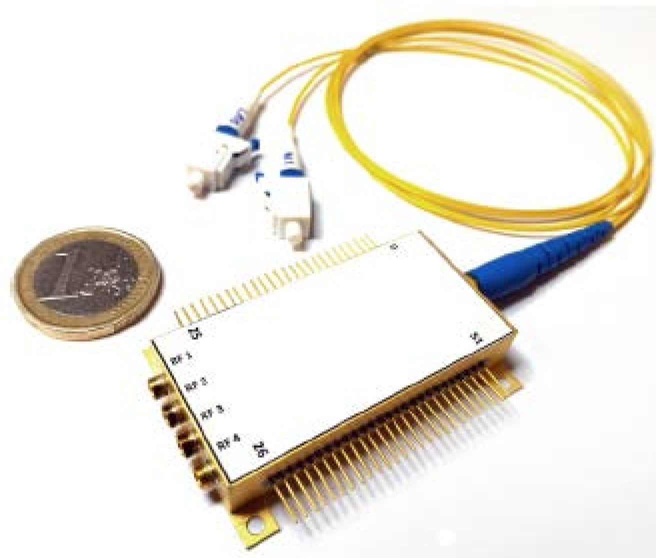

Packaged chip

A monolithic integrated photonic microwave filter

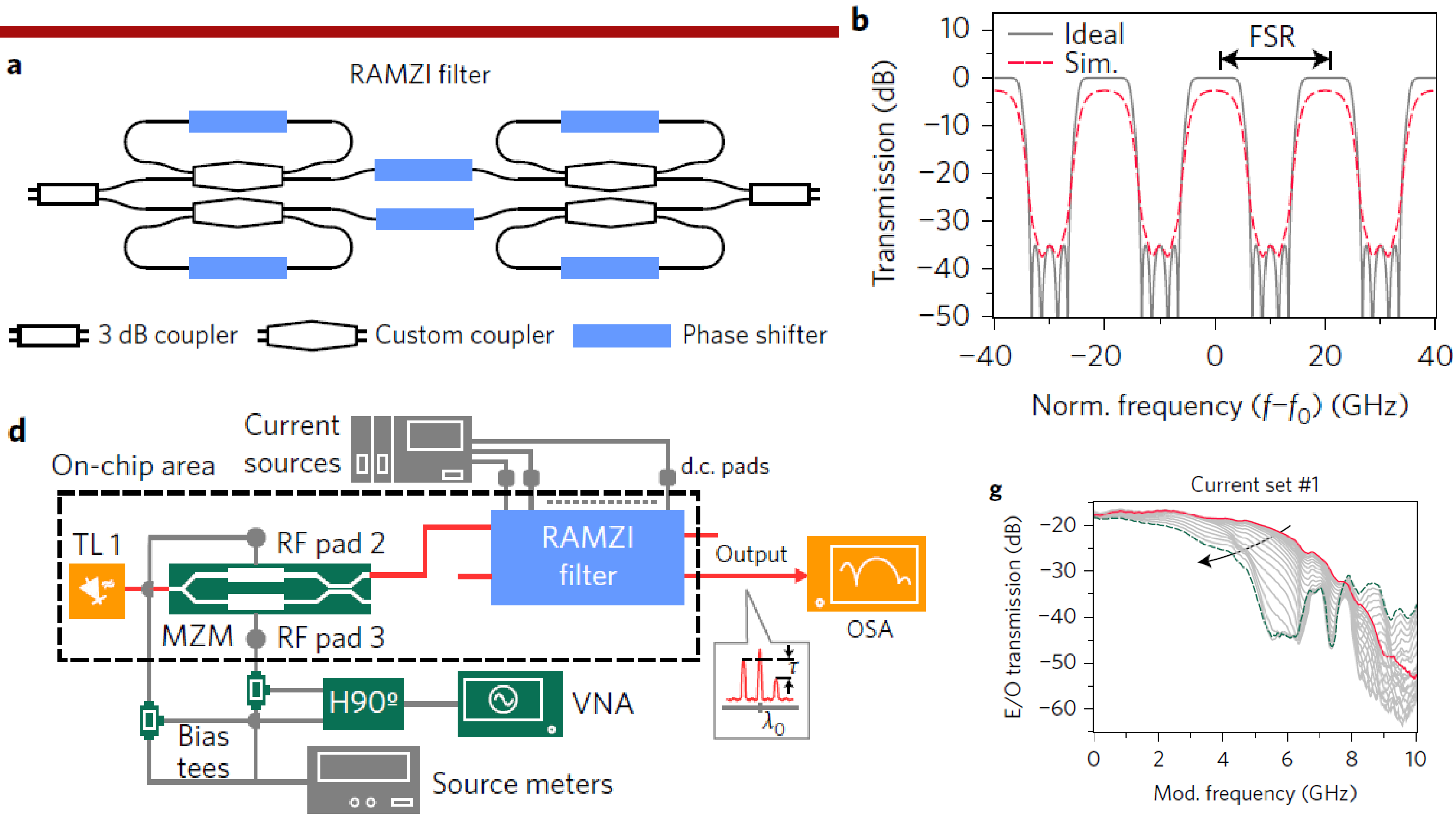

A monolithic integrated photonic microwave filter

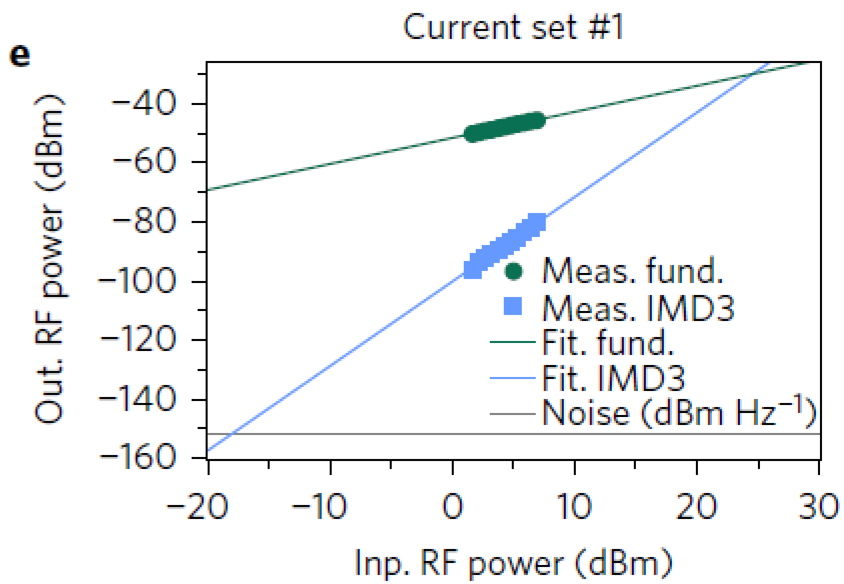

Measured powers of the fundamental signal and the IMD3 when the filter is tuned at 1.4 GHz

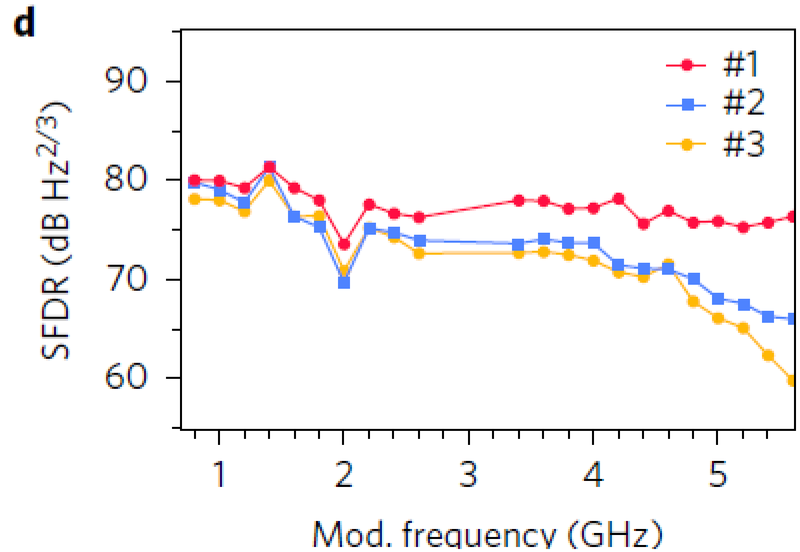

Measured spurious-free dynamic range (SFDR) for these three cases as a function of modulation frequency

Outline

- Introduction to Microwave Photonics (MWP)
- SiP-based MWP systems
  - Photonic generation of microwave waveforms
  - Photonic processing of microwave signals
  - A fully SiP integrated MWP filter
- InP-based signal processing
  - A fully reconfigurable photonic signal processor
  - A fully InP integrated MWP filter
- SiN-based MWP systems
  - **True time delay beamforming**
  - Reconfigurable signal processor
- Conclusion

Squint-free beamforming - true time delay (TTD)

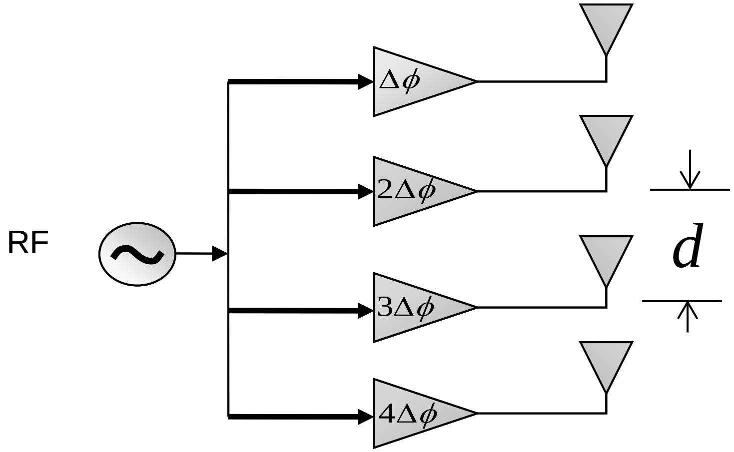

Phased Array Antenna System based on phase shifters

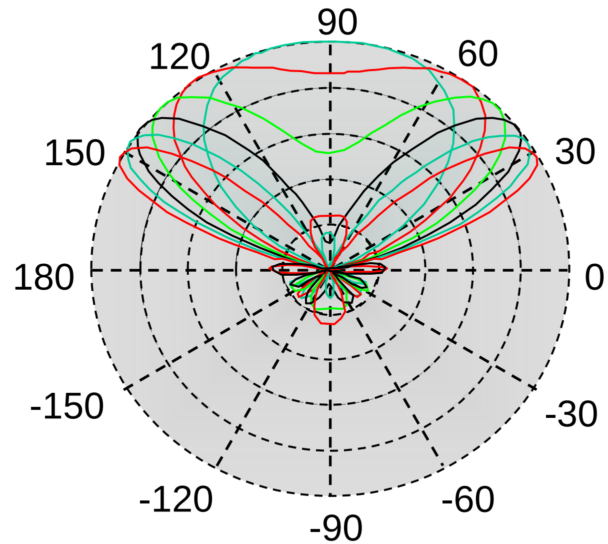

Example of beam squint with electrical phase shift technique

$$\theta = \sin^{-1}\left(\frac{\Delta\phi\lambda}{2\pi d}\right)$$

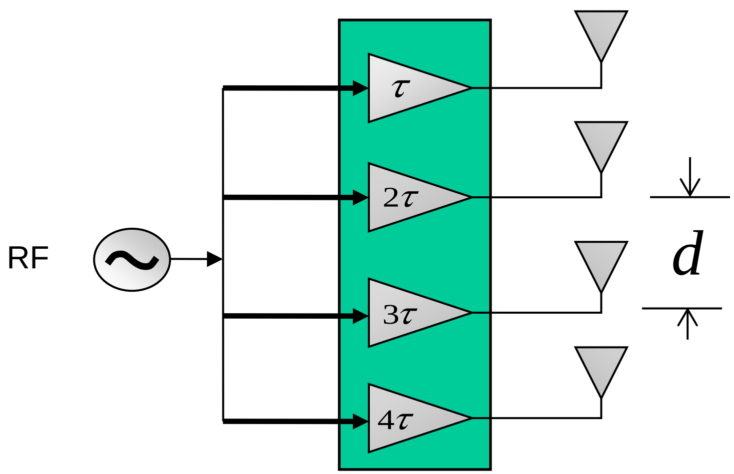

Phased Array Antenna System based on TTD

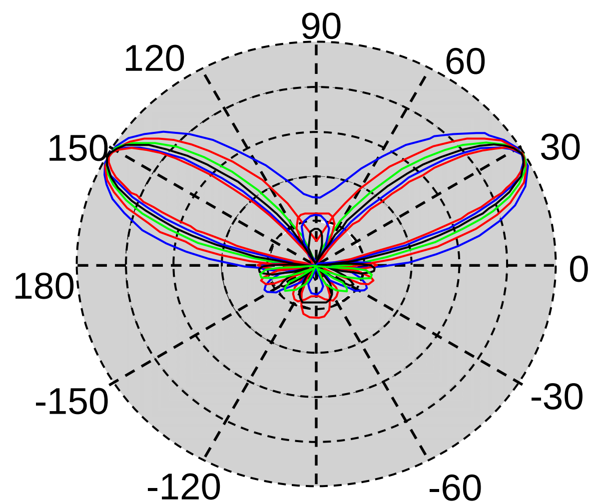

Example of beam squint-free pattern with true-time delay

$$\theta = \sin^{-1}\left(\frac{\tau}{d}\right)$$

 IPC2017

Single-Chip Ring Resonator-Based 1 × 8 Optical Beam Forming Network in CMOS-Compatible Waveguide Technology

L. Zhuang, *Student Member, IEEE*, C. G. H. Roeloffzen, *Member, IEEE*, R. G. Heideman, A. Borreman, A. Meijerink, *Member, IEEE*, and W. van Etten, *Senior Member, IEEE*

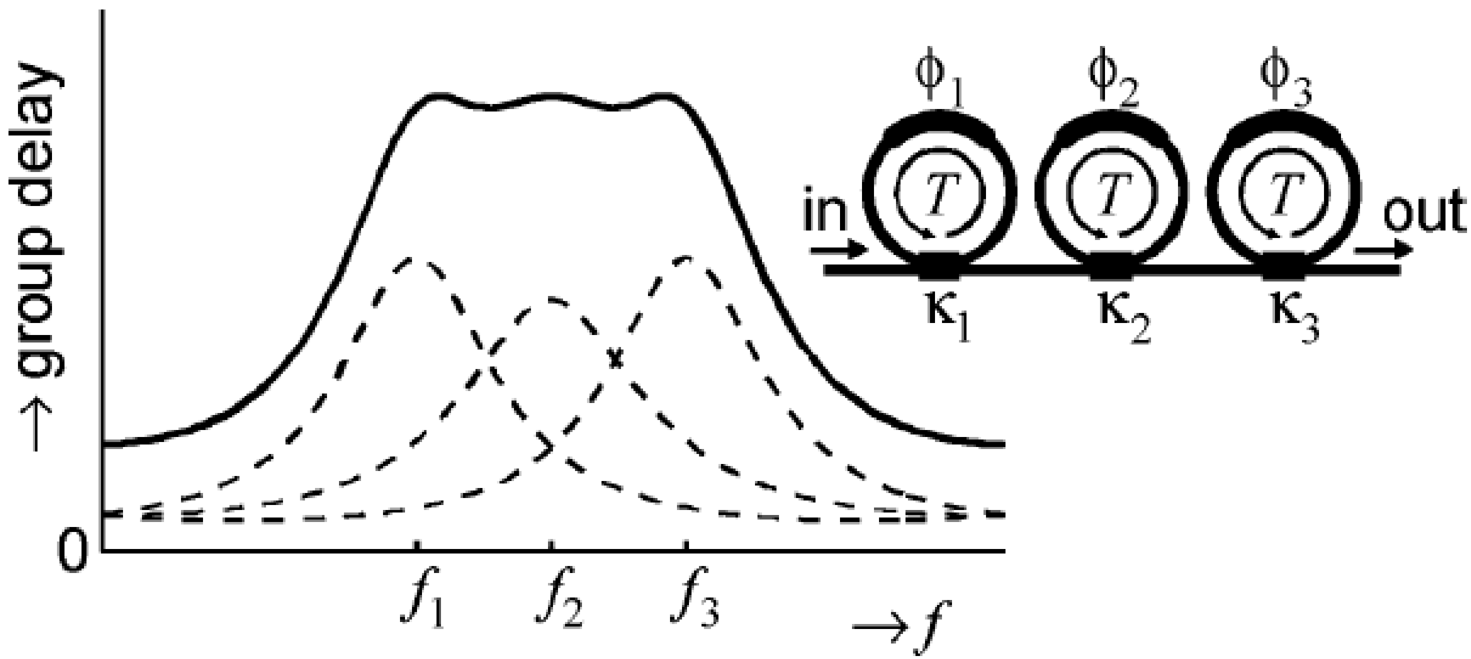

True time delay beamforming

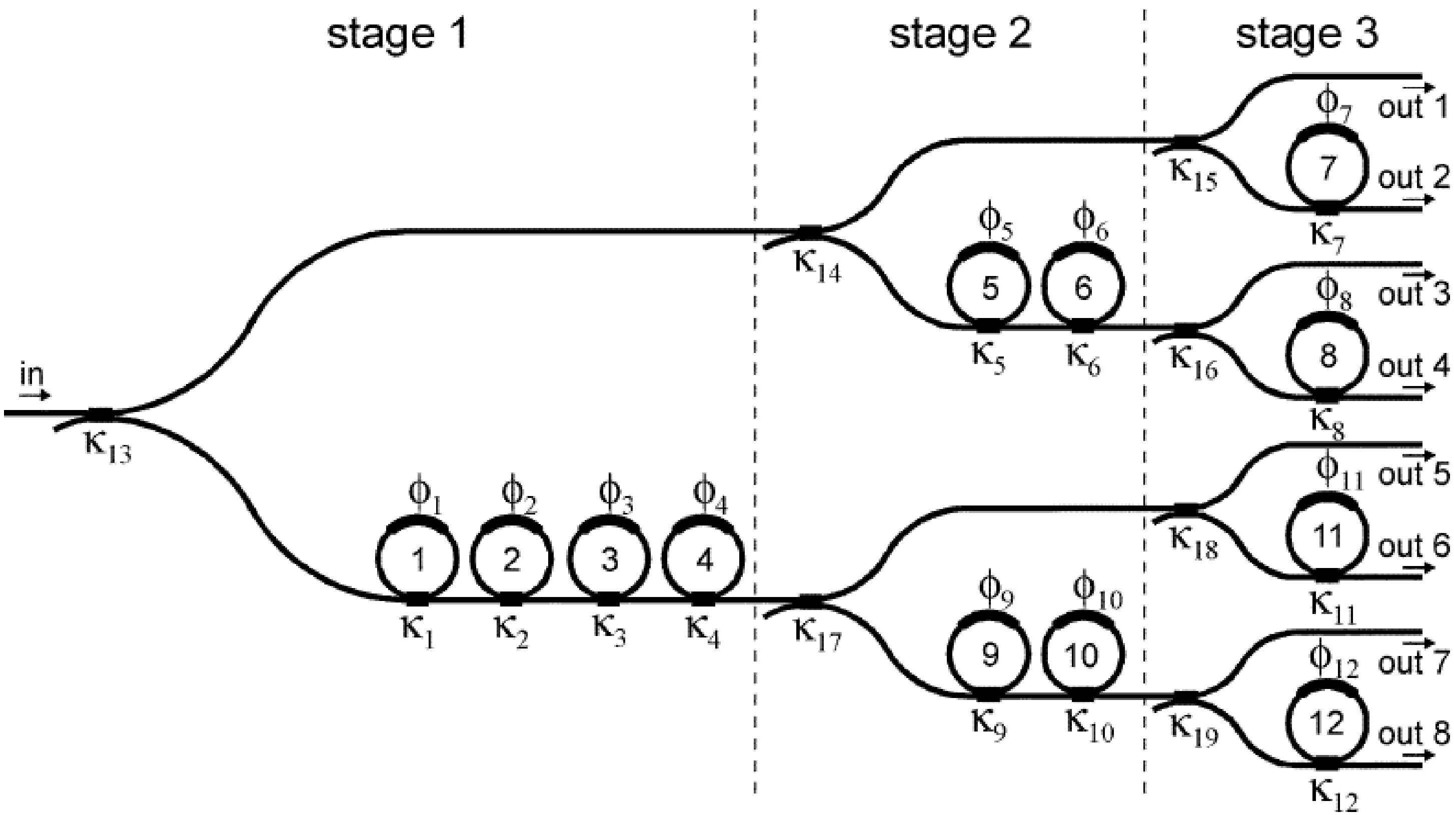

Fig. 2. Binary tree-based 1 × 8 OBFN for transmitter system, consisting of 12 ORRs and seven tunable splitters.

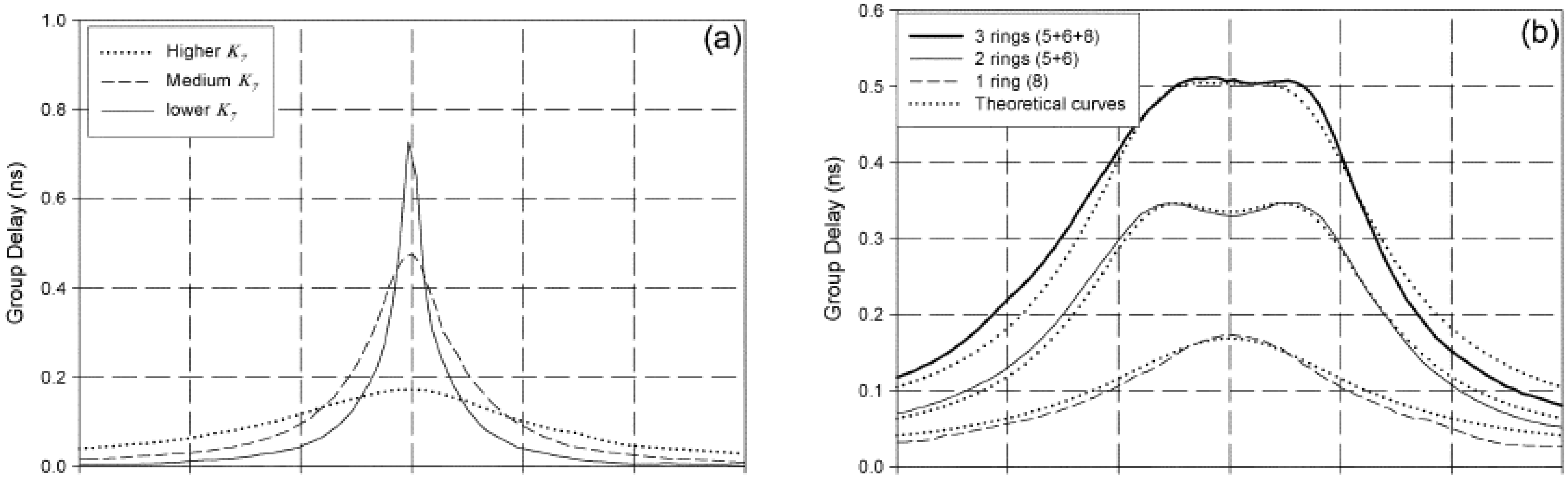

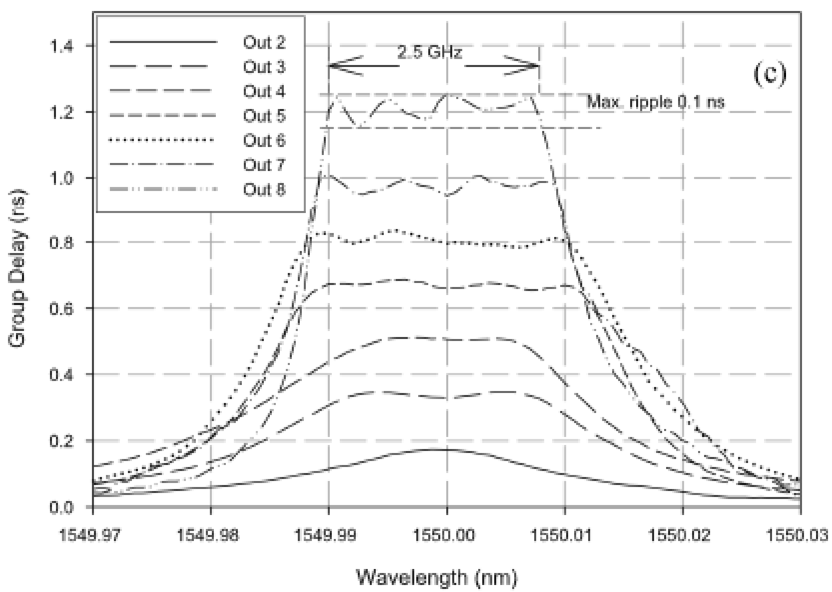

Fig. 5. Measurement results of different outputs of the 1 8 OBFN chip: (a) and (b) show group delay responses of Outputs 2 and 4, respectively; (c) shows the linearly increasing delay at all outputs of the 1 8 OBFN chip.

System integration and radiation pattern measurements of a phased array antenna employing an integrated photonic beamformer for radio astronomy applications

1 March 2012 / Vol. 51, No. 7 / APPLIED OPTICS 789

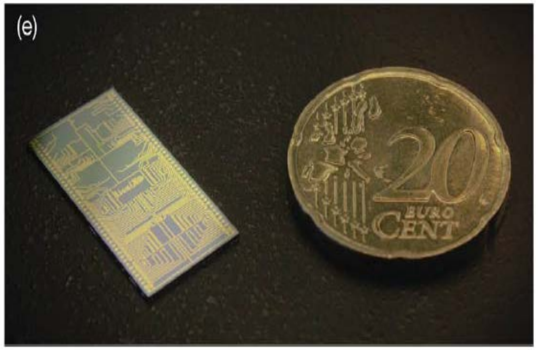

Maurizio Burla,[1,*] Chris G. H. Roeloffzen,[1] Leimeng Zhuang,[1] David Marpaung,[1] Muhammad Rezaul Khan,[1] Peter Maat,[2] Klaas Dijkstra,[2] Arne Leinse,[3] Marcel Hoekman,[3] and René Heideman[3]

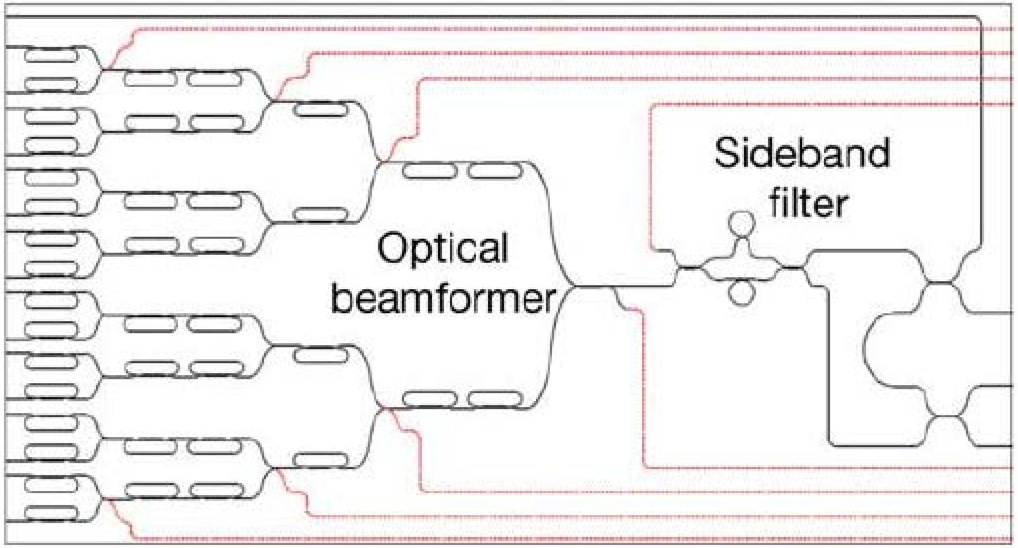

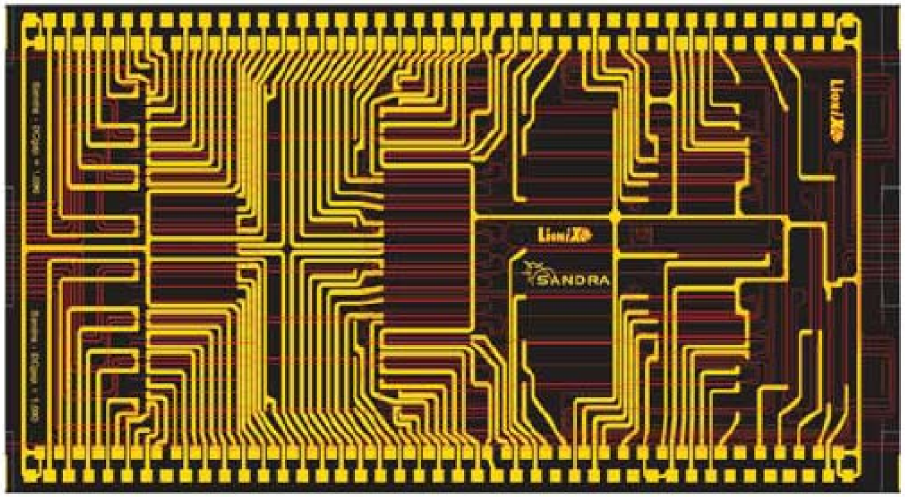

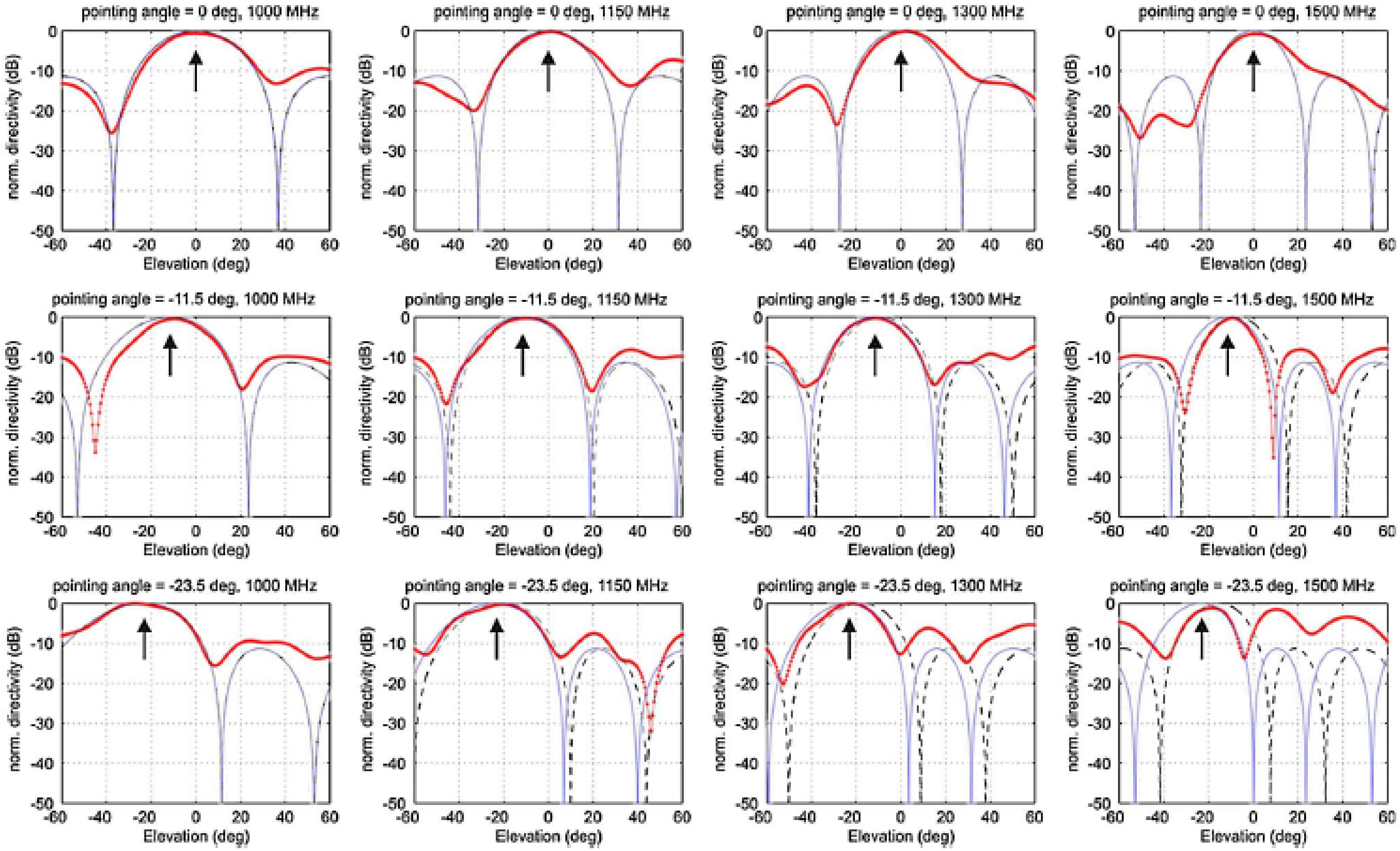

Fig. 10. (Color online) Measured (thick lines) versus simulated (thin solid lines) radiation patterns (E-plane) for three different pointing angles of the main beam: 0 degrees (top), –11.5 degrees (center), and –23.5 degrees (bottom). The measurements are also compared with the patterns that would be obtained in case phase shifters are used (dashed lines). Measurements at four frequencies (left to right: 1000 MHz, 1150 MHz, 1300 MHz, 1500 MHz) show the absence of beam squinting for the main lobe (indicated by the arrows) over the whole frequency range. Note the shift to the right of the leftmost null of radiation and the irregular shape assumed by the main lobe, in several of the measured patterns, as a consequence of parasitic effects in the measurement setup.

Silicon photonics - TTD beamforming

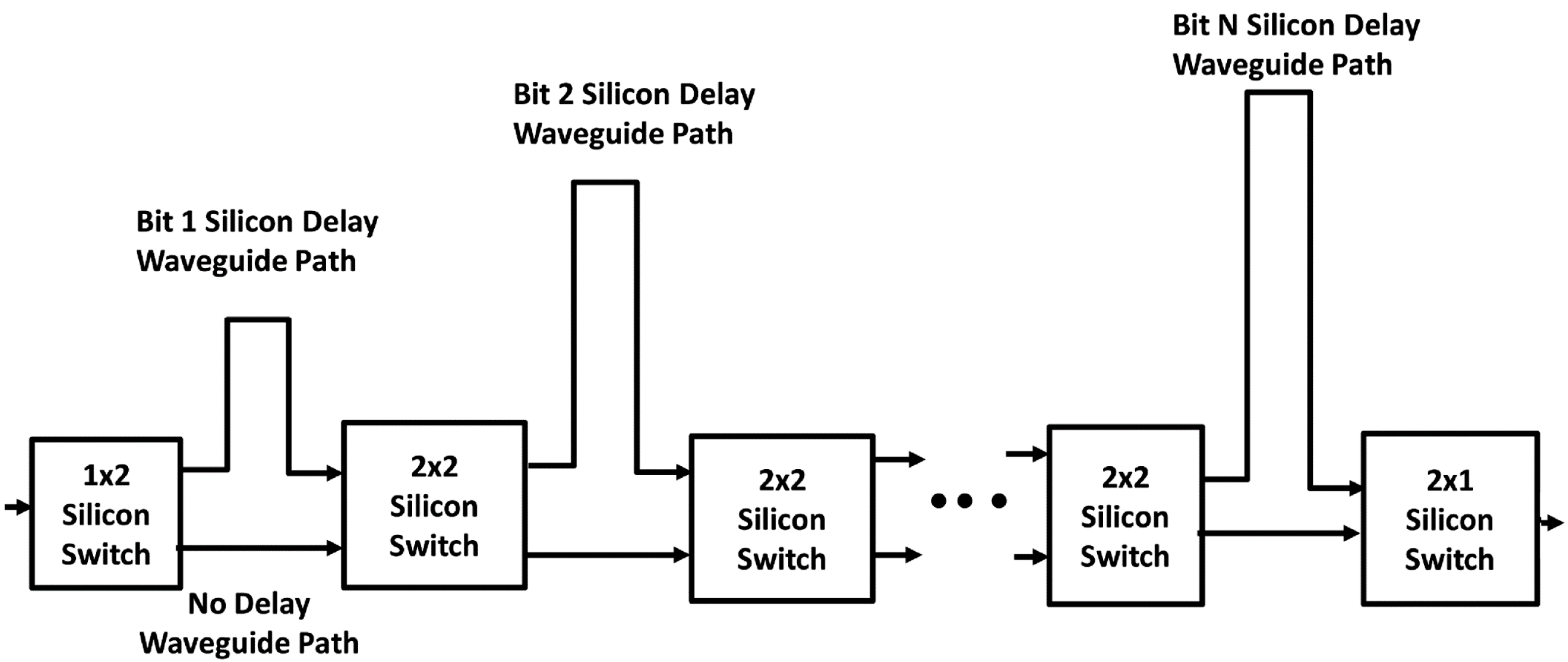

Silicon photonics - TTD beamforming

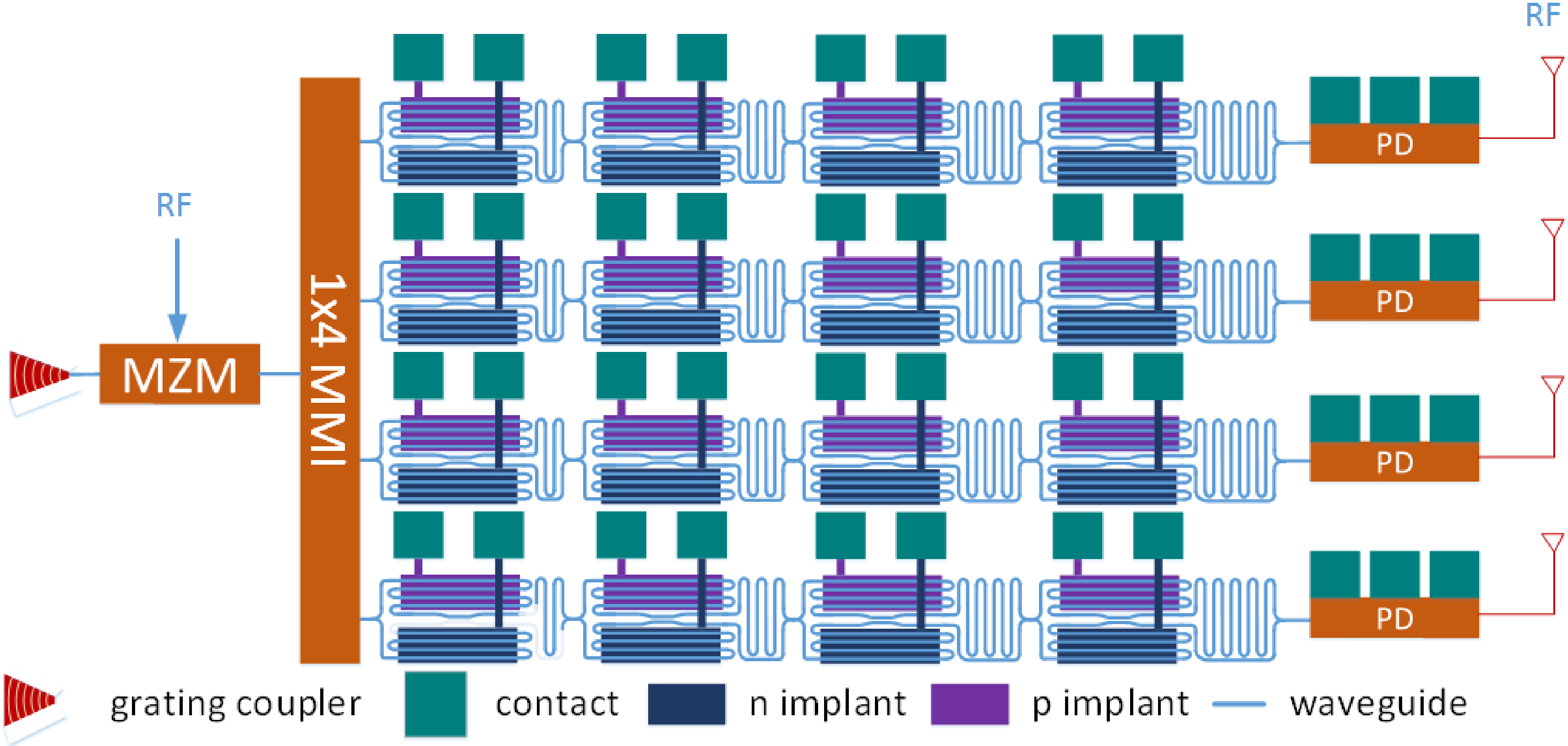

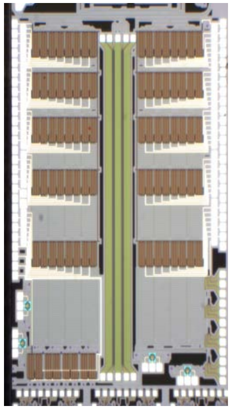

Outline

- Introduction to Microwave Photonics (MWP)
- SiP-based MWP systems
  - Photonic generation of microwave waveforms
  - Photonic processing of microwave signals
  - A fully SiP integrated MWP filter
- InP-based signal processing
  - A fully reconfigurable photonic signal processor
  - A fully InP integrated MWP filter
- SiN-based MWP systems
  - True time delay beamforming
  - **Reconfigurable signal processor**
- Conclusion

Research Article Vol. 2, No. 10 / October 2015 / *Optica* 854

IPC2017

optica

Programmable photonic signal processor chip for radiofrequency applications

Leimeng Zhuang,[1,*] Chris G. H. Roeloffzen,[2] Marcel Hoekman,[3] Klaus-J. Boller,[4] and Arthur J. Lowery[1,5]

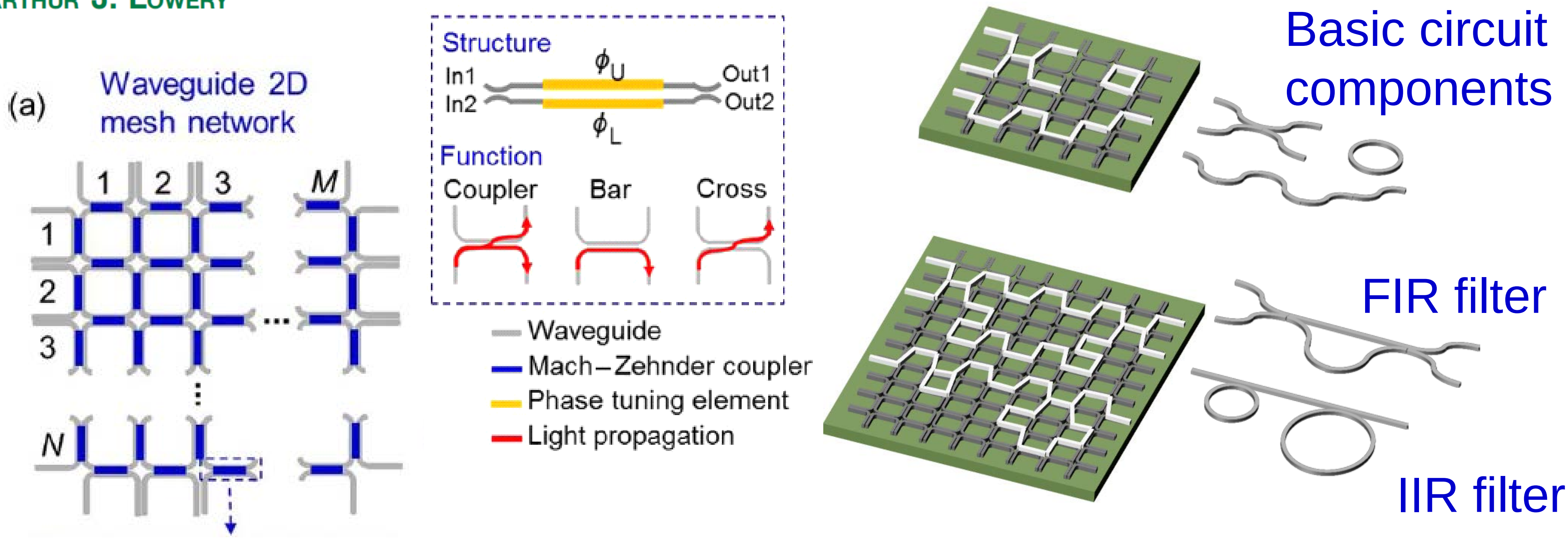

Programmable photonic signal processor chip for radiofrequency applications

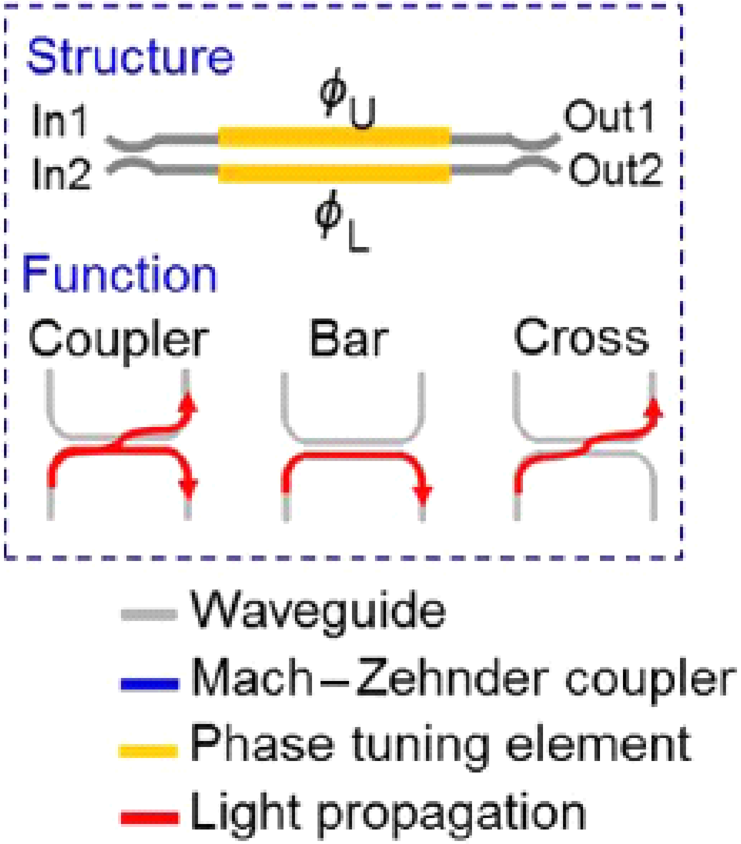

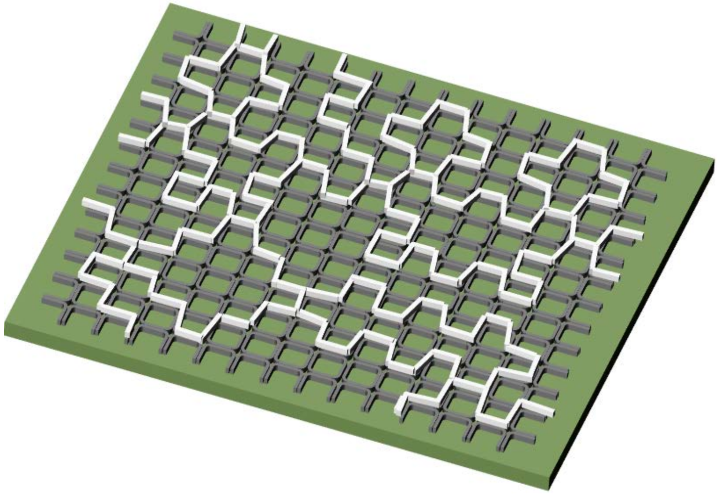

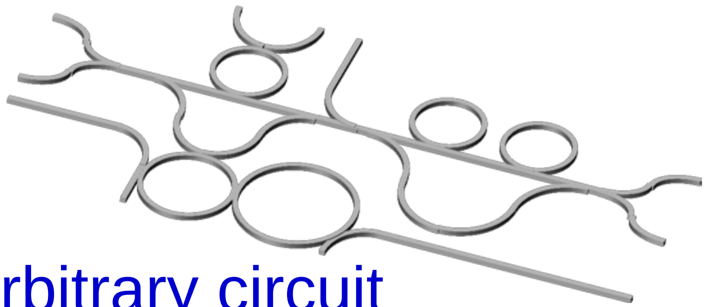

Arbitrary circuit topology

Proof-of-concept demonstration

Silicon Nitride (TriPleX)

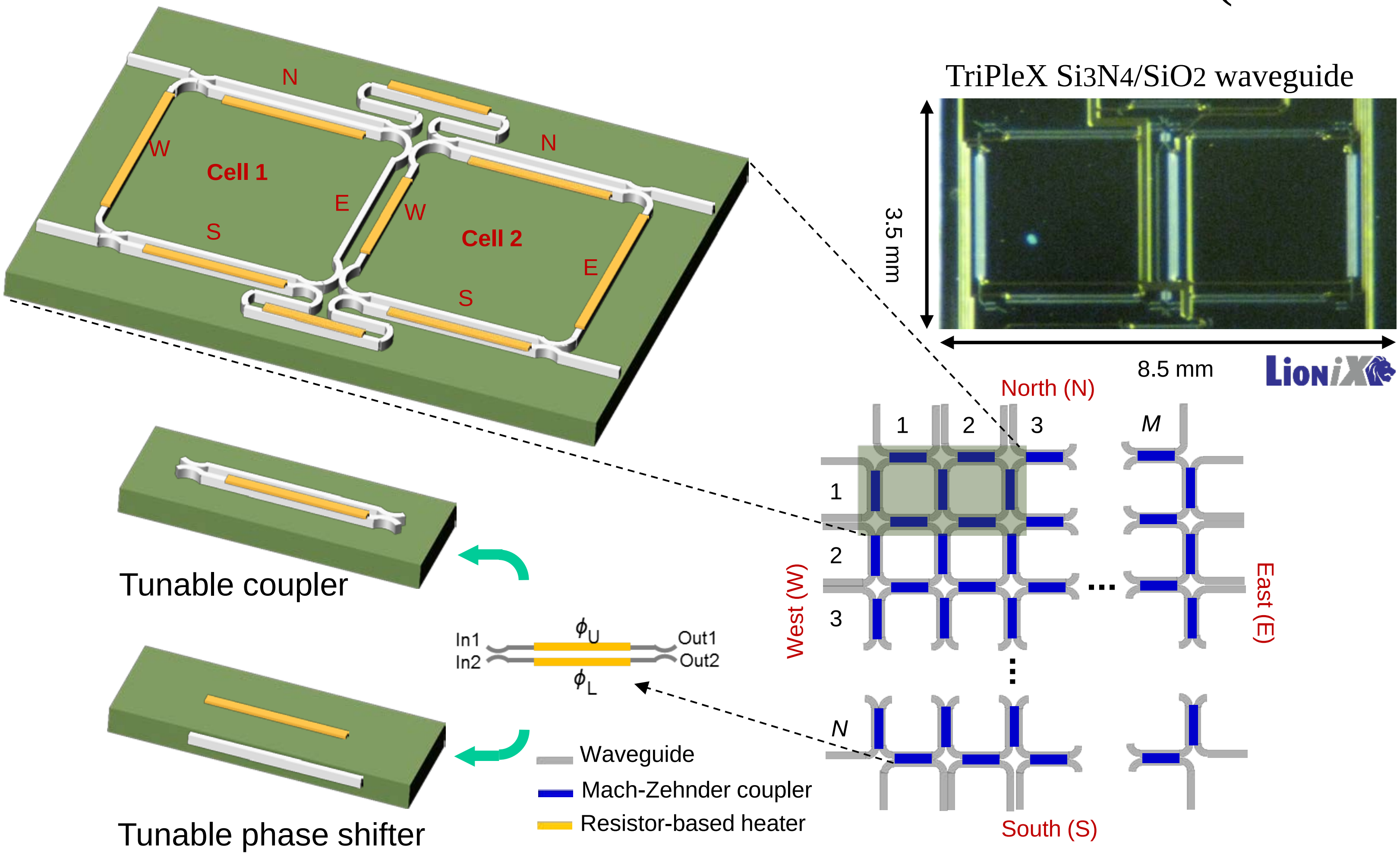

Proof-of-concept demonstration

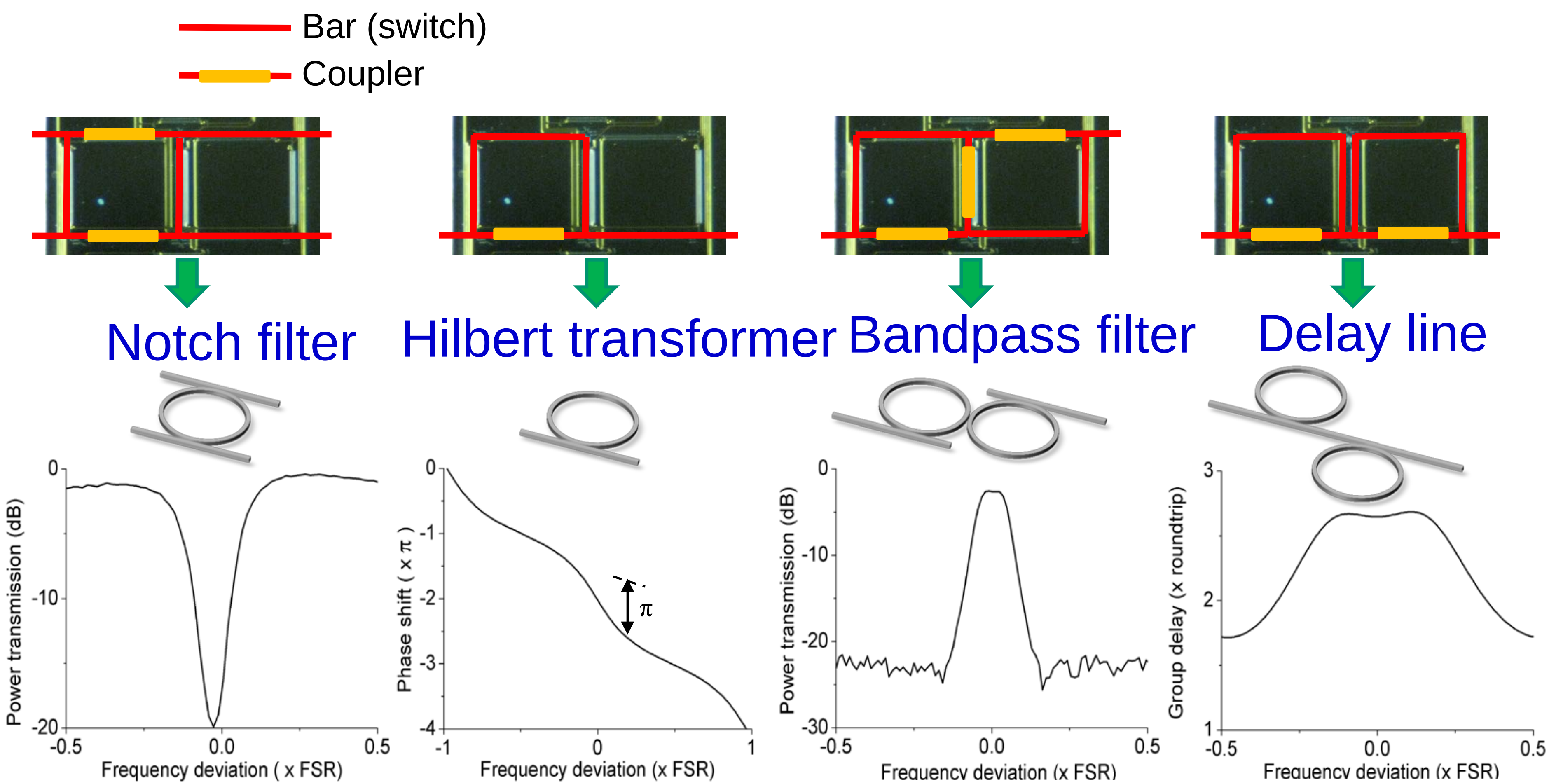

nature COMMUNICATIONS

ARTICLE

DOI: 10.1038/s41467-017-00714-1 OPEN

Multipurpose silicon photonics signal processor core

Daniel Pérez[1], Ivana Gasulla[1], Lee Crudgington[2], David J. Thomson[2], Ali Z. Khokhar[2], Ke Li[2], Wei Cao[2], Goran Z. Mashanovich[2,3] & José Capmany[1]

Published 21 September 2017

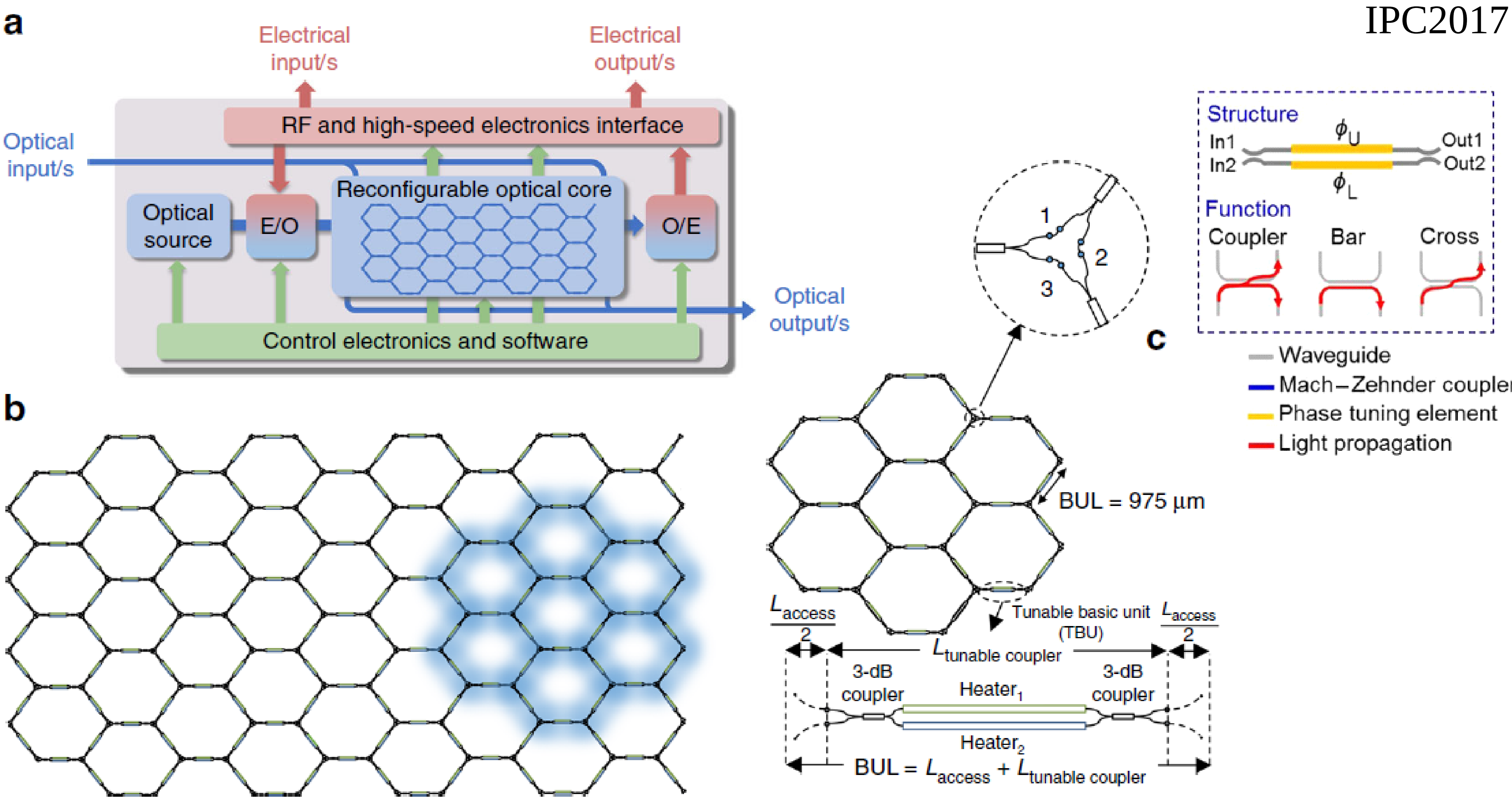

Fig. 1 Software-defined general-purpose photonic processor and its waveguide mesh reconfigurable core. **a** Architecture of the processor showing the reconfigurable core as its central element and the different possible electrical, optical and control input/output signals (E/O: External modulator. O/E: Optical receiver). **b** Schematic of the hexagonal waveguide mesh; a 7 unit cell structure is marked in *blue*. **c** Layout detail of the 7-cell hexagonal waveguide mesh designed and fabricated, including a zoom (*lower*) of a hexagon side of length 1 basic unit length (*BUL*) implemented by means of a 3-dB Mach Zehnder Interferometer (*MZI*) and a zoom (*upper*) of an optical interconnection node. TBU, tuneable basic unit

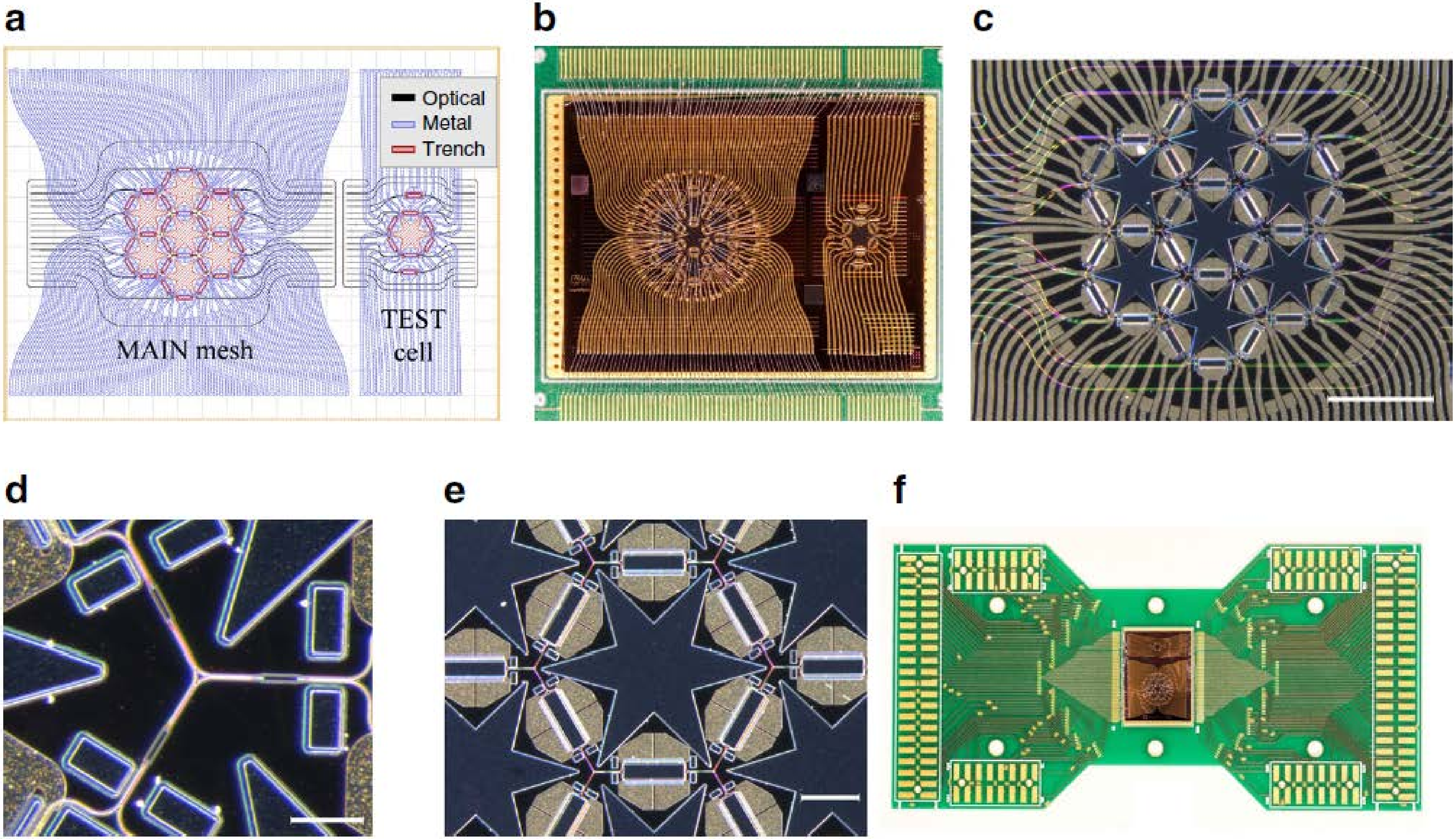

Fig. 2 Fabricated hexagonal waveguide mesh chip. **a** Design layers (optical, electrical, and thermal) of the 7-cell hexagonal waveguide mesh and the auxiliary test cell. **b** Fabricated silicon on insulator (*SOI*) chip of footprint 15 × 20 mm. **c** Zoomed vision of the 7-cell hexagonal waveguide mesh. *Scale bar* of 2 mm. In the *right bottom* corner **d** zoomed image of an optical interconnection node of three tuneable basic units (TBUs). *Scale bar* of 100 μm. In the *right bottom* corner **e** zoomed image of a single hexagonal cell showing the Mach Zehnder Interferometer (*MZI*). *Scale bar* of 500 μm. In the *right bottom* corner, tuning heaters, and star-type thermal isolation trenches. **f** Printed circuit board with the waveguide mesh chip mounted and wired bonded

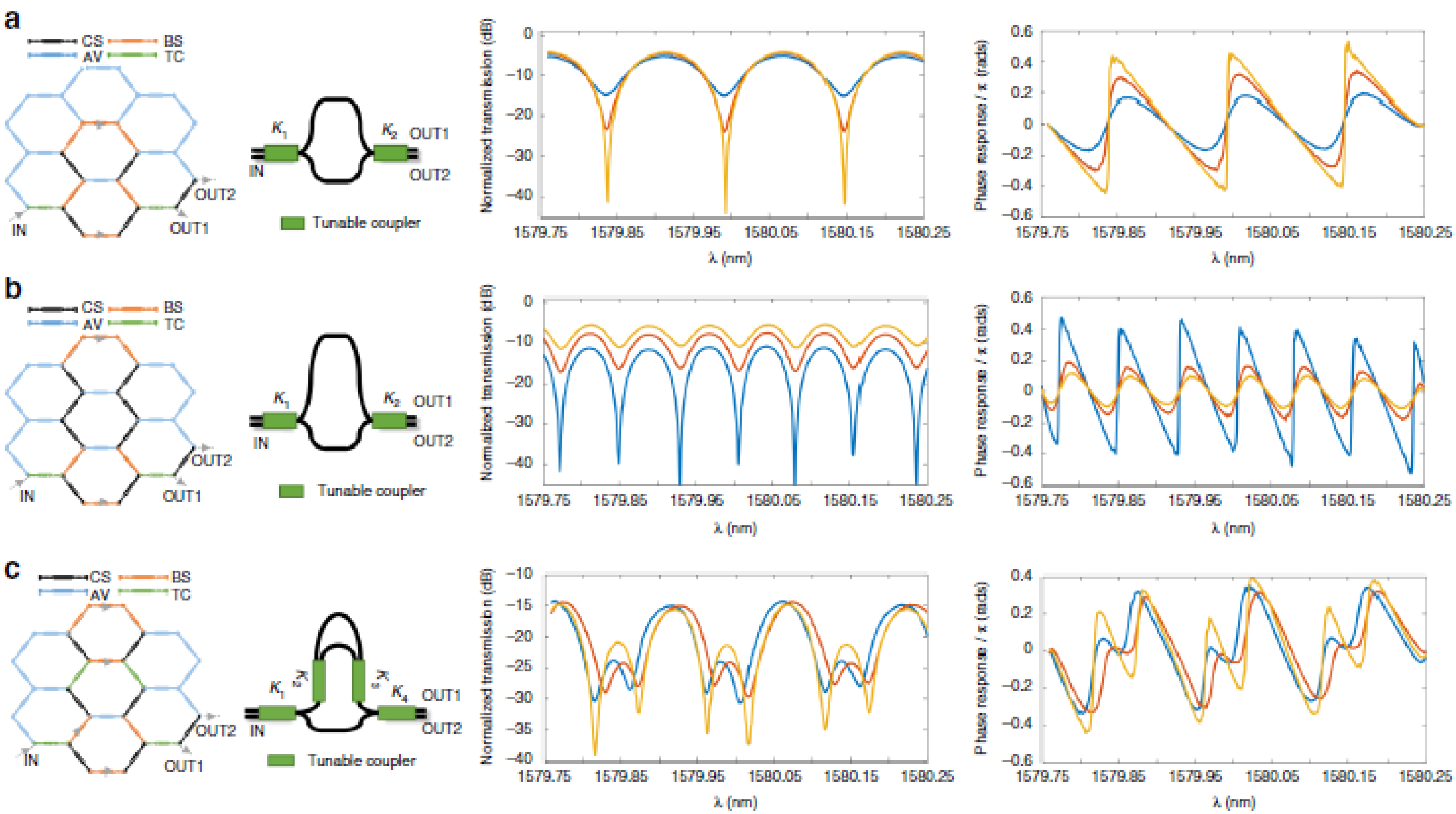

Fig. 3 Experimental results for tuneable unbalanced Mach Zehnder Interferometers and finite impulse response filters. Waveguide mesh connection diagram, circuit layout and measured modulus, and phase transfer function for different values of the coupling constants K_1 and K_2 in the case of **a** a 4-BUL unbalanced Mach-Zehnder Interferometer (*UMZI*) filter; **b** an 8-BUL UMZI filter; **c** a 4-BUL basic delay 3-tap transversal filter. For each case, the first column shows the 7-cell hexagonal waveguide mesh configuration, where each Mach Zehnder Interferometer (*MZI*) device is represented by a given color depending on whether it is activated as a cross (*black*) or bar (*orange*) switch, a tuneable coupler (*green*) or not used/available (*blue*). The *second column* shows the layout of the implemented structure, while the *third* and *fourth columns* show, respectively, the measured modulus and corresponding phase (calibrated by the shortest path) for the synthesized configuration where the input is in the IN port and the output is the OUT1 port. Measured curves are displayed for different values of the coupling constants K_1 and K_2, which are tuned by changing the injection currents to the heater elements of the input and output MZI devices of the UMZI. Changing these values alters the position of the zero in the UMZI transfer function bringing it closer or farther to the unit circle[42]. The closer the zero is to the unit circle, the deeper are the notches in the transfer function are and the higher is the phase shift step in the transfer function is ref. [42]. BUL, basic unit length; CS, cross state; BS, bar state; AV, available; TC, tuneable coupler

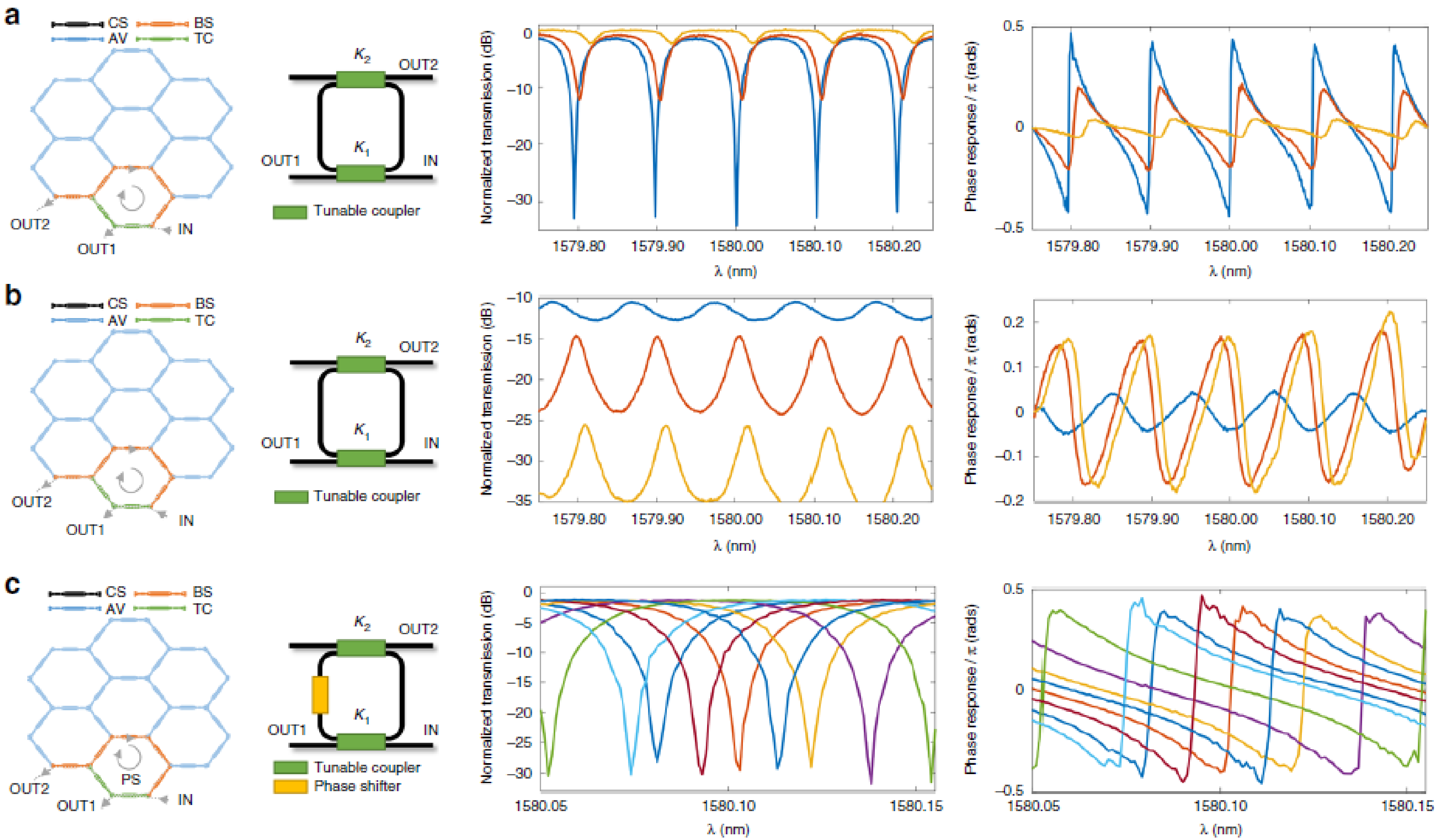

Fig. 4 Experimental results for 6-BUL ring resonator infinite impulse response and combined finite impulse response and infinite impulse response filters. Waveguide mesh connection diagram, circuit layout and measured modulus, and phase transfer function for **a** a 6-BUL optical ring resonator (*ORR*) infinite impulse response (*IIR*) filter for different values of the coupling constants K_1 and K_2; **b** a 6-BUL ORR finite impulse response (FIR) + IIR filter for different values of the coupling constants K_1 and K_2; **c** a 6-BUL ORR IIR filter along a full spectral period for different values of the optical ring resonator round-trip phase shift. BUL, basic unit length; CS, cross state; BS, bar state; AV, available; TC, tuneable coupler

Conclusion

- MWP has been extensively investigated, but its applications are limited due to large size and high cost of discrete components.

- The use of PICs is a solution to reduce the size and cost.

- The 3 materials systems have their own limitations
  - SiP – no light amplification, no light source
  - InP – large size, high loss, and complexity in fabrication
  - SiN – passive only devices

- **Hybrid Integration (SiP + InP)** may be needed to produce laser sources and optical amplifiers using III-V materials - a key challenge for wide applications of silicon photonics.

Acknowledgments

CMC Microsystems

NSERC Si-EPIC program
NSERC Discovery grant program
NSERC Strategic partnership grant program